Integrated Approaches to Modeling Late Paleozoic Petroleum Reservoirs in the Greater Midcontinent, U.S.

Part 4 – Lithofacies, Petrophysics, and Petrofacies

Short Course

AAPG - Southwest Section

December 8, 2008 -- Abilene, Texas

December 9, 2008 -- Ft. Worth, Texas

W. Lynn Watney
Senior Scientific Fellow
Kansas Geological Survey
1930 Constant Avenue
Lawrence, KS 66047
Ph: 785-864-2184
Fax: 785-864-5317
Email: lwatney@kgs.ku.edu

Schedule

- 9:00-10:00 – 1. Approach to Modeling Late Paleozoic Petroleum Reservoirs.
- 10-12 noon – 2. Regional structural and tectonic framework during the late Paleozoic and significance to reservoir systems.
  - **~10:30-10:45 -- Break –**
- **Noon-1:00 pm – Lunch**
- 1:00-3:00 pm -- 3. Sequence stratigraphy and reservoir architecture of late Paleozoic strata in the Midcontinent.
  - **~3:00-3:15 – Break –**
- 3:00-4:30 pm -- 4. Reservoir Lithofacies and Petrofacies.
- **4:30-5:00 pm – 5. Wrap-up & Summary**.

Take Home Points of Short Course

- Basement structures and distal tectonic events affecting them are important in defining location and properties of reservoirs.
- Process-based field, outcrop, and Recent analogs provide more appropriate, accurate interpolation of reservoir properties.
- Late Paleozoic reservoirs are dominated by depositional fabric selective diagenesis, both early and late both.
- Establishing petrofacies and pore types is essential to accurate calculations of water saturations, volumetrics, ROIP, establishing permeability correlations and predicting fluid flow.
- Infill locations and new pays within oil and gas fields remain significant targets for IOR in mature regions; requires comprehensive, integrated approach.
- Re-exploration and exploitation of mature producing areas can be substantially benefited by access to and mining of large data sets – digital and electronic data – logs, production, core/samples and descriptions, *in an integrated and quantitative manner.*

4. Reservoir Lithofacies and Petrofacies

- Modern ooid shoals – geometries, textures, processes
- Example – role of establishing temporal geometries and importance of texture in permeability and flow unit designation.
  - Hall Gurney CO2 pilot, Central Kansas Uplift, Kansas (Upper Missourian Plattsburg Limestone)
- Petrophysics Overview
  - Solving the Archie equation for Sw and establishing the cementation exponent, m
  - Significance of bulk volume water, (BVW = Sw*Ø) and pore type
  - Examples –
    - Marmaton Altamont Limestone – volumetrics of an oomoldic reservoir using varying “m”, the cementation exponent
    - Waddell Field – San Andres oomoldic and karsted reservoir, significance of structure and diagenesis
    - Norcan East Field -- Calibrating pay in a shaly estuarine valley-fill sandstone (Atokan, western Ks)

Slides on Modern ooid shoals from the Bahamas provided by Eugene C. Rankey University of Kansas

Oolitic Carbonate Shoals

Conceptual Facies Models

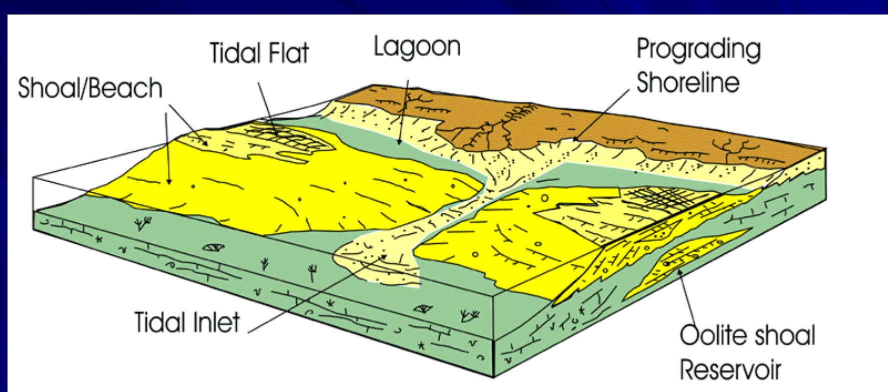

After Handford, 1988

Is this the best we can do?

- Qualitative
- Not predictive

E.C. Rankey, KU

Dunham Carbonate Classification

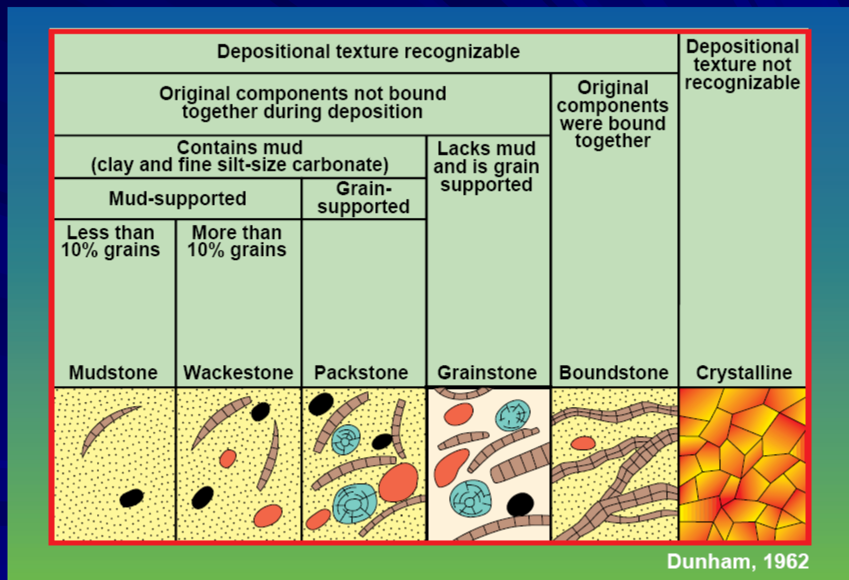

Moore (1988)

Goals

- Examine **geomorphology** of marine (oolitic) sand bodies
- Explore **grain sizes and types** within a hydro-geomorphic framework
- Explain patterns in terms of **fundamental processes**

Courtesy of Gene Rankey
Department of Geology
The University of Kansas

Marine Sand Belt - Character

- Large-scale sand body parallel shelf margin
- Parabolic bars superimposed; flood/ebb
- Individual sand waves, varied orientation
- Cross-laminated – troughs, perhaps wave rippled
- Increase in energy upwards

Lily Bank Marine Sand Belt

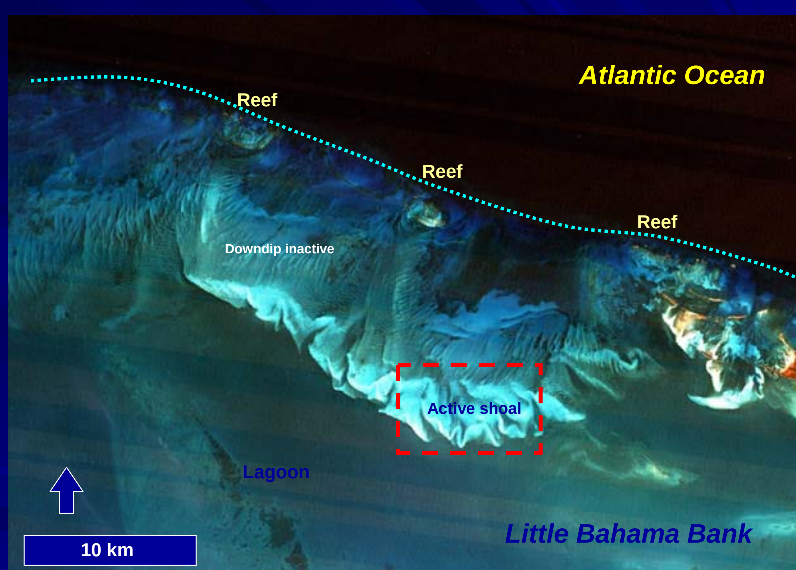

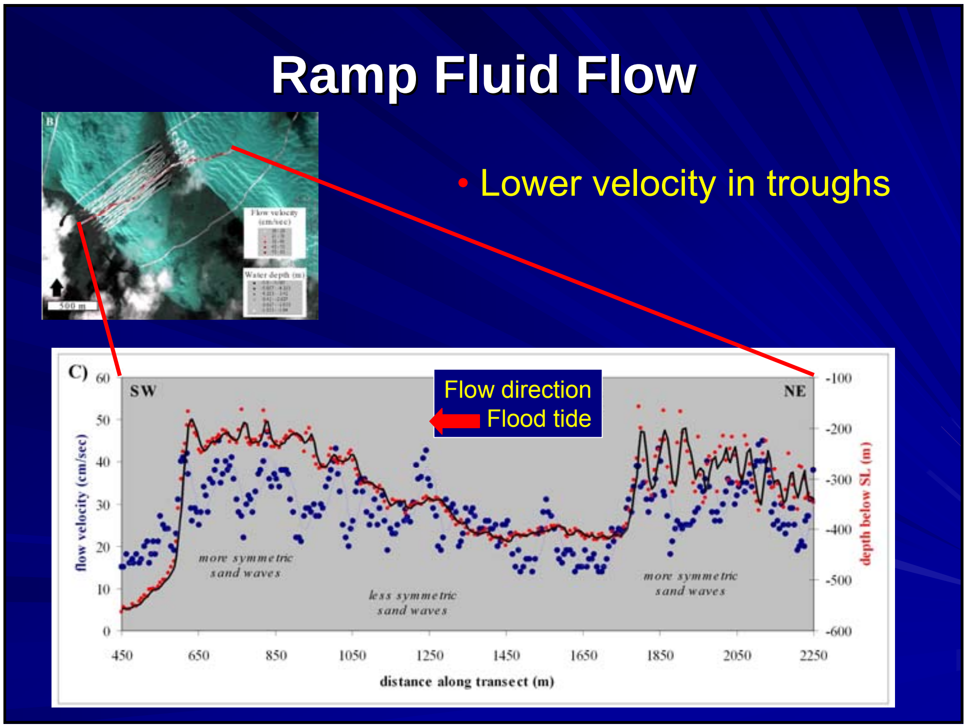
Ramp Fluid Flow
• Lower velocity in troughs
Flow direction
Flood tide
SW
NE
more symmetric sand waves
less symmetric sand waves
more symmetric sand waves
flow velocity (cm/sec)
depth below SL (m)
distance along transect (m)
500 m

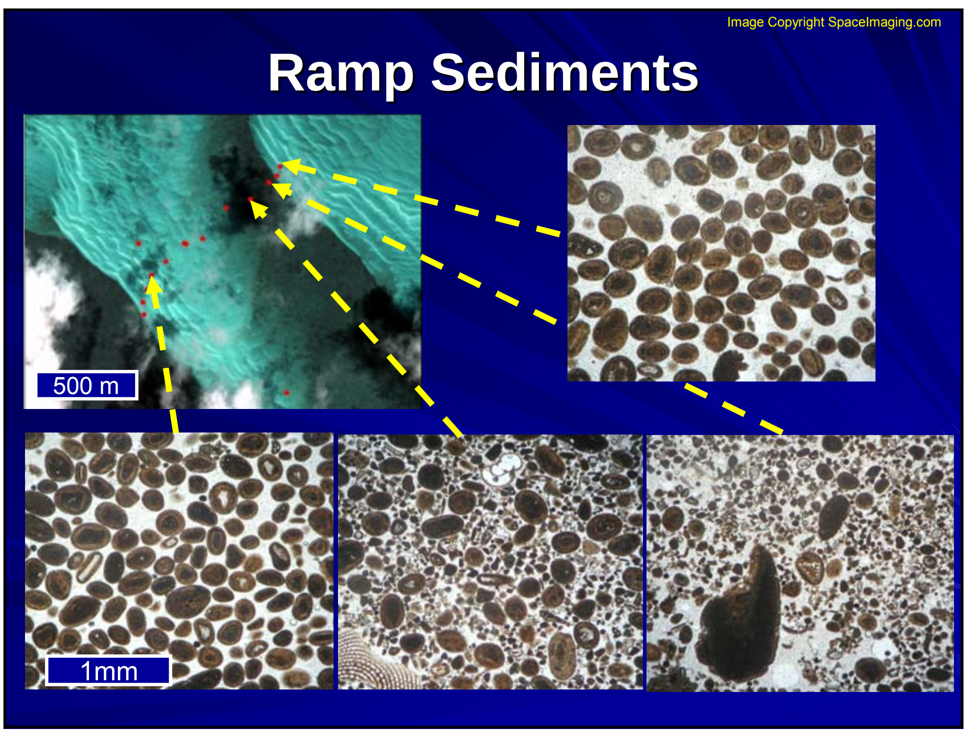
Image Copyright SpaceImaging.com
Ramp Sediments
500 m
1mm

Ramp Sediments

- Relative to troughs, crests:
  - Are coarser
  - Are better sorted

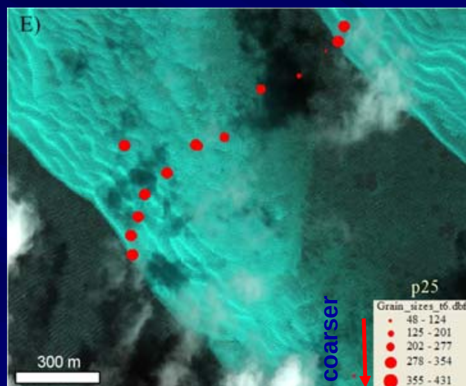

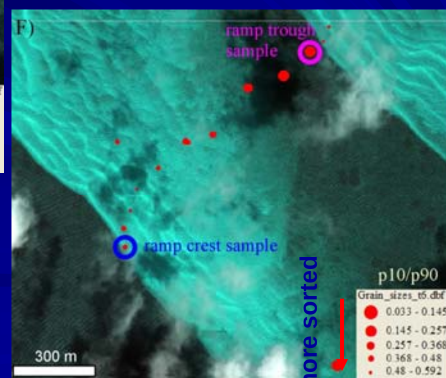

Carbonate Tidal Deltas

Mostly from Stacy Reeder PhD

Tidal Deltas - Character

- Lobate forms; most commonly flood deltas
- Commonly (not always) associated with bedrock islands
  - clasts/rocky bottom
  - 'Fixed' location
- Even if flood-oriented, shaped by both flood and ebb tides
- Not commonly interpreted in geologic record

Ebb-Dominated Tidal Delta on Little Bahama Bank

• Ebb flow over shoal

• Decreasing current velocity with distance

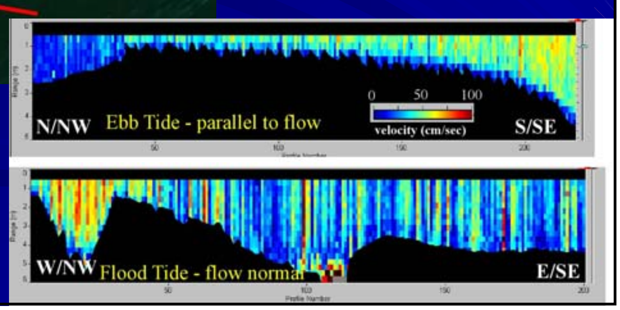

Tidal Sand Ridges

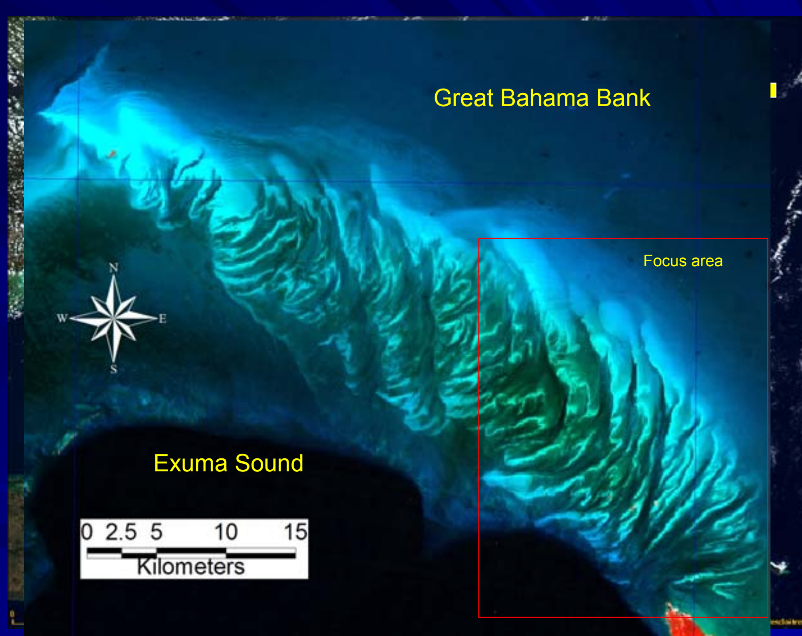

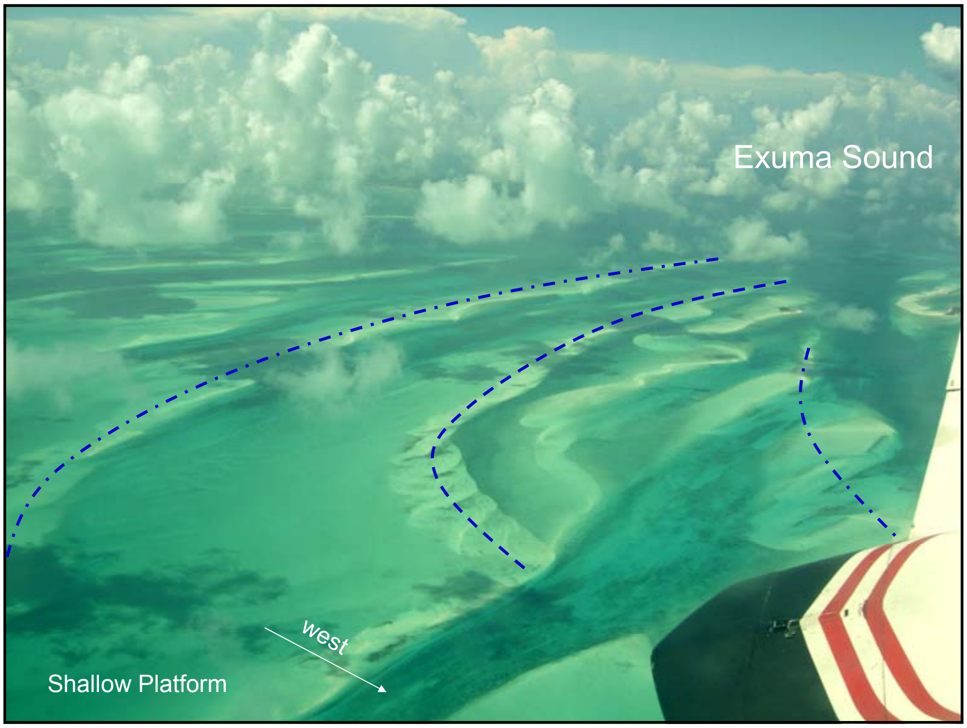
Exuma Sound
west
Shallow Platform

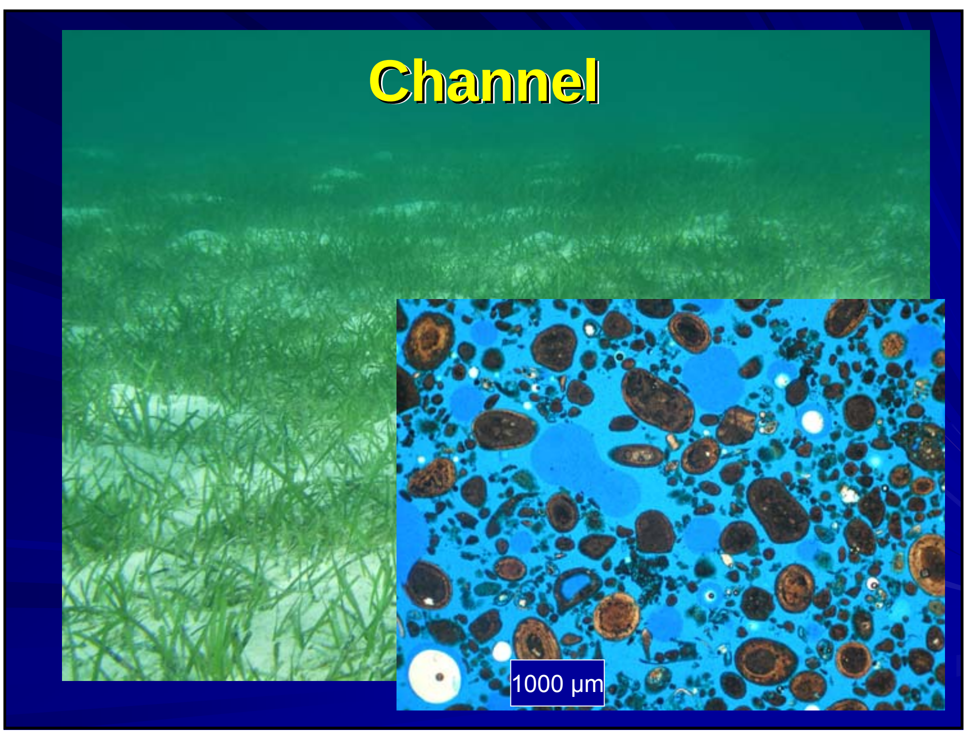
Channel
1000 µm

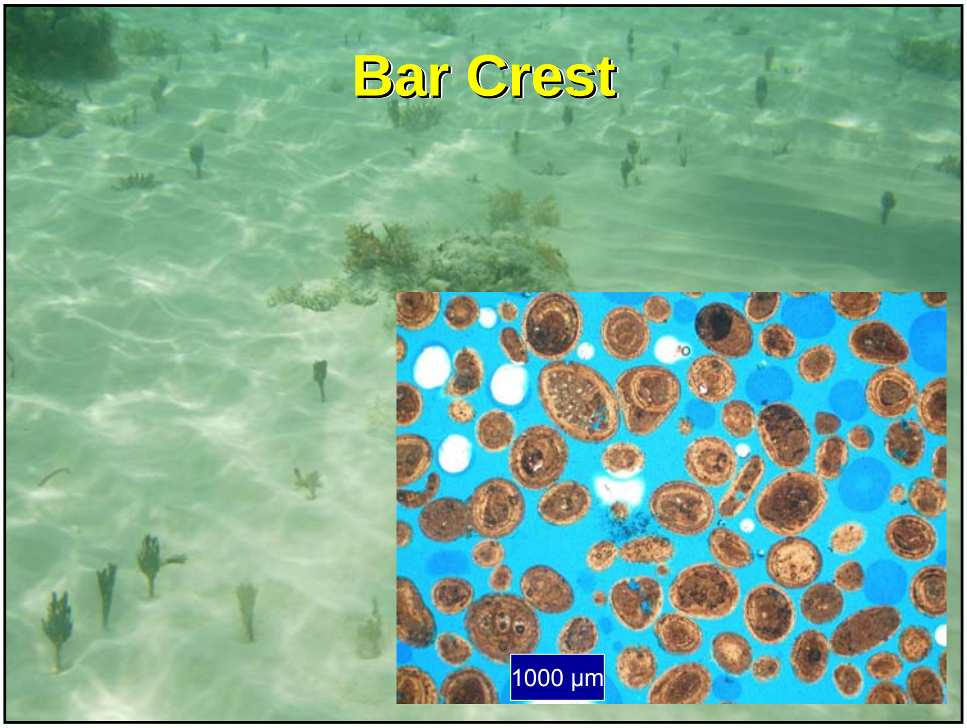

Conclusions from Modern

- Feedbacks between bathymetry and hydrodynamics lead to predictable geomorphic trends
- Ooid sorting improves along crest of shoals

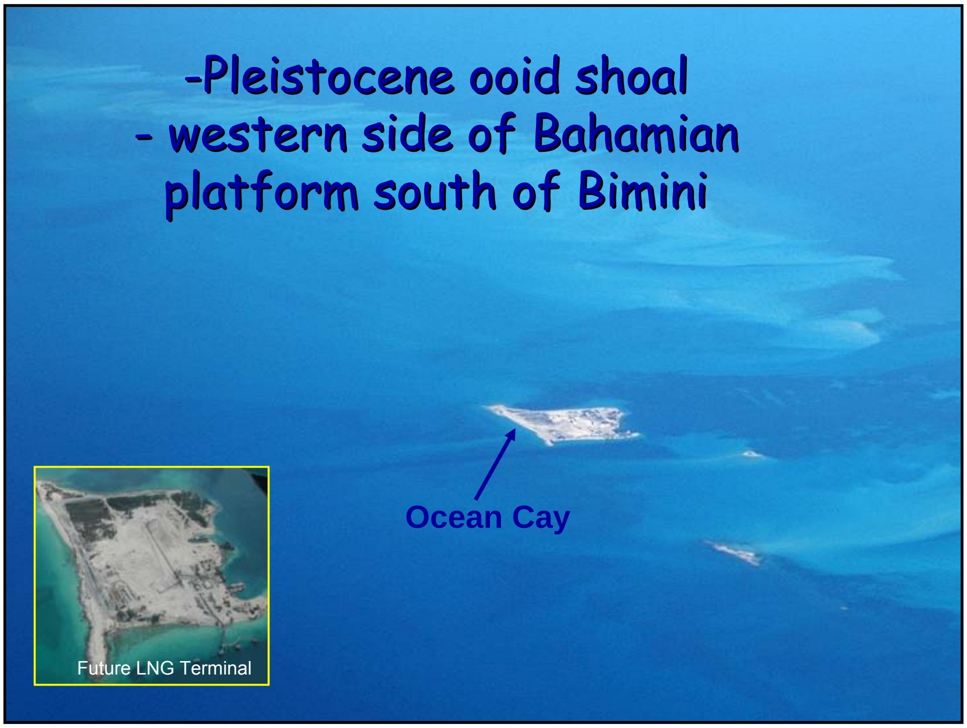
-Pleistocene ooid shoal
- western side of Bahamian platform south of Bimini
Ocean Cay
Future LNG Terminal

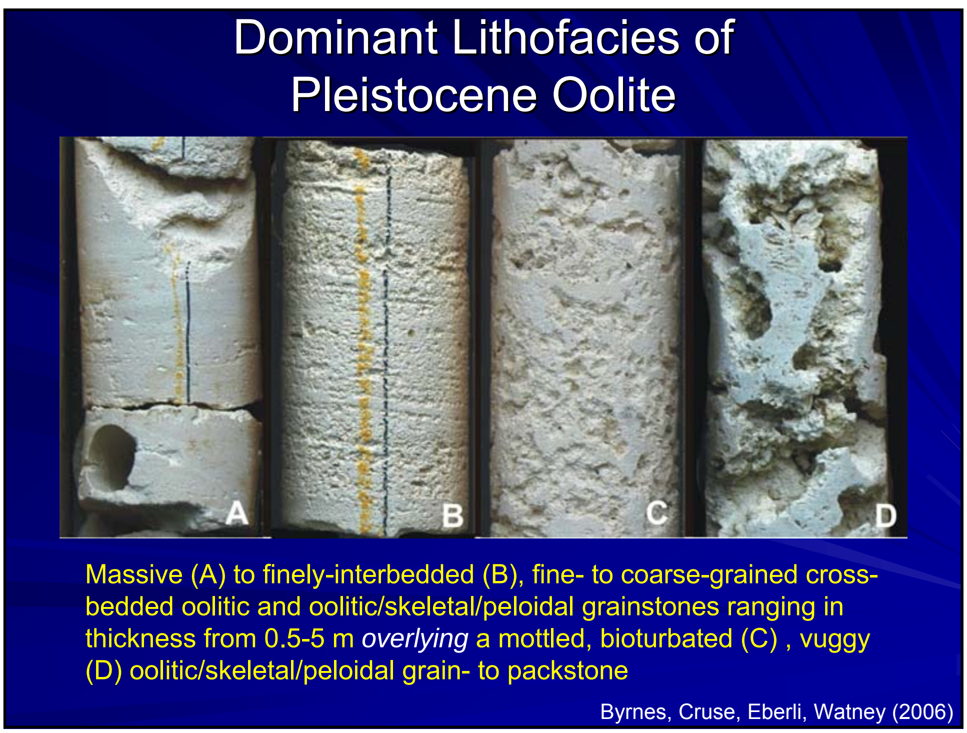
Dominant Lithofacies of Pleistocene Oolite
A
B
C
D
Massive (A) to finely-interbedded (B), fine- to coarse-grained cross-bedded oolitic and oolitic/skeletal/peloidal grainstones ranging in thickness from 0.5-5 m *overlying* a mottled, bioturbated (C) , vuggy (D) oolitic/skeletal/peloidal grain- to packstone
Byrnes, Cruse, Eberli, Watney (2006)

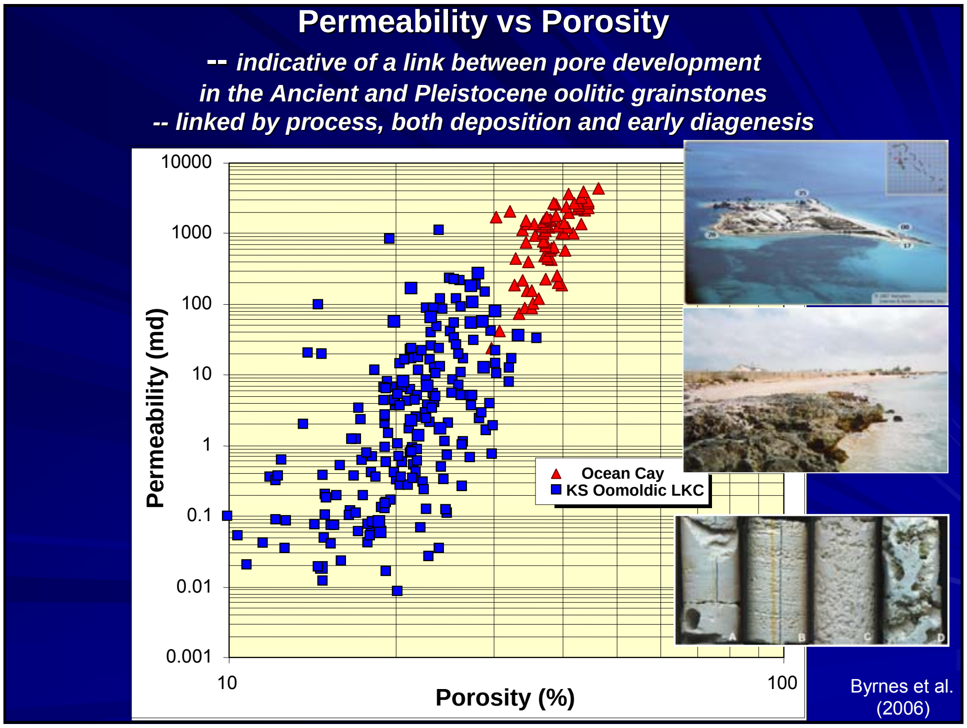
Permeability vs Porosity
-- indicative of a link between pore development in the Ancient and Pleistocene oolitic grainstones
-- linked by process, both deposition and early diagenesis
Permeability (md)
Porosity (%)
Ocean Cay
KS Oomoldic LKC
Byrnes et al. (2006)

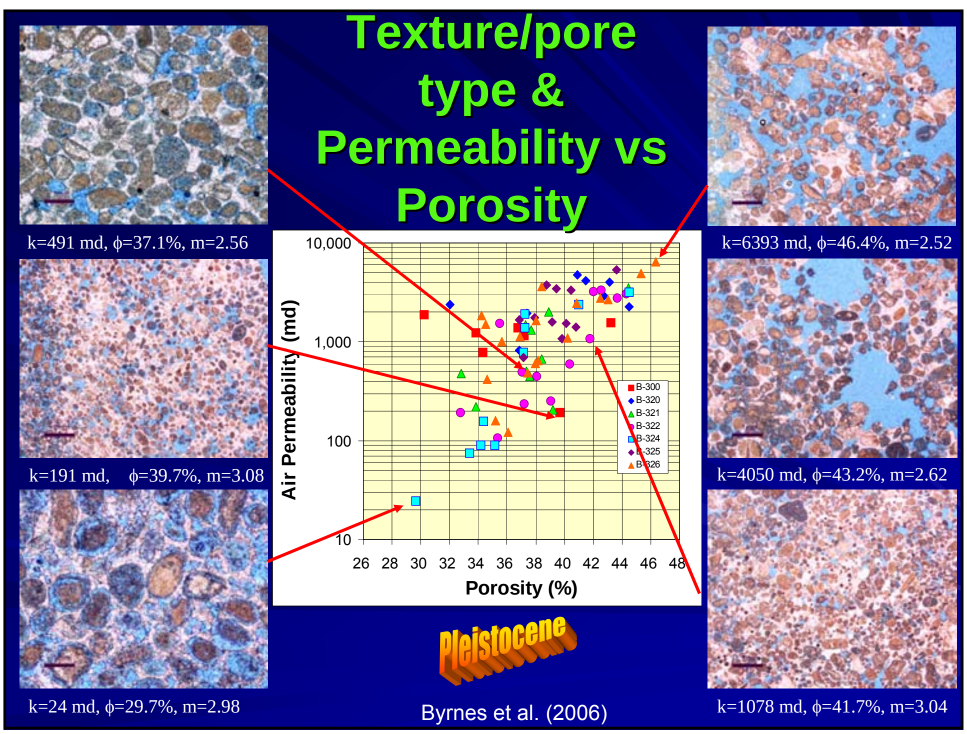
Texture/pore type & Permeability vs Porosity
k=491 md, ϕ=37.1%, m=2.56
k=191 md, ϕ=39.7%, m=3.08
k=24 md, ϕ=29.7%, m=2.98
k=6393 md, ϕ=46.4%, m=2.52
k=4050 md, ϕ=43.2%, m=2.62
k=1078 md, ϕ=41.7%, m=3.04
Air Permeability (md)
Porosity (%)
Pleistocene
Byrnes et al. (2006)

LKC Permeability vs Porosity

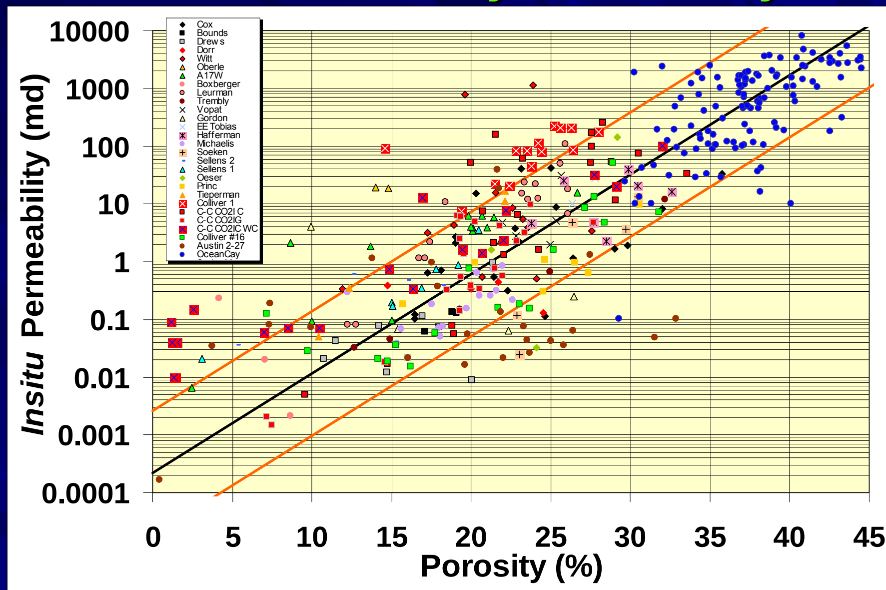

$\log_{10}k_i = 0.154\ \phi - 3.21$ (SE=6X)
$\log_{10}k_i = 0.090\ \phi + 0.47\ MCI - 3.2$ (SE=5.5X)

Permeability and Pore Diameter

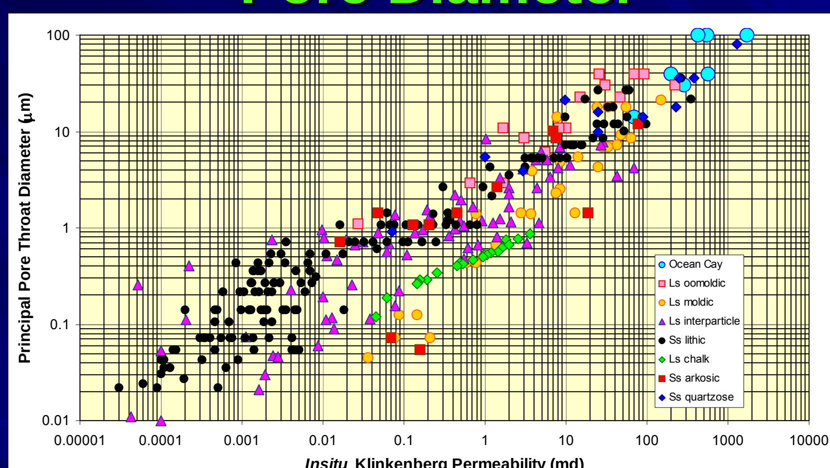

Pleistocene cores (*light blue*) exhibit correlation of permeability and principal pore throat diameter consistent with trend of other lithologies.

Byrnes et al. (2006)

Application of Modern and Pleistocene to the Pennsylvanian

- Lobate and linear oolitic shoals form complex geometries
- Granulometric attributes of Modern and Ancient ooid shoals are comparable
- Oomoldic porosity is extensive in Pleistocene and older rocks (*for aragonitic-rich ooid*)
- Size, sorting, packing of Pennsylvanian and Pleistocene oomolds are closely related
- Oomoldic pores are closely related to depositional fabric and near surface subaerial diagenesis, modified by later burial diagenesis

Pleistocene, Ocean Cay *w/ alz-r stain*

Pennsylvanian, Bethany Falls Ls. unstained

Lansing-Kansas City Production and CO_2 Project Location

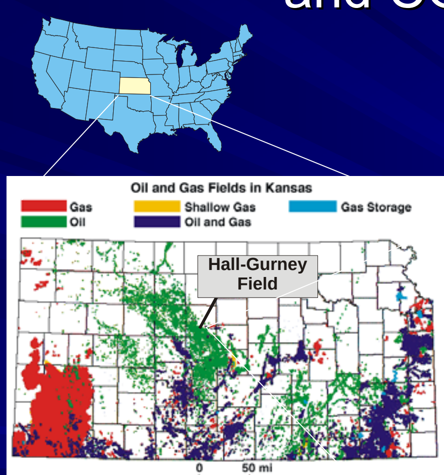

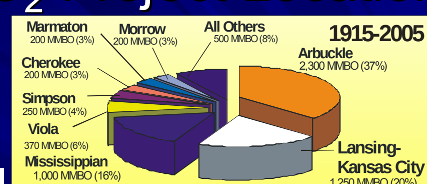

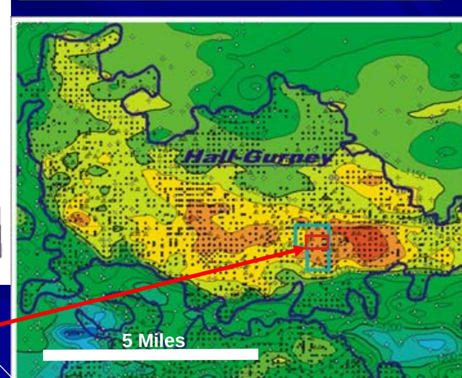

CO2 Pilot Study Area

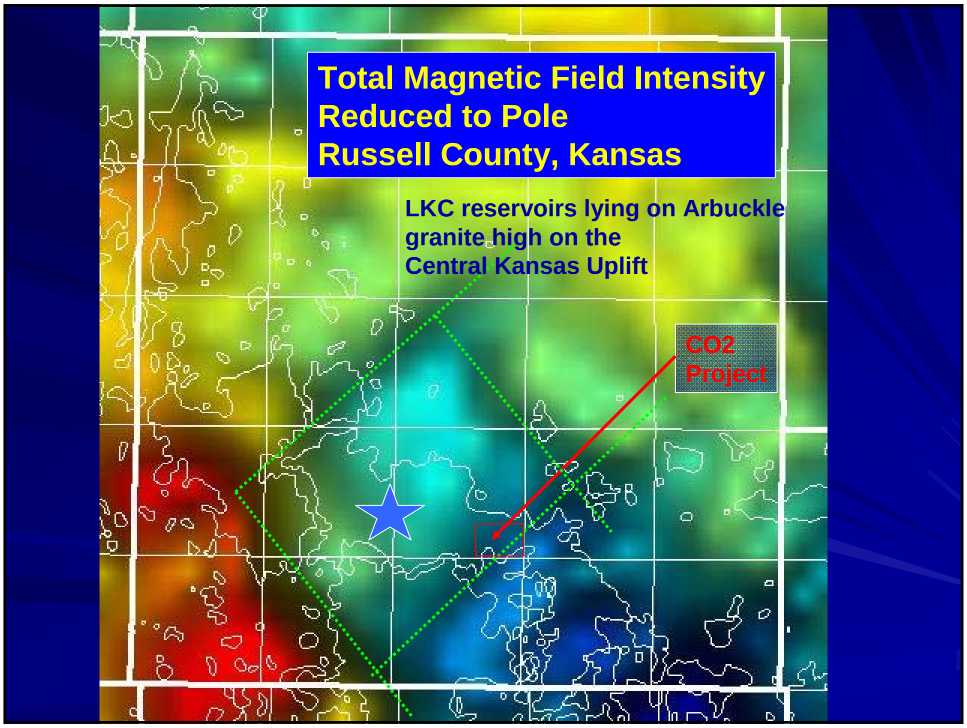
Total Magnetic Field Intensity
Reduced to Pole
Russell County, Kansas
LKC reservoirs lying on Arbuckle granite high on the Central Kansas Uplift
CO2 Project

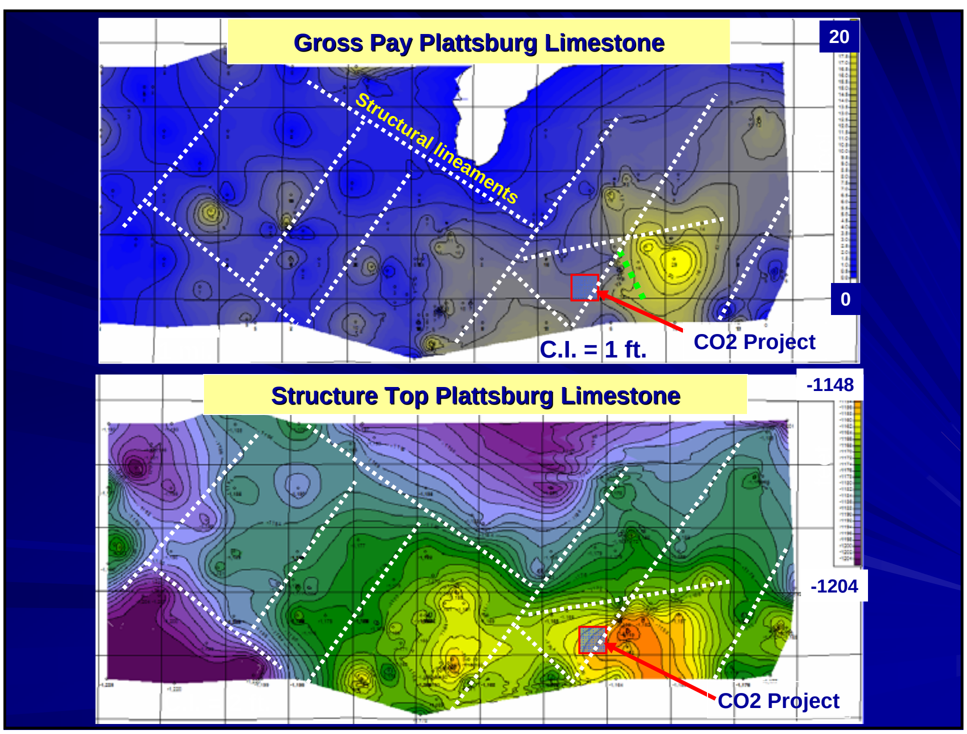
Gross Pay Plattsburg Limestone
20
Structural lineaments
0
C.I. = 1 ft.
CO2 Project
Structure Top Plattsburg Limestone
-1148
-1204
CO2 Project

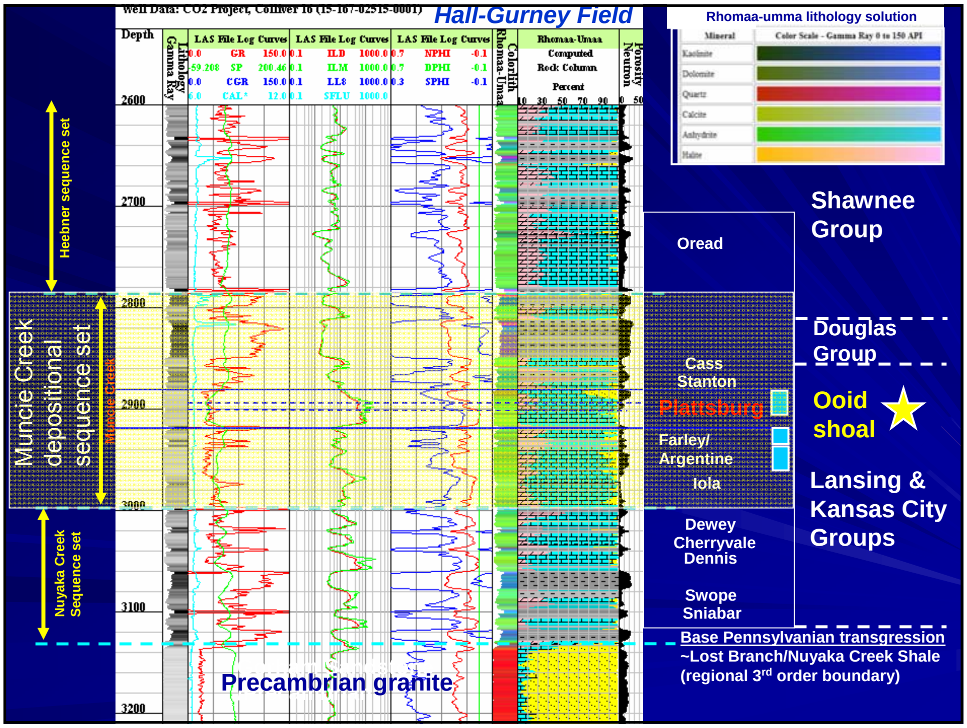
Hall-Gurney Field
Rhomaa-umma lithology solution
Kaolinite
Dolomite
Quartz
Calcite
Anhydrite
Halite
Heebner sequence set
Muncie Creek depositional sequence set
Muncie Creek
Nuyaka Creek Sequence set
Shawnee Group
Oread
Douglas Group
Cass
Stanton
Plattsburg
Ooid shoal
Farley/ Argentine
Iola
Lansing & Kansas City Groups
Dewey
Cherryvale
Dennis
Swope
Sniabar
Base Pennsylvanian transgression
~Lost Branch/Nuyaka Creek Shale
(regional 3rd order boundary)
Precambrian granite
Depth
2600
2700
2800
2900
3000
3100
3200

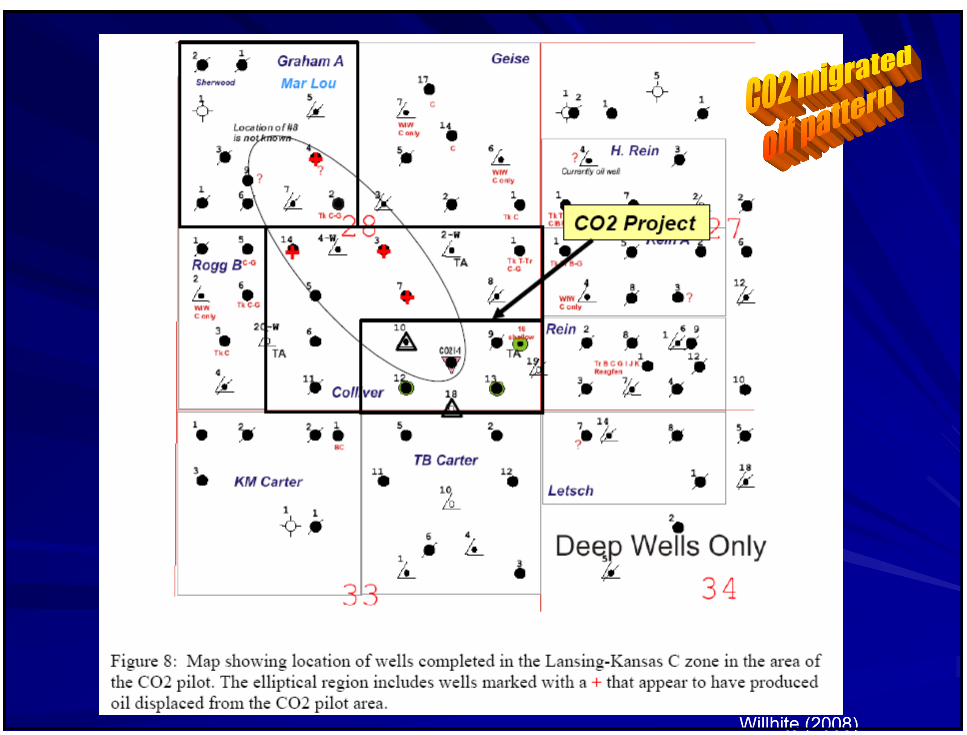
CO2 migrated oil pattern
Graham A
Mar Lou
Geise
H. Rein
CO2 Project
Rogg B
Rein
Colliver
TB Carter
KM Carter
Letsch
Deep Wells Only
28
27
33
34
Figure 8: Map showing location of wells completed in the Lansing-Kansas C zone in the area of the CO2 pilot. The elliptical region includes wells marked with a + that appear to have produced oil displaced from the CO2 pilot area.
Willhite (2008)

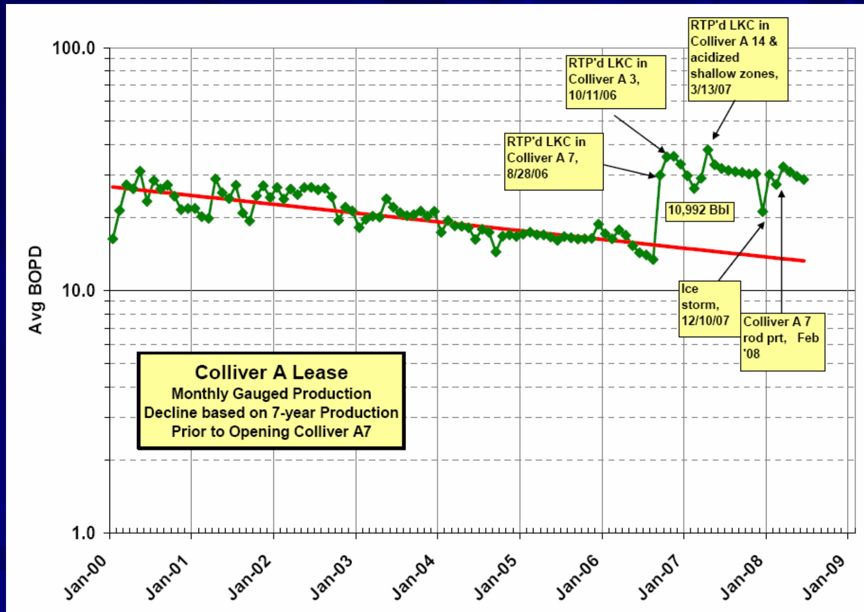

Figure 10: Colliver A lease production after C zone was opened in Colliver A #7, Colliver A#3 and Colliver A#14. Willhite (2008)

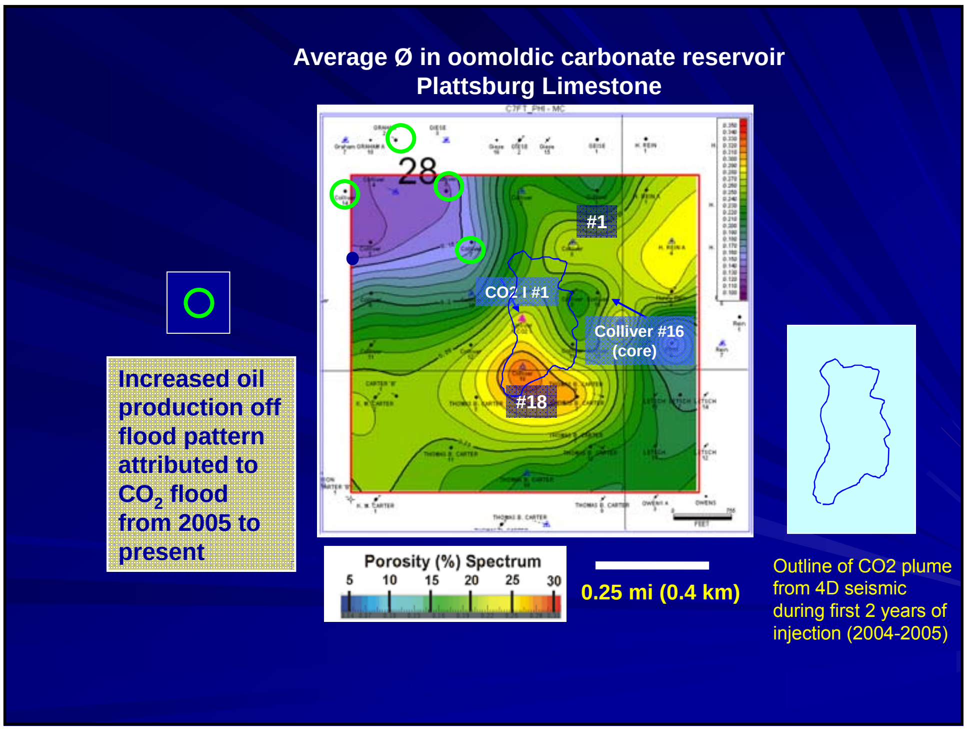

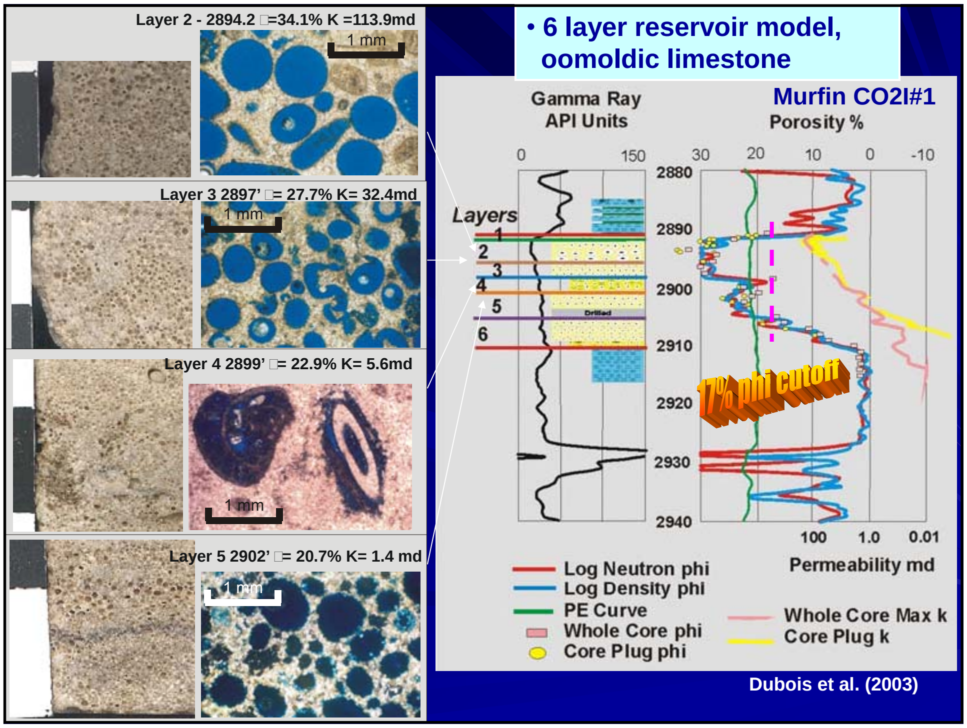
• 6 layer reservoir model, oomoldic limestone
Layer 2 - 2894.2 =34.1% K =113.9md
Layer 3 2897' = 27.7% K= 32.4md
Layer 4 2899' = 22.9% K= 5.6md
Layer 5 2902' = 20.7% K= 1.4 md
1 mm
Gamma Ray API Units
Murfin CO2I#1
Porosity %
Layers
17% phi cutoff
Permeability md
Log Neutron phi
Log Density phi
PE Curve
Whole Core phi
Core Plug phi
Whole Core Max k
Core Plug k
Dubois et al. (2003)

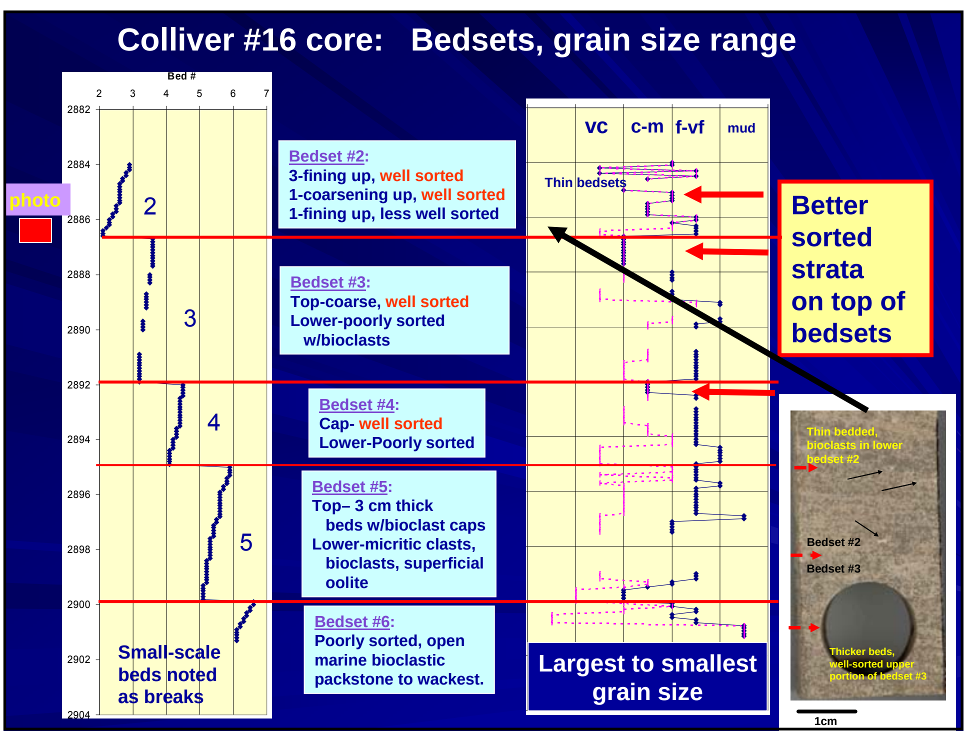
Colliver #16 core: Bedsets, grain size range
Bed #
photo
Bedset #2:
3-fining up, well sorted
1-coarsening up, well sorted
1-fining up, less well sorted
Bedset #3:
Top-coarse, well sorted
Lower-poorly sorted w/bioclasts
Bedset #4:
Cap- well sorted
Lower-Poorly sorted
Bedset #5:
Top– 3 cm thick beds w/bioclast caps
Lower-micritic clasts, bioclasts, superficial oolite
Bedset #6:
Poorly sorted, open marine bioclastic packstone to wackest.
Small-scale beds noted as breaks
vc c-m f-vf mud
Thin bedsets
Largest to smallest grain size
Better sorted strata on top of bedsets
Thin bedded, bioclasts in lower bedset #2
Bedset #2
Bedset #3
Thicker beds, well-sorted upper portion of bedset #3
1cm

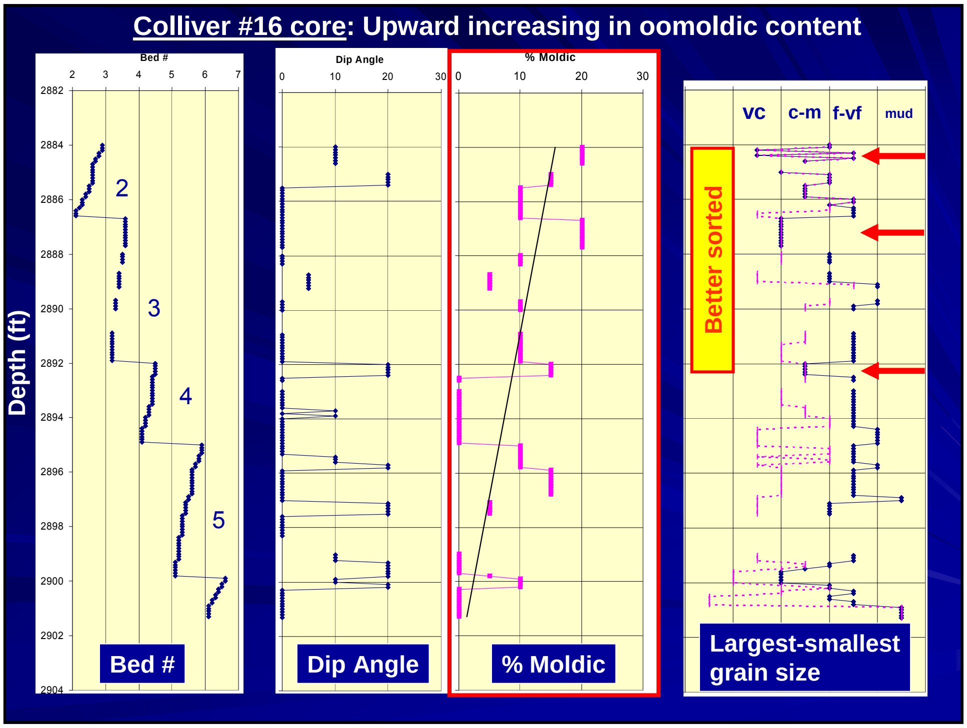
Colliver #16 core: Upward increasing in oomoldic content
Bed #
Dip Angle
% Moldic
Depth (ft)
Better sorted
vc
c-m
f-vf
mud
Largest-smallest grain size

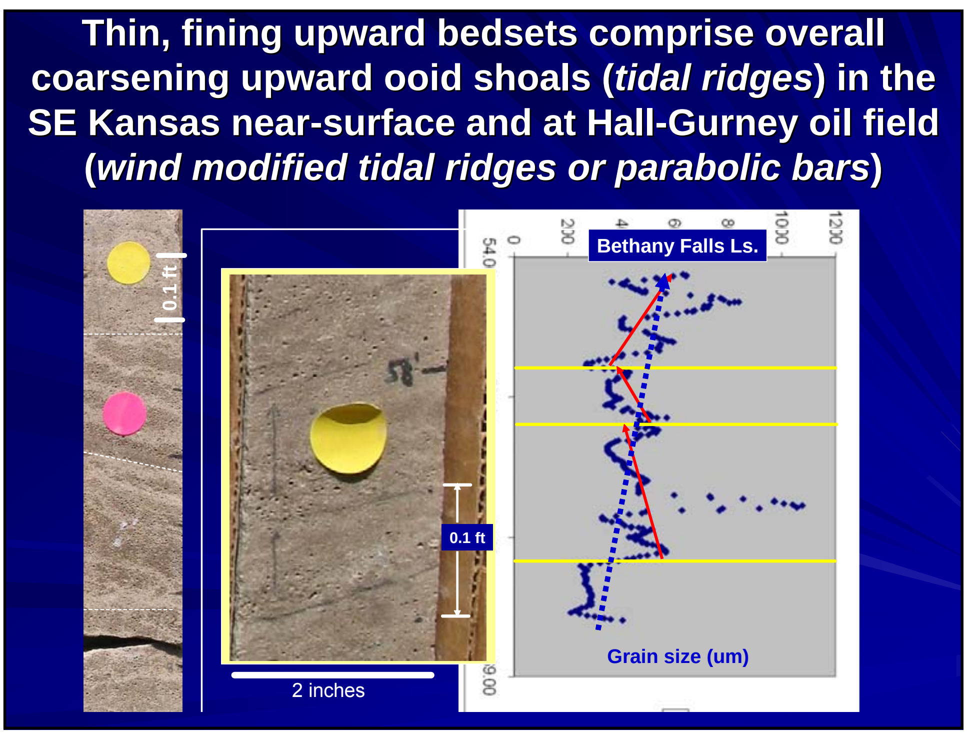
Thin, fining upward bedsets comprise overall coarsening upward ooid shoals (*tidal ridges*) in the SE Kansas near-surface and at Hall-Gurney oil field (*wind modified tidal ridges or parabolic bars*)
0.1 ft
0.1 ft
2 inches
Bethany Falls Ls.
Grain size (um)

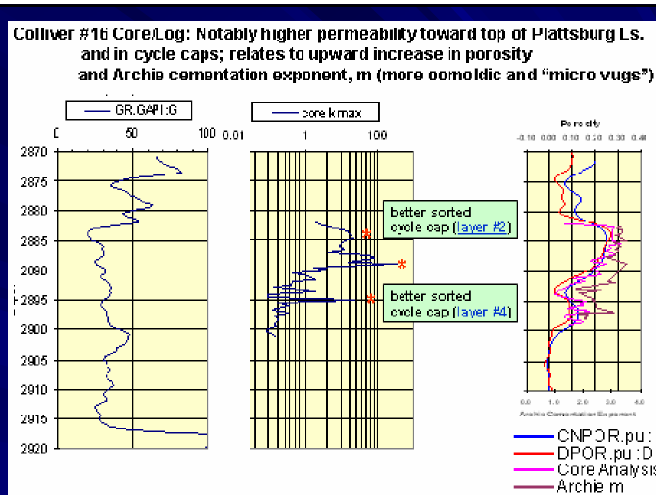

- Depth profile of the "C" zone showing gamma ray, maximum permeability, and Archie cementation exponent, m, compared to various measures of porosity.
- Note that cementation exponent, m, increases upward from around 2 to near 3.5. Higher m indicates more tortuous paths for fluid to move as m increases.
- Higher m in Archie water saturation equation raises Sw

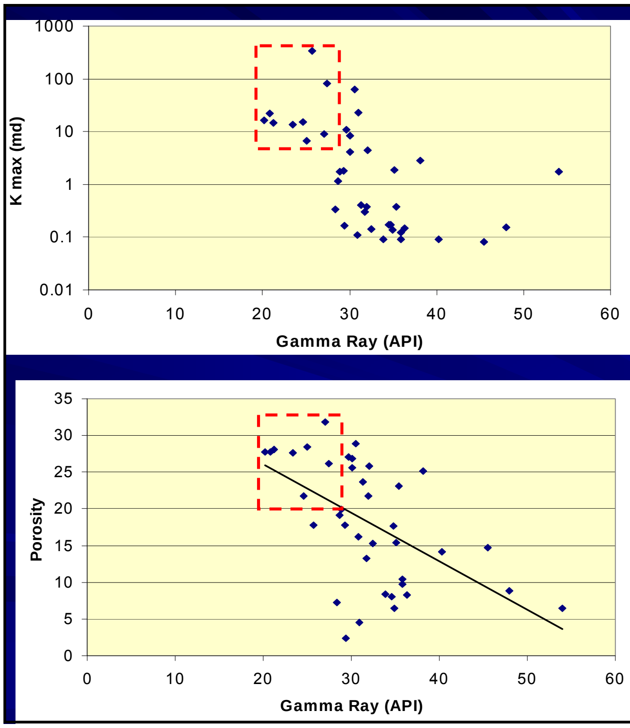

Clean (lower gamma ray), better-sorted oolite/ oomoldic

- **Higher permeability, >10 md**
- Correlation with: better sorting, packing, and interconnected oomolds *(microvugs & associated high Archie cementation exponent)*
- **Clean, better sorted higher porosity in cycle caps,** porosity highest near top of shallowing upward succession
- Better sorted bar crests in Modern ooid shoals

Colliver #16 core data

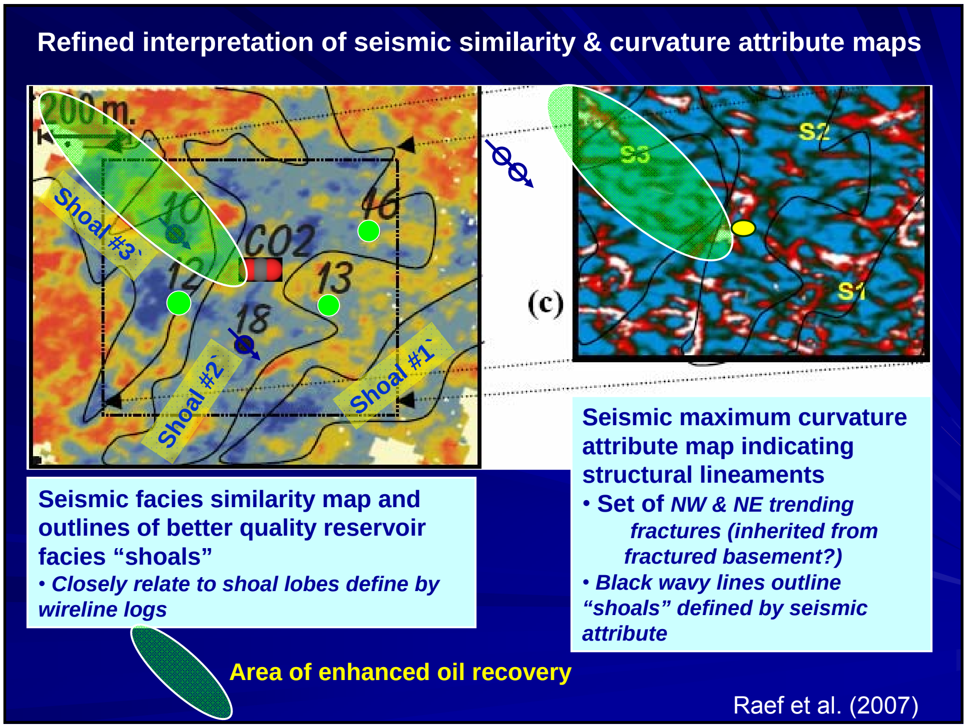
Refined interpretation of seismic similarity & curvature attribute maps
200 m.
Shoal #3
10
CO2
46
12
13
18
Shoal #2
Shoal #1
(c)
S3
S2
S1
Seismic facies similarity map and outlines of better quality reservoir facies "shoals"
• Closely relate to shoal lobes define by wireline logs
Seismic maximum curvature attribute map indicating structural lineaments
• Set of NW & NE trending fractures (inherited from fractured basement?)
• Black wavy lines outline "shoals" defined by seismic attribute
Area of enhanced oil recovery
Raef et al. (2007)

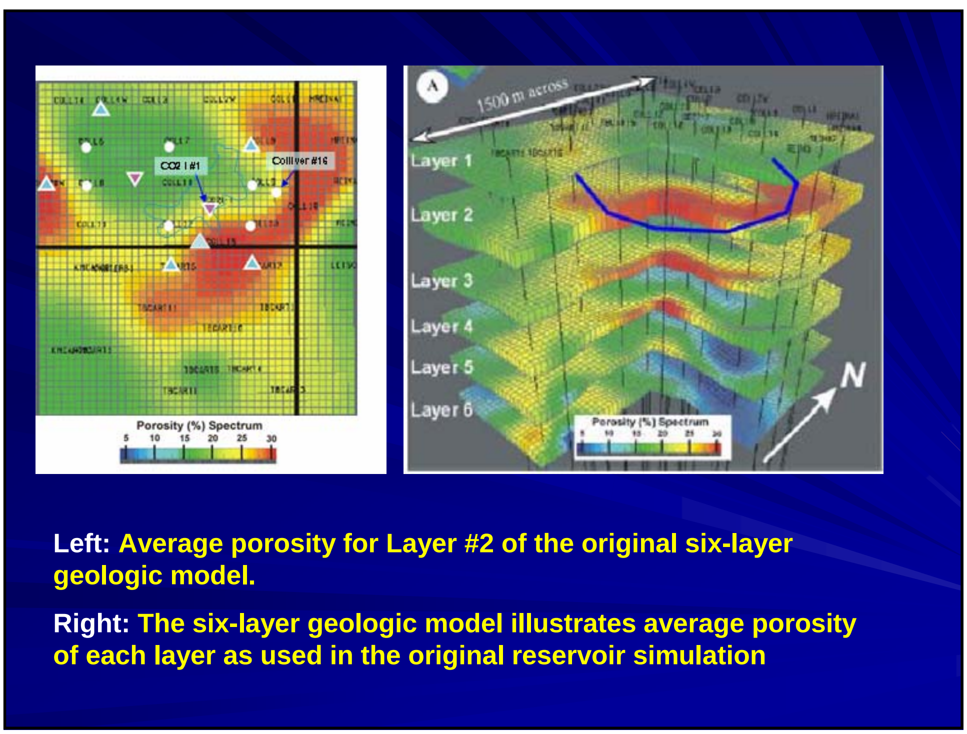
CO2 I #1
Colliver #16
Porosity (%) Spectrum
5 10 15 20 25 30
A
1500 m across
Layer 1
Layer 2
Layer 3
Layer 4
Layer 5
Layer 6
N
Porosity (%) Spectrum
Left: Average porosity for Layer #2 of the original six-layer geologic model.
Right: The six-layer geologic model illustrates average porosity of each layer as used in the original reservoir simulation

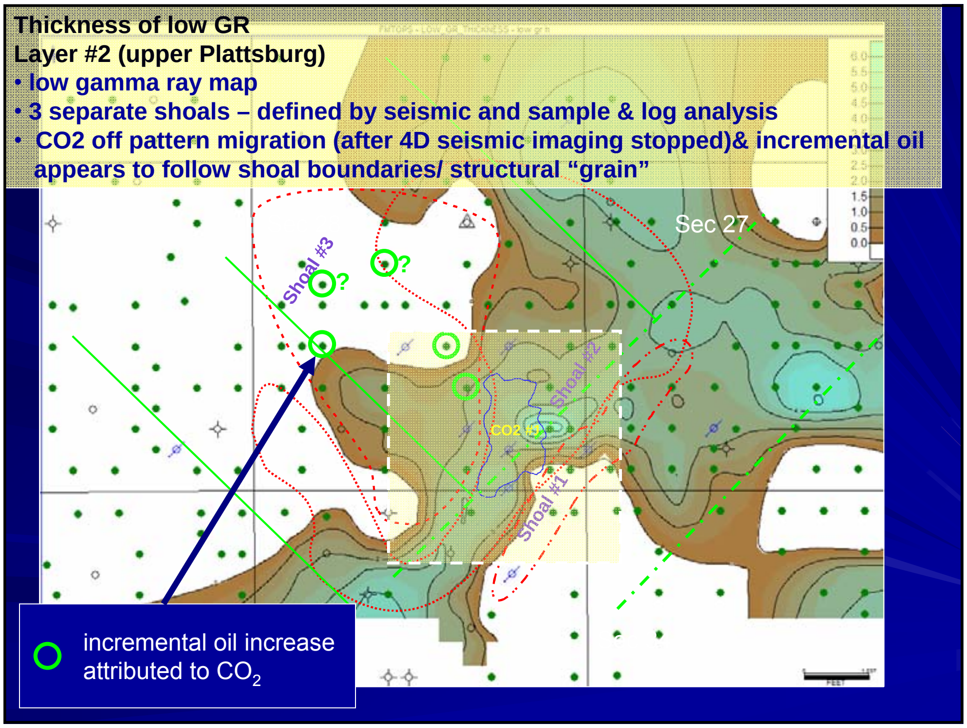
Thickness of low GR
Layer #2 (upper Plattsburg)
• low gamma ray map
• 3 separate shoals – defined by seismic and sample & log analysis
• CO2 off pattern migration (after 4D seismic imaging stopped)& incremental oil appears to follow shoal boundaries/ structural "grain"
Sec 27
Shoal #3
Shoal #2
Shoal #1
CO2 #1
incremental oil increase attributed to CO_2

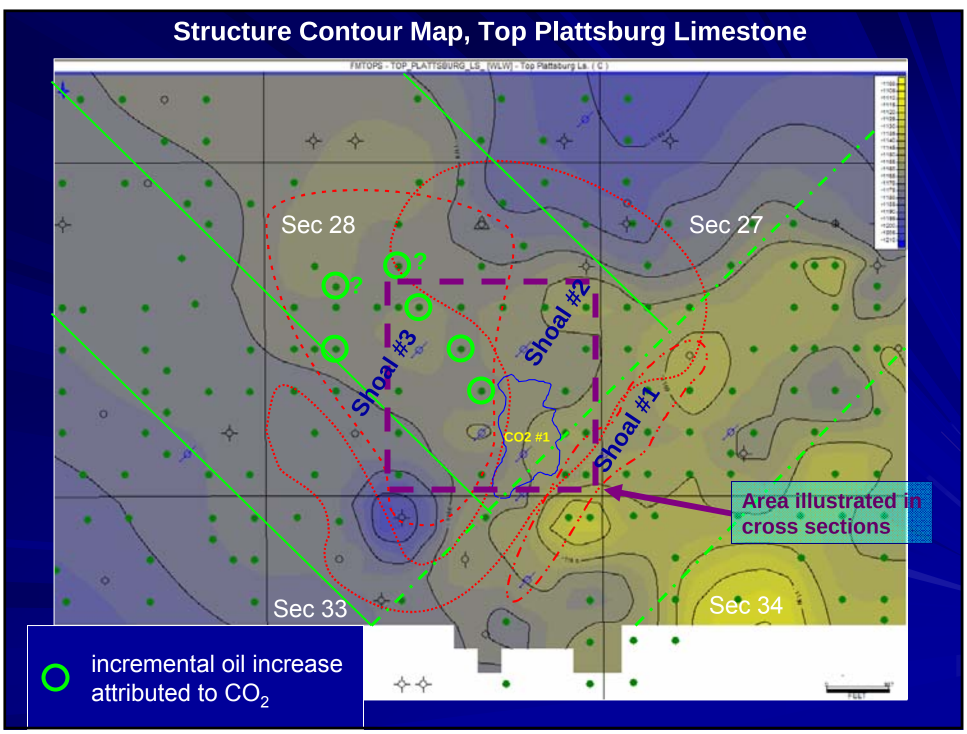
Structure Contour Map, Top Plattsburg Limestone
Sec 28
Sec 27
Sec 33
Sec 34
Shoal #3
Shoal #2
Shoal #1
CO2 #1
Area illustrated in cross sections
incremental oil increase attributed to CO_2

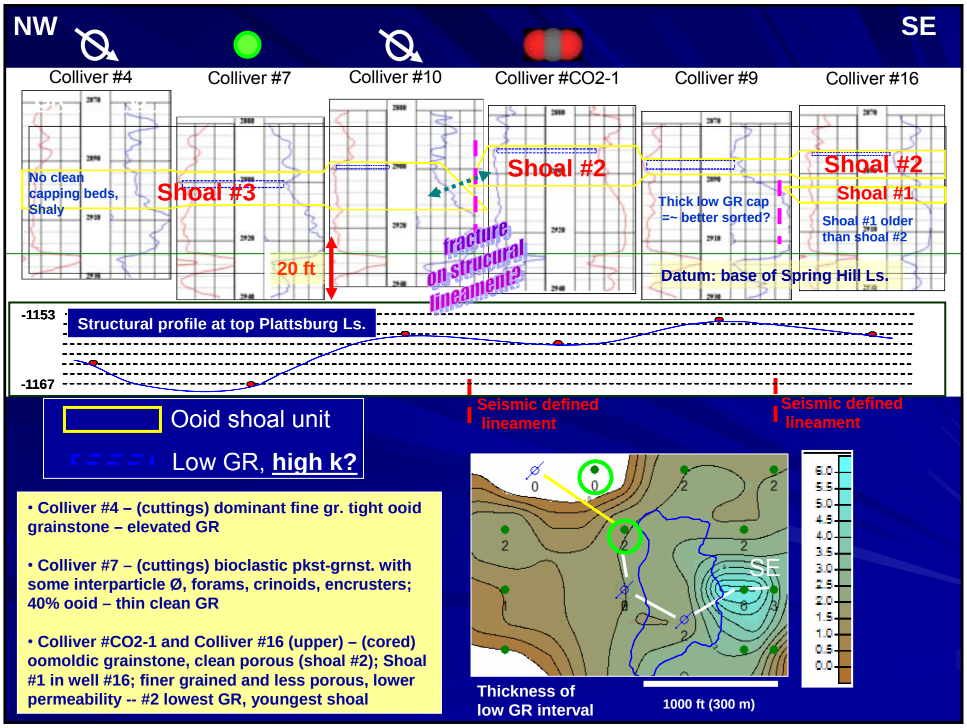
NW
SE
Colliver #4
Colliver #7
Colliver #10
Colliver #CO2-1
Colliver #9
Colliver #16
No clean capping beds, Shaly
Shoal #3
Shoal #2
Shoal #2
Shoal #1
Thick low GR cap =~ better sorted?
Shoal #1 older than shoal #2
fracture on strucural lineament?
20 ft
Datum: base of Spring Hill Ls.
-1153
-1167
Structural profile at top Plattsburg Ls.
Seismic defined lineament
Seismic defined lineament
Ooid shoal unit
Low GR, high k?
• Colliver #4 – (cuttings) dominant fine gr. tight ooid grainstone – elevated GR
• Colliver #7 – (cuttings) bioclastic pkst-grnst. with some interparticle Ø, forams, crinoids, encrusters; 40% ooid – thin clean GR
• Colliver #CO2-1 and Colliver #16 (upper) – (cored) oomoldic grainstone, clean porous (shoal #2); Shoal #1 in well #16; finer grained and less porous, lower permeability -- #2 lowest GR, youngest shoal
SE
Thickness of low GR interval
1000 ft (300 m)

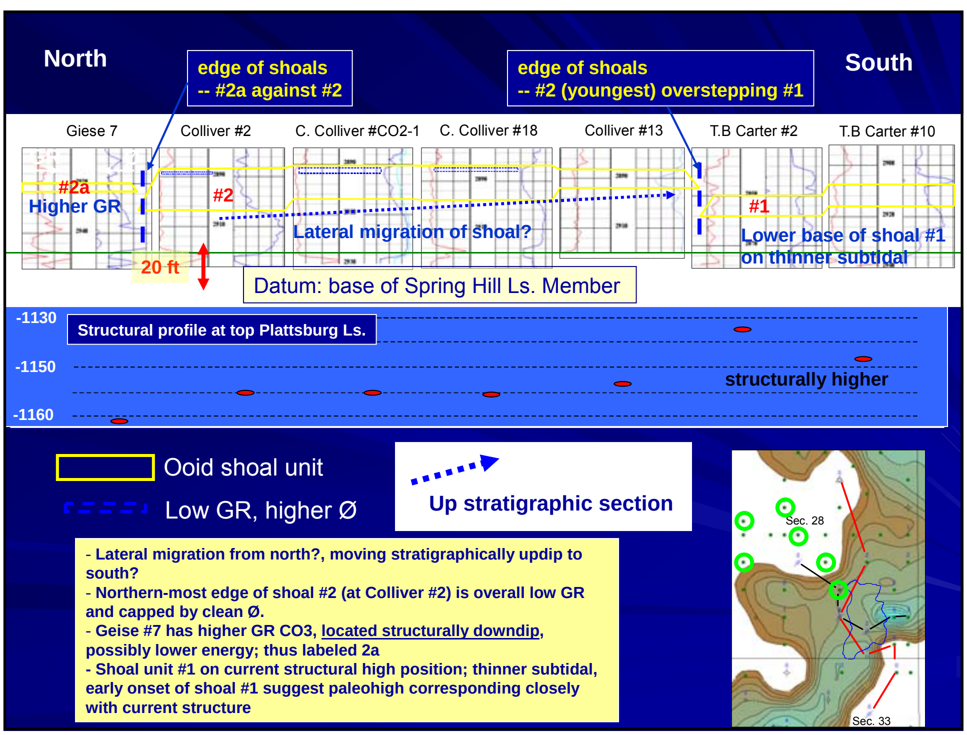
North
edge of shoals -- #2a against #2
edge of shoals -- #2 (youngest) overstepping #1
South
Giese 7
Colliver #2
C. Colliver #CO2-1
C. Colliver #18
Colliver #13
T.B Carter #2
T.B Carter #10
#2a
Higher GR
#2
Lateral migration of shoal?
#1
Lower base of shoal #1 on thinner subtidal
20 ft
Datum: base of Spring Hill Ls. Member
-1130
-1150
-1160
Structural profile at top Plattsburg Ls.
structurally higher
Ooid shoal unit
Low GR, higher Ø
Up stratigraphic section
- Lateral migration from north?, moving stratigraphically updip to south?
- Northern-most edge of shoal #2 (at Colliver #2) is overall low GR and capped by clean Ø.
- Geise #7 has higher GR CO3, located structurally downdip, possibly lower energy; thus labeled 2a
- Shoal unit #1 on current structural high position; thinner subtidal, early onset of shoal #1 suggest paleohigh corresponding closely with current structure
Sec. 28
Sec. 33

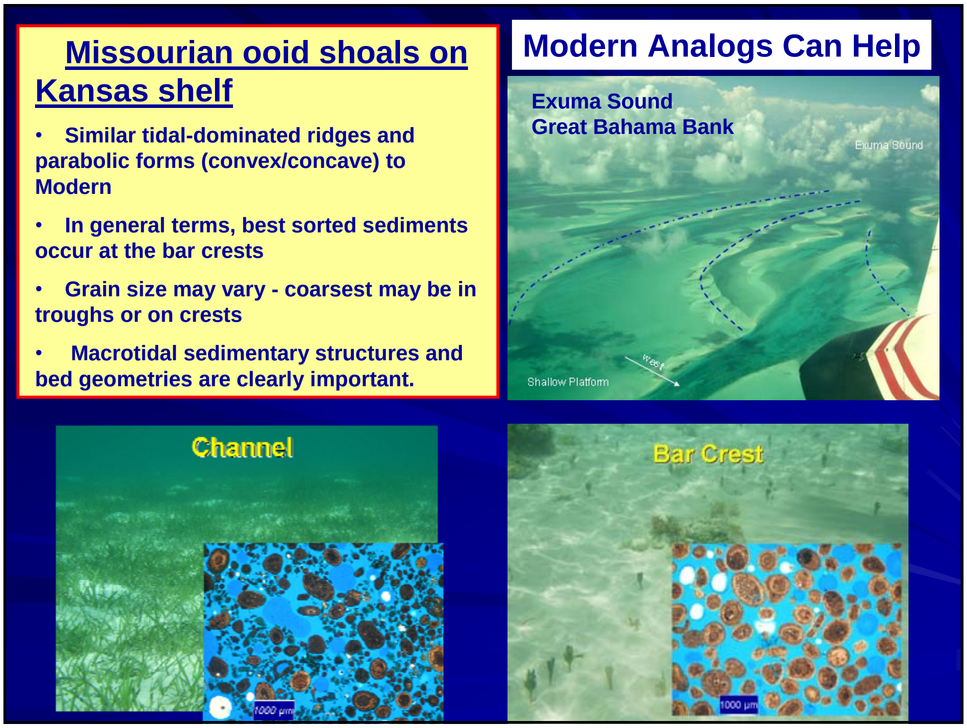

Missourian ooid shoals on Kansas shelf
• Similar tidal-dominated ridges and parabolic forms (convex/concave) to Modern
• In general terms, best sorted sediments occur at the bar crests
• Grain size may vary - coarsest may be in troughs or on crests
• Macrotidal sedimentary structures and bed geometries are clearly important.
Modern Analogs Can Help
Exuma Sound
Great Bahama Bank
Exuma Sound
Shallow Platform
west
Channel
Bar Crest
1000 μm
1000 μm

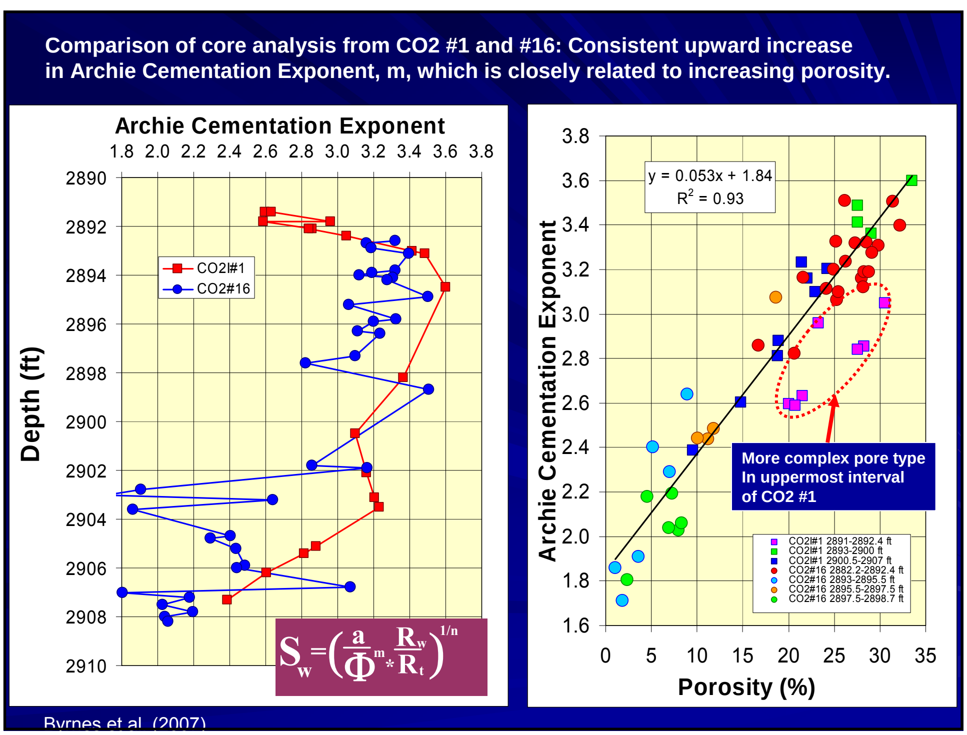

Comparison of core analysis from CO2 #1 and #16: Consistent upward increase in Archie Cementation Exponent, m, which is closely related to increasing porosity.
Archie Cementation Exponent
1.8 2.0 2.2 2.4 2.6 2.8 3.0 3.2 3.4 3.6 3.8
Depth (ft)
2890 2892 2894 2896 2898 2900 2902 2904 2906 2908 2910
CO2I#1
CO2#16
$S_w = \left(\frac{a}{\Phi^m} * \frac{R_w}{R_t}\right)^{1/n}$
y = 0.053x + 1.84
R^2 = 0.93
Archie Cementation Exponent
3.8 3.6 3.4 3.2 3.0 2.8 2.6 2.4 2.2 2.0 1.8 1.6
0 5 10 15 20 25 30 35
Porosity (%)
More complex pore type In uppermost interval of CO2 #1
CO2I#1 2891-2892.4 ft
CO2I#1 2893-2900 ft
CO2I#1 2900.5-2907 ft
CO2#16 2882.2-2892.4 ft
CO2#16 2893-2895.5 ft
CO2#16 2895.5-2897.5 ft
CO2#16 2897.5-2898.7 ft
Byrnes et al. (2007)

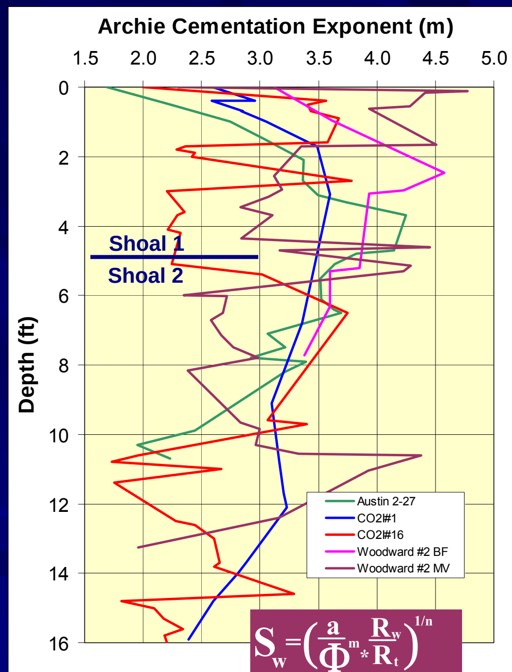

$$S_w = \left(\frac{a}{\Phi^m} * \frac{R_w}{R_t}\right)^{1/n}$$

Byrnes et al. (2007)

Archie Cementation Exponent, m

$m \neq 2$

$1.8 < m < 5$

m varies with depth mirroring k

- Note CO2#16 stacked shoals – m pattern starts from top of each shoal
- Similar pattern for Woodward #2 Mound Valley & Bethany Falls (near-surface analog in SE Kansas)

LKC Pc-Sw is sensitive to height & permeability

krow is sensitive to permeability & Soi

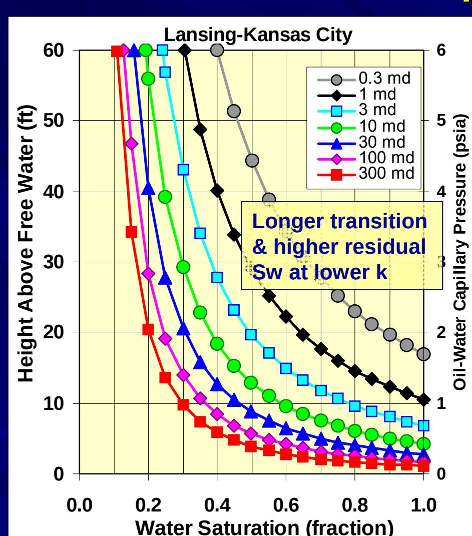

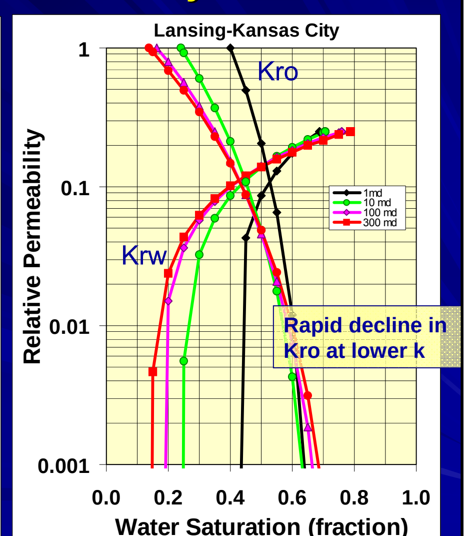

(after Byrnes & Bhattacharya, 2006; SPE 99736)

m vs ϕ

- $m = f(\phi, A_{pore})$
- $m = f(\phi, k)$
- $m = (-0.019 \log_{10} k + 0.085)\phi + 1.5$

Model for estimating m in oomoldic petrofacies knowing k and phi

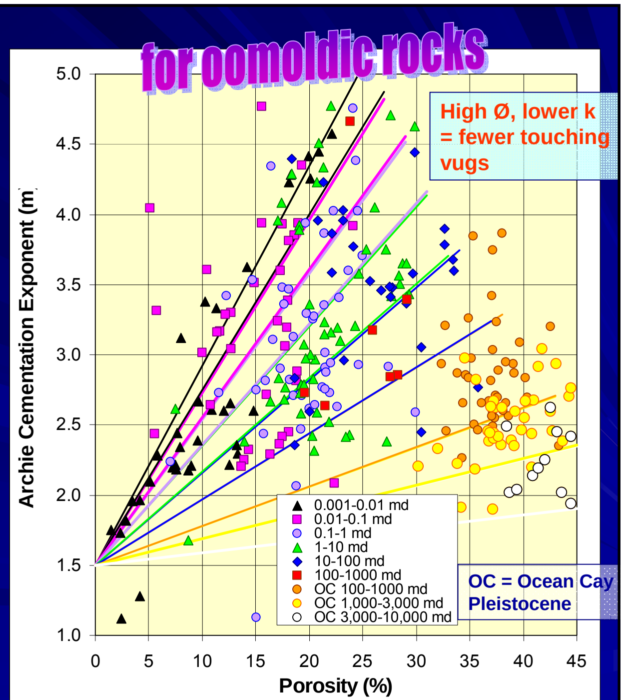

Byrnes et al. (2007)

Take home points for Hall-Gurney CO2 project

- Revised geologic model for "C" zone to incorporate
  - Remap effective flow units by delineation of low gamma ray, high porosity intervals
  - Incorporate directional permeability in northwesterly trend in shoal #3 overlying structural saddle/flexure to incorporate preferred direction for open fractures
  - Open fractures in NW-trend consistent with seismic coherency analysis compared to production in nearby field
- CO_2 IOR in West Texas/New Mexico San Andres indicates that fracture networks are also very important and vuggy porosity can be very discontinuous

Petrophysics Overview

Solving for water saturation ... the Archie equation

$$S_w = \left(\frac{a}{\Phi^m} * \frac{R_w}{R_t}\right)^{1/n}$$

READING THE ROCKS FROM WIRELINE LOGS

John Doveton
Kansas Geological Survey
1930 Constant Avenue
Lawrence, KS 66047
Phone: 785-864-2100
Email: doveton@kgs.ku.edu

m in sandstones

Archie (1942) observed the range in value of *m* in sandstones:

1.3	unconsolidated sandstones
1.4 - 1.5	very slightly cemented
1.6 - 1.7	slightly cemented
1.8 - 1.9	moderately cemented
2.0 - 2.2	highly cemented

m in carbonates

- **Interparticle**: intergranular and intercrystalline porosity

  m=2

- **Fracture** porosity

  m<2

- **Vug**: moldic porosity or vugs that are larger than the grains

  m>2<5

Prediction of fluid PRODUCTION from BVW = *Sw x Ø*

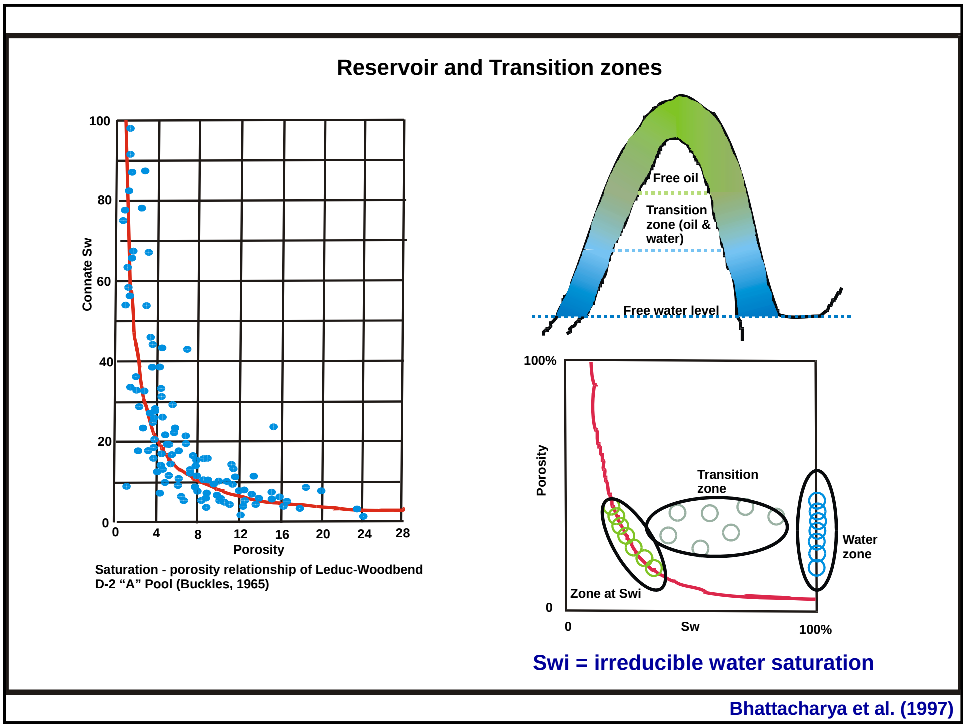
Reservoir and Transition zones
Connate Sw
Porosity
Saturation - porosity relationship of Leduc-Woodbend D-2 "A" Pool (Buckles, 1965)
Free oil
Transition zone (oil & water)
Free water level
Porosity
Transition zone
Water zone
Zone at Swi
Sw
Swi = irreducible water saturation
Bhattacharya et al. (1997)

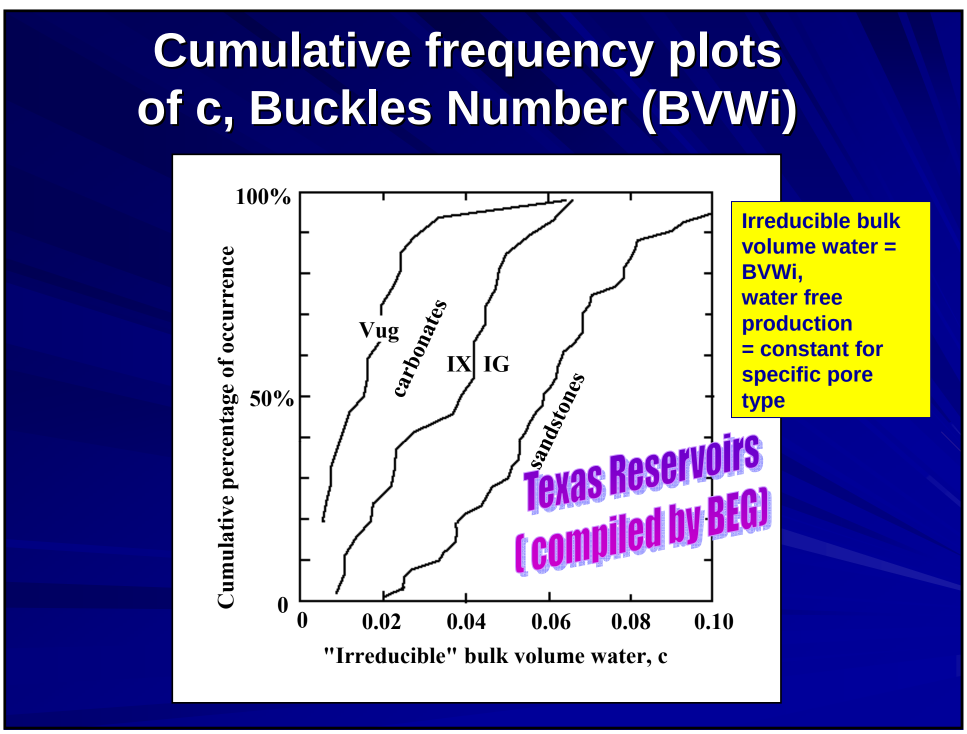
Cumulative frequency plots of c, Buckles Number (BVWi)
Cumulative percentage of occurrence
"Irreducible" bulk volume water, c
Vug
carbonates
IX
IG
sandstones
Irreducible bulk volume water = BVWi, water free production = constant for specific pore type
Texas Reservoirs (compiled by BEG)

Texas carbonate reservoir data by formation

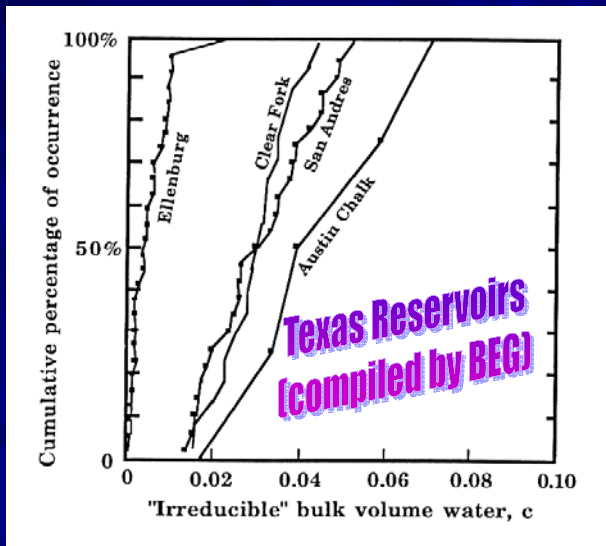

The Pickett Plot

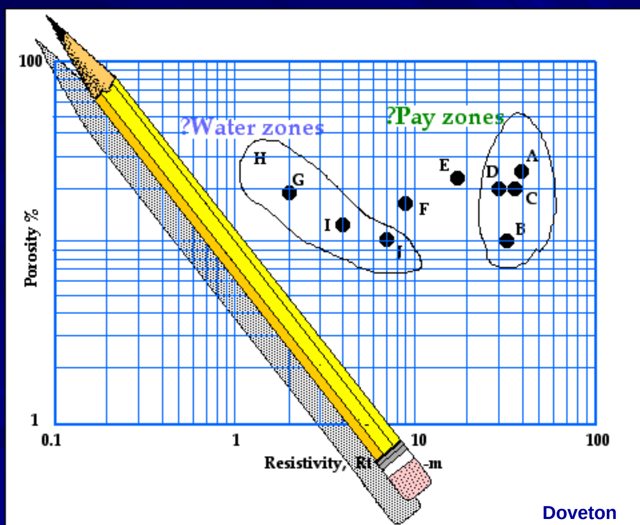

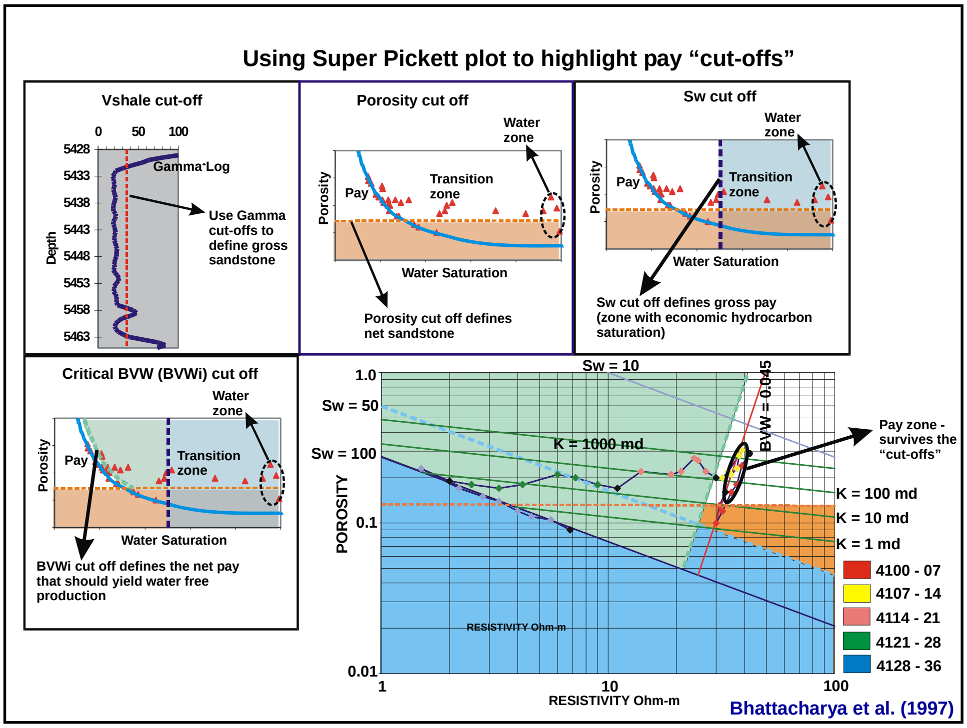

Using Super Pickett plot to highlight pay "cut-offs"
Vshale cut-off
Gamma Log
Use Gamma cut-offs to define gross sandstone
Depth
Porosity cut off
Water zone
Transition zone
Pay
Water Saturation
Porosity cut off defines net sandstone
Sw cut off
Sw cut off defines gross pay (zone with economic hydrocarbon saturation)
Critical BVW (BVWi) cut off
BVWi cut off defines the net pay that should yield water free production
Sw = 10
Sw = 50
Sw = 100
BVW = 0.045
K = 1000 md
Pay zone - survives the "cut-offs"
K = 100 md
K = 10 md
K = 1 md
4100 - 07
4107 - 14
4114 - 21
4121 - 28
4128 - 36
POROSITY
RESISTIVITY Ohm-m
Bhattacharya et al. (1997)

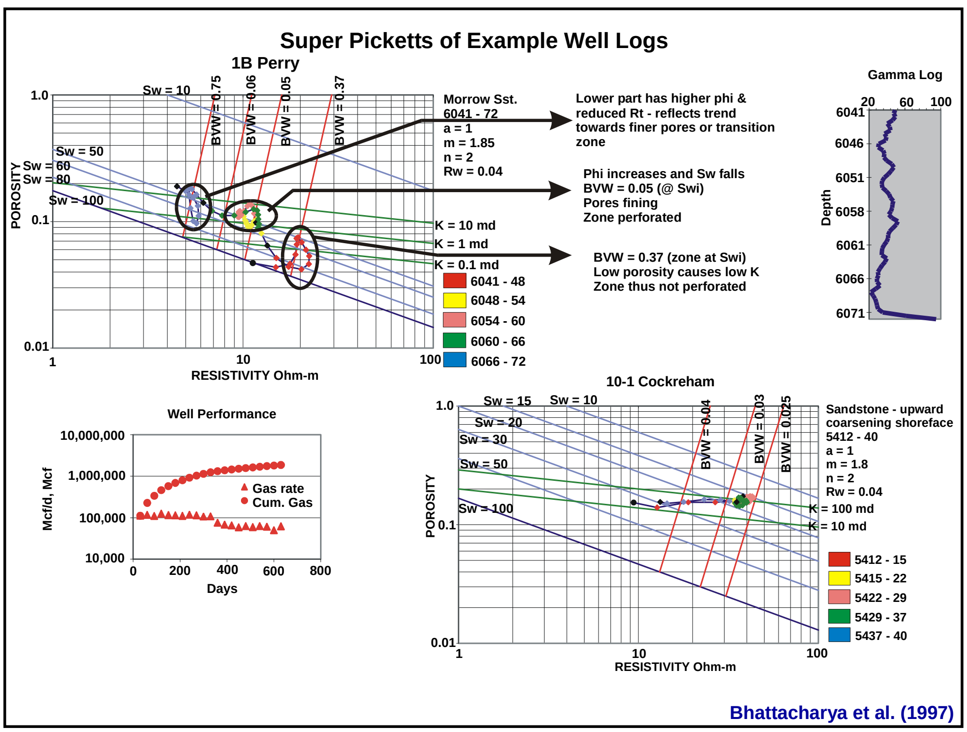

Super Picketts of Example Well Logs
1B Perry
Morrow Sst.
6041 - 72
a = 1
m = 1.85
n = 2
Rw = 0.04
Lower part has higher phi & reduced Rt - reflects trend towards finer pores or transition zone
Phi increases and Sw falls
BVW = 0.05 (@ Swi)
Pores fining
Zone perforated
BVW = 0.37 (zone at Swi)
Low porosity causes low K
Zone thus not perforated
K = 10 md
K = 1 md
K = 0.1 md
6041 - 48
6048 - 54
6054 - 60
6060 - 66
6066 - 72
Gamma Log
Depth
RESISTIVITY Ohm-m
POROSITY
Well Performance
Gas rate
Cum. Gas
Mcf/d, Mcf
Days
10-1 Cockreham
Sandstone - upward coarsening shoreface
5412 - 40
a = 1
m = 1.8
n = 2
Rw = 0.04
K = 100 md
K = 10 md
5412 - 15
5415 - 22
5422 - 29
5429 - 37
5437 - 40
Bhattacharya et al. (1997)

Common Signatures on Super Pickett plot

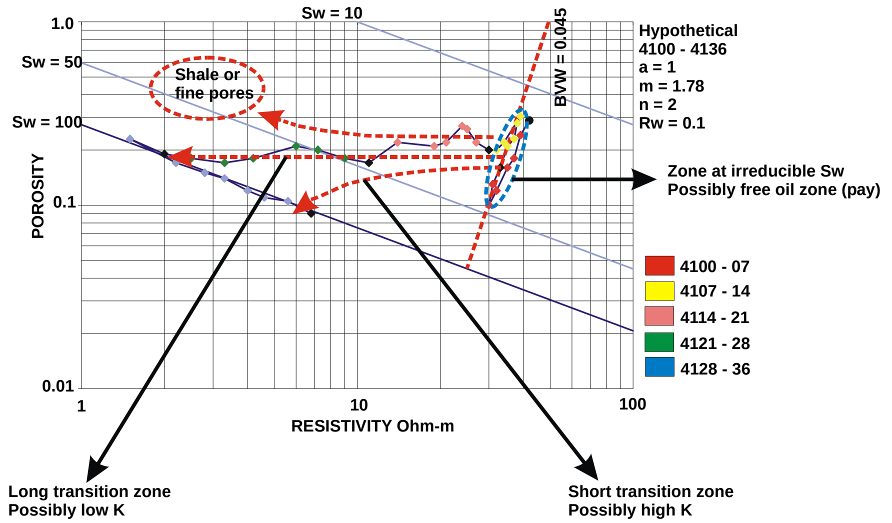

Inferences from Super Pickett signatures:

Low BVW at low phi - zone may be at Swi but low phi may result low K
Cluster of points hanging around a BVW line - zone at Swi
Phi increasing with decrease in resistivity - finer pores or transition
Constant Phi with decreasing resistivity and increasing Sw - transition zone

Bhattacharya et al. (1997)

From Geomodels to Engineering Models – Opportunities for Spreadsheet Computing

Saibal Bhattacharya, W. Lynn Watney, Willard J. Guy, John H. Doveton, Geoff Bohling, and Paul M. Gerlach

Kansas Geological Survey
1930 Constant Avenue – Campus West
Lawrence, Kansas 66047

1999 GCSSEPM Foundation Research Conference –
Advanced Reservoir Characterization for the Twenty-First Century

OOIP calculations for estimating waterflood potential in Pennsylvanian oomoldic reservoir

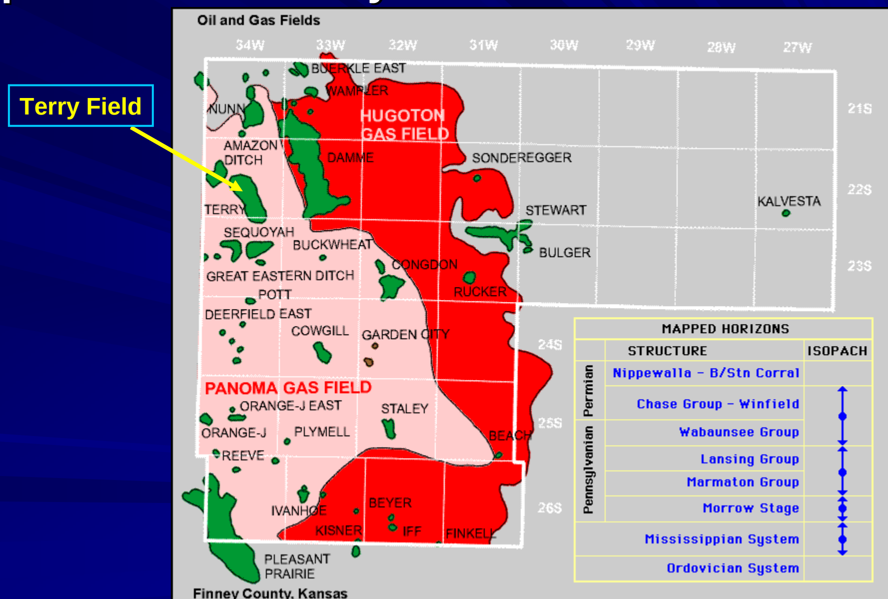

OOIP calculations for estimating waterflood potential in Pennsylvanian oomoldic reservoir

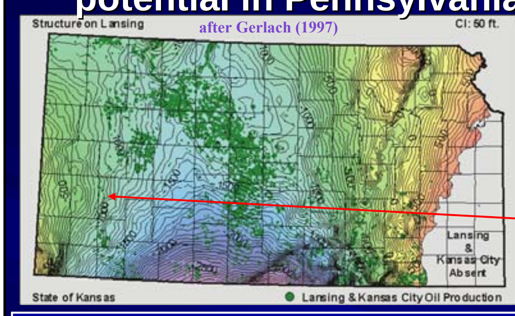

Target:
- Complex stacked carbonate oil reservoirs
- Field scale

Data:
- Core, DST, well logs, perfs & IP, production history
  Oil properties

Tools:
Rock catalog, production & DST analyst, PVT,
log analysis, well profile (marked log), cross section,
mapping-volumetric analysis,
KHAN (Kansas Hydrocarbon Association Navigator)

Terry Field, Finney County

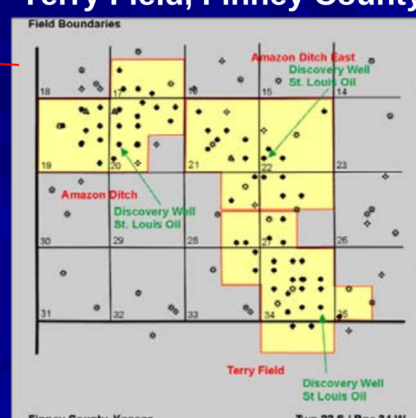

Maps from the Digital Petroleum Atlas

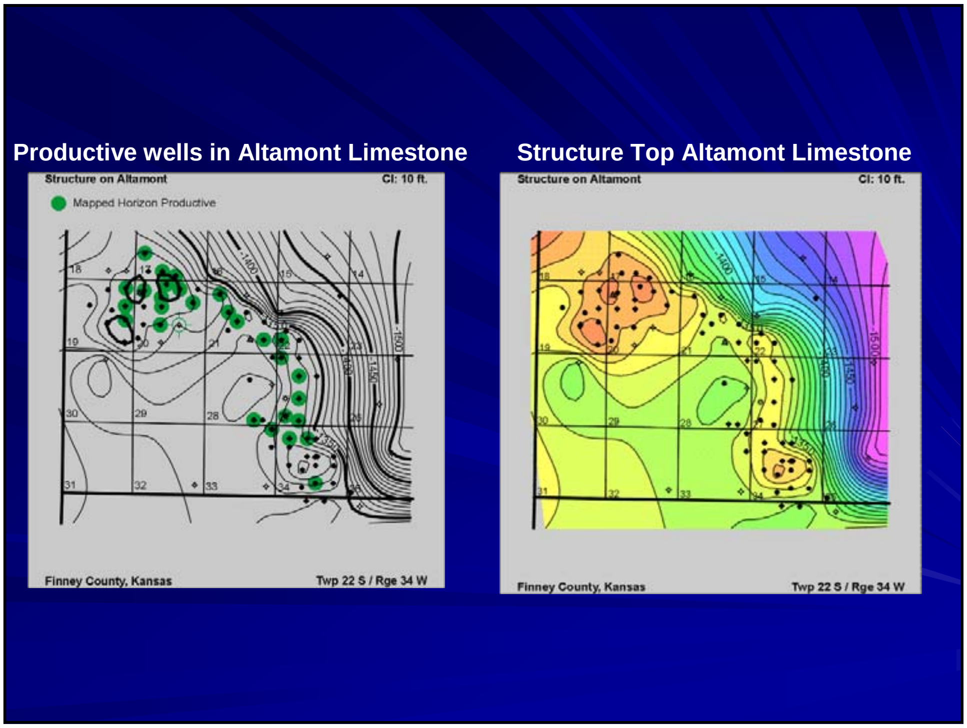
Productive wells in Altamont Limestone
Structure Top Altamont Limestone
Structure on Altamont
CI: 10 ft.
Mapped Horizon Productive
Finney County, Kansas
Twp 22 S / Rge 34 W
Structure on Altamont
CI: 10 ft.
Finney County, Kansas
Twp 22 S / Rge 34 W

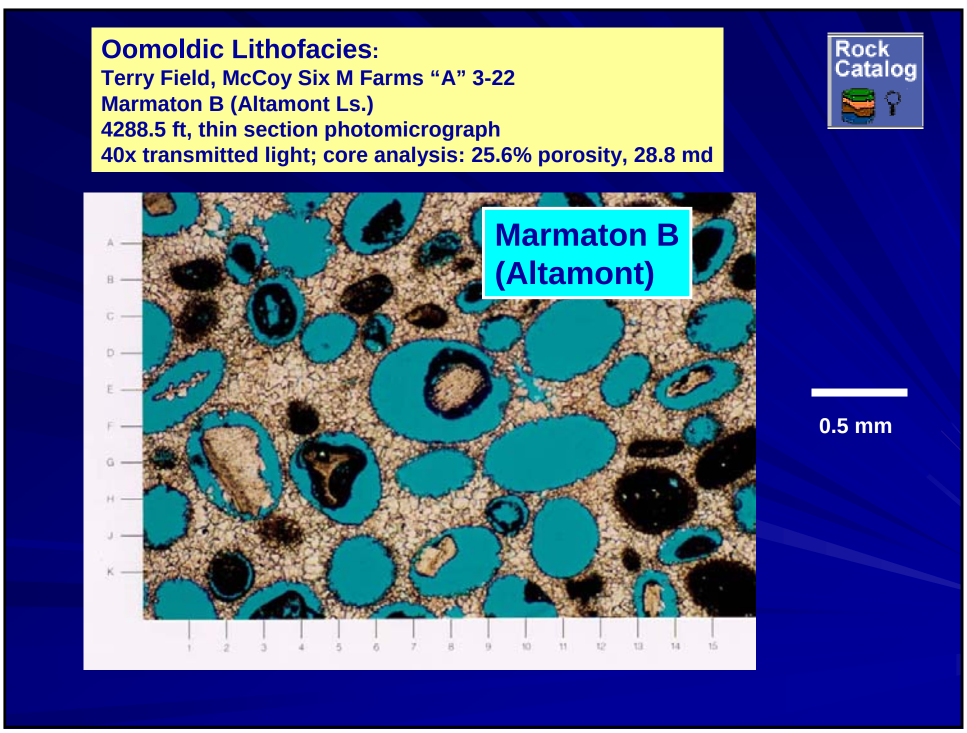
Oomoldic Lithofacies:
Terry Field, McCoy Six M Farms "A" 3-22
Marmaton B (Altamont Ls.)
4288.5 ft, thin section photomicrograph
40x transmitted light; core analysis: 25.6% porosity, 28.8 md
Rock Catalog
Marmaton B (Altamont)
0.5 mm

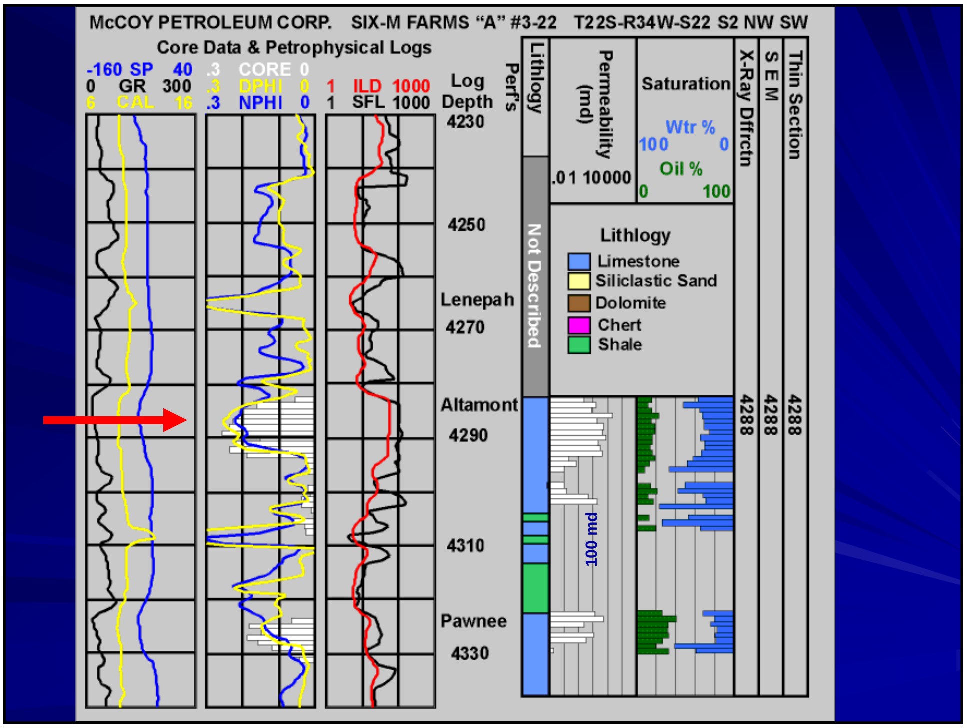

NW-SE Petrophysical Cross Section through Altamont Limestone in Terry Field

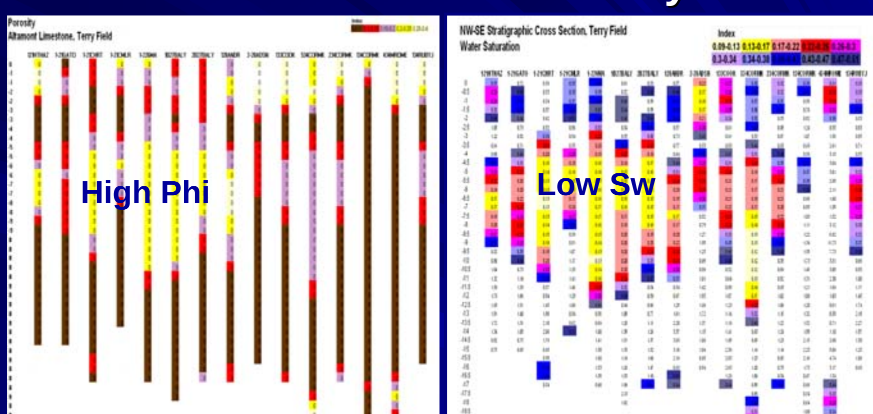

Datum: Top Altamont

- Sweet spots of reservoir (high phi, low Sw, low BVW) likely more permeable, well drained areas
- Waterflood effectiveness include ways to access oil in marginal areas of reservoir.

Petrophysics of the oomoldic Altamont limestone

Archie Cementation Exponent

Oomoldic limestones from Kansas and globally exhibit extremely high Archie cementation exponents. This is consistent with the interpretation that the oomoldic pores are similar to micro-vugs. Modified Archie parameters for the Carter-Colliver Lease rocks are: **m=1.36, a=9.59.** Conversely, if m is considered to change with porosity then m can be predicted for the higher porosity rocks using: **m = 0.05*Porosity(%) + 1.9.** Cementation exponents are near 2.0 in the bioclastic wackestone overlying the 'C' zone. Cementation exponents increase into the top of the 'C' and then decrease with increasing depth to the base. This is associated with the higher porosity at the top of the 'C' zone but is also influenced by pore structure changes associated with the unconformity surface.

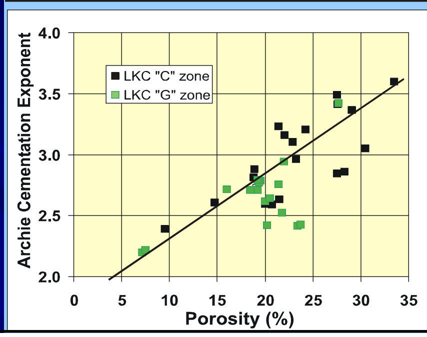

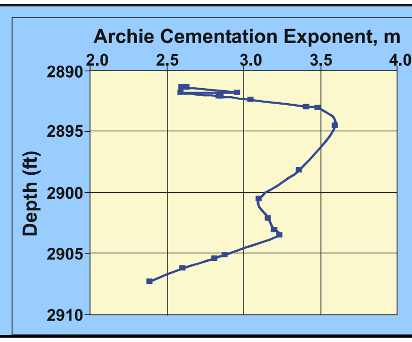

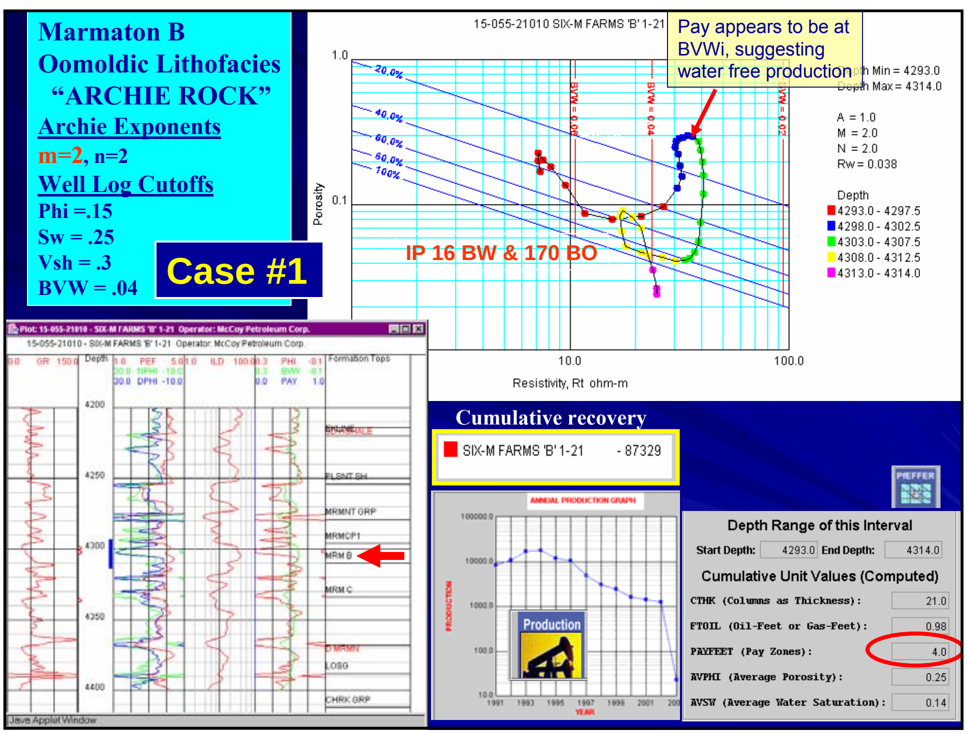

Marmaton B

Case #2

Log calibration as defined by core analysis of highly oomoldic LKC limestones from CKU

Archie Exponents
m=3.5, n=2

Well Log Cutoffs
Phi =.17
Sw = .55
Vsh = .3
BVW = .097

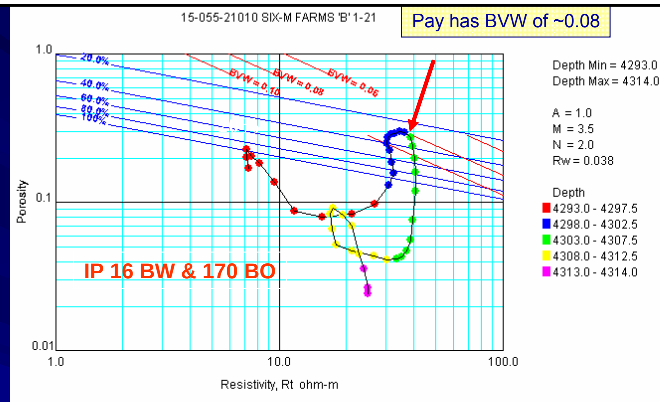

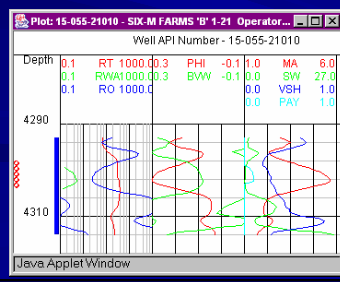

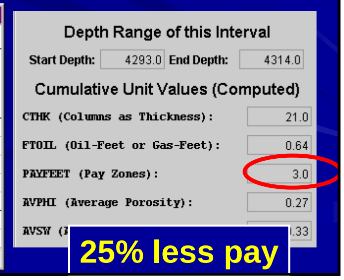

Volumetrics

Marmaton B
Terry Field
Finney County, Kansas

Oomoldic Reservoir

Compare impact of two sets of cutoffs

Case #1	Case #2
Marmaton B Initial log cutoffs	Marmaton B Log calibration utilizing core analysis of highly oomoldic LKC limestones from CKU
Archie Exponents m=2, n=2	Archie Exponents m=3.5, n=2
Well Log Cutoffs Phi =.15 Sw = .25 Vsh = .3 BVW = .04	Well Log Cutoffs Phi =.17 Sw = .55 Vsh = .3 BVW = .097

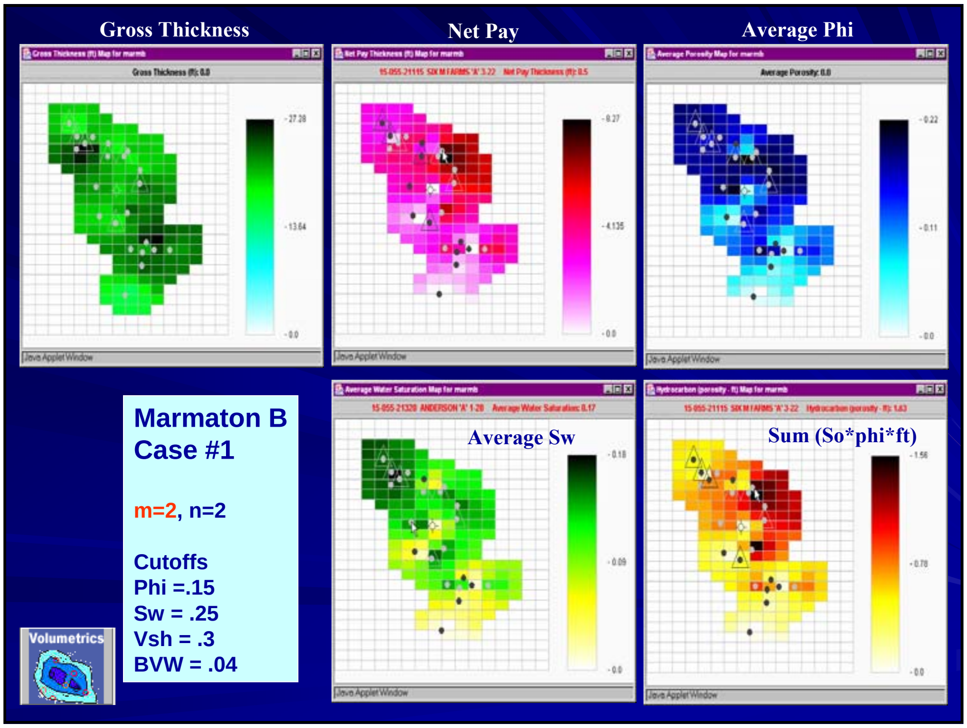
Gross Thickness
Net Pay
Average Phi
Marmaton B
Case #1
m=2, n=2
Cutoffs
Phi =.15
Sw = .25
Vsh = .3
BVW = .04
Volumetrics
Average Sw
Sum (So*phi*ft)

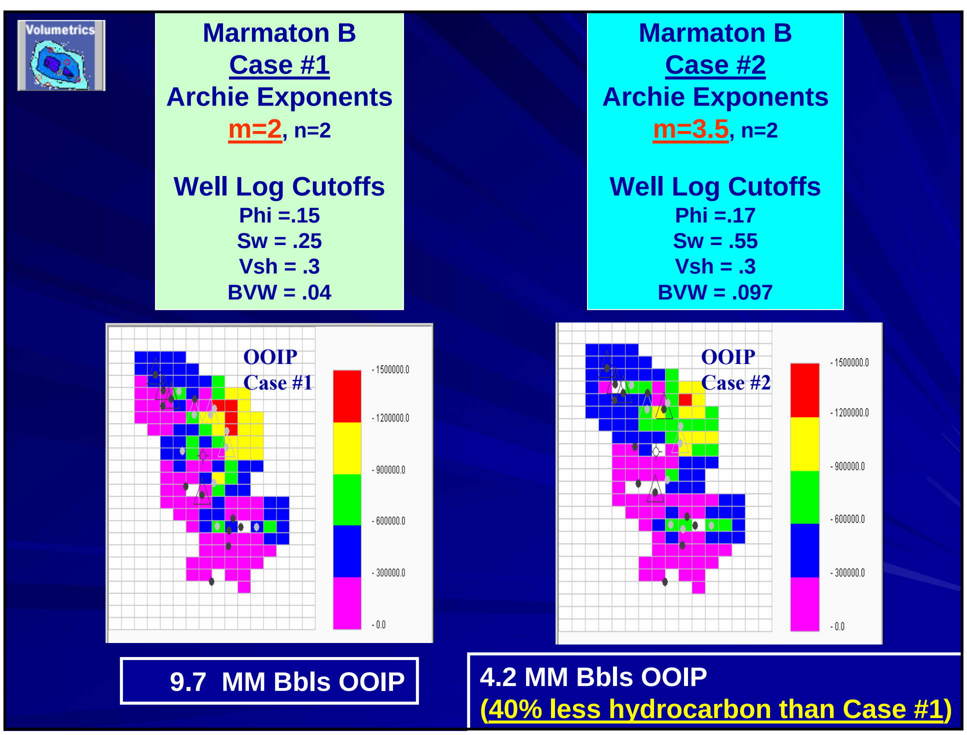
Volumetrics
Marmaton B
Case #1
Archie Exponents
m=2, n=2
Well Log Cutoffs
Phi =.15
Sw = .25
Vsh = .3
BVW = .04
Marmaton B
Case #2
Archie Exponents
m=3.5, n=2
Well Log Cutoffs
Phi =.17
Sw = .55
Vsh = .3
BVW = .097
OOIP
Case #1
OOIP
Case #2
9.7 MM Bbls OOIP
4.2 MM Bbls OOIP
(40% less hydrocarbon than Case #1)

Pennsylvanian

- Lobate and linear oolitic shoals form complex geometries
- Granulometric attributes of Modern and ancient ooid shoals are comparable
- Oomoldic porosity is pervasive
- Size, sorting, packing of Pennsylvanian and Pleistocene oomolds are closely related
- Archie cementation exponent, m, is critical measurement affecting Sw calculations and OOIP.
- Relative permeability to oil of lower perm oomoldic rocks is generally defined by steep decline with increasing Sw

Pleistocene, Ocean Cay
w/ alz-r stain

Pennsylvanian, Bethany Falls Ls.
unstained

Conclusions

- **Geometries, scales, and facies distributions of Pennsylvanian oolite shoals suggest analogs to Modern, tidally influenced ooid tidal ridges and parabolic bars.**
- **Accurate and precise characterization of connected (effective) oomoldic pores is critical in IOR modeling and prediction:**
  - *Better sorted, cleaner (low GR), highly porous (>17%) oomoldic grainstone appear to be more permeable;*
  - *In Plattsburg Limestone at Hall-Gurney Field, best sorting noted in upper portion of shallowing upward high frequency cycles and bedsets, probably delimiting separate ooid shoal development*
  - *Moldic porosity increases upward in shallowing bedsets and high frequency cycles*
- **Structural control of oolite reservoirs likely at various scales augmenting and possibly influencing depositional and diagenetic fabrics.**
- **Geophysicists, engineers, and geologists needed for model development and validation**

Conclusions

- In a oomoldic thin-bed reservoir standard log analysis is misleading
- Equations for k, Pc, kr, m presented provide improved prediction for oomoldic LKC
- Archie m is <u>not</u> 2, m = f(ϕ, k)
- Many/most LKC are thin-bed reservoirs
  - require advanced log analysis
- Even if you run DST accurate k, kr, Sw is needed for waterflood prediction
- Proposed log-analysis methodology should provide improved k and Sw prediction in LKC

Paper in progress

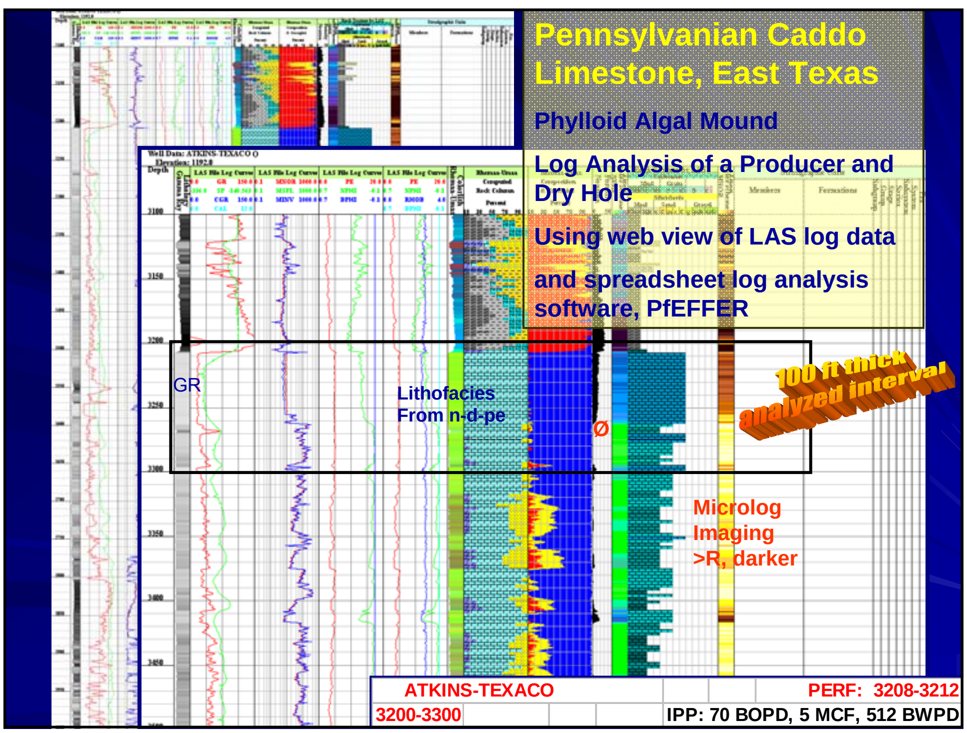

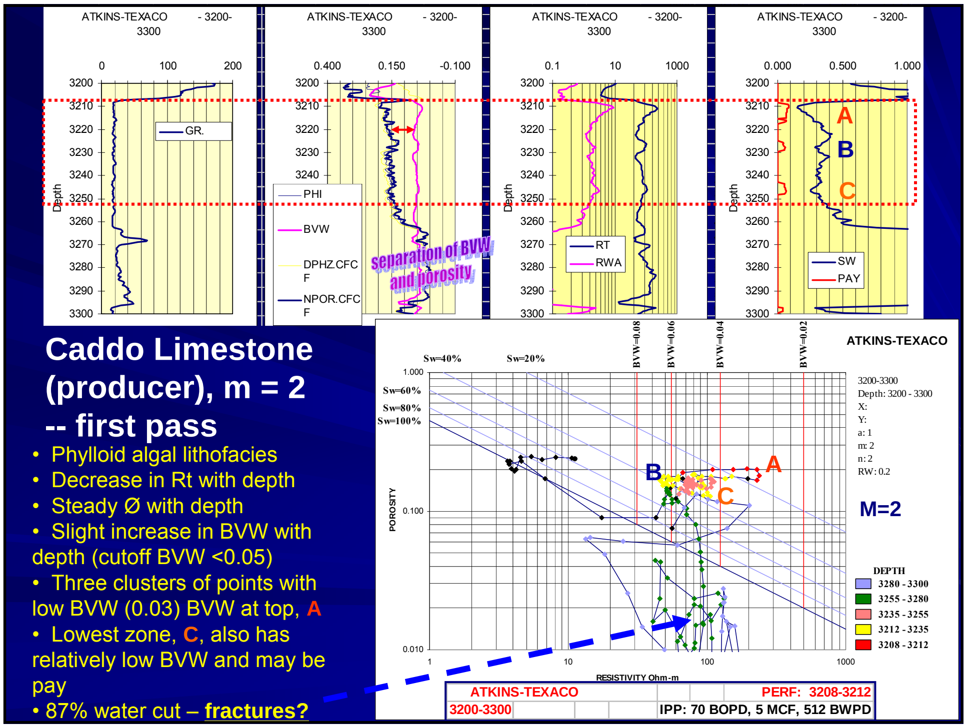
ATKINS-TEXACO - 3200-3300
GR.
PHI
BVW
DPHZ.CFC F
NPOR.CFC F
separation of BVW and porosity
RT
RWA
SW
PAY
A
B
C
Depth
Caddo Limestone (producer), m = 2 -- first pass
• Phylloid algal lithofacies
• Decrease in Rt with depth
• Steady Ø with depth
• Slight increase in BVW with depth (cutoff BVW <0.05)
• Three clusters of points with low BVW (0.03) BVW at top, A
• Lowest zone, C, also has relatively low BVW and may be pay
• 87% water cut – fractures?
ATKINS-TEXACO
Sw=40%
Sw=20%
Sw=60%
Sw=80%
Sw=100%
BVW=0.08
BVW=0.06
BVW=0.04
BVW=0.02
POROSITY
RESISTIVITY Ohm-m
3200-3300
Depth: 3200 - 3300
X:
Y:
a: 1
m: 2
n: 2
RW: 0.2
M=2
DEPTH
3280 - 3300
3255 - 3280
3235 - 3255
3212 - 3235
3208 - 3212
ATKINS-TEXACO
PERF: 3208-3212
3200-3300
IPP: 70 BOPD, 5 MCF, 512 BWPD

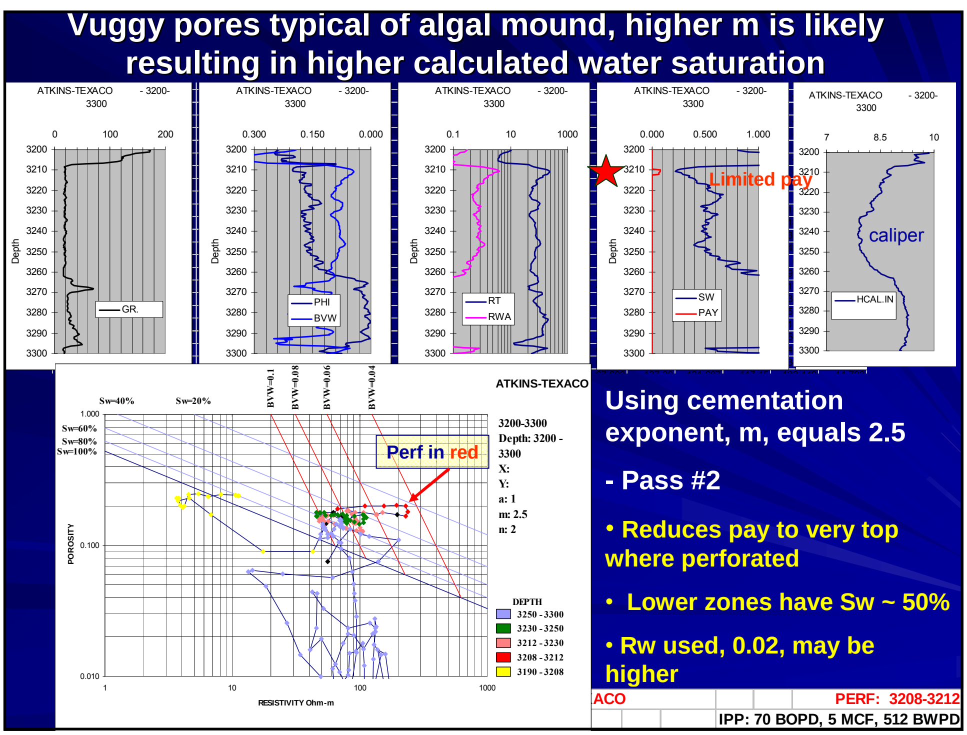
Vuggy pores typical of algal mound, higher m is likely resulting in higher calculated water saturation
ATKINS-TEXACO - 3200-3300
GR.
PHI
BVW
RT
RWA
SW
PAY
Limited pay
caliper
HCAL.IN
Depth
ATKINS-TEXACO
Sw=40%
Sw=20%
Sw=60%
Sw=80%
Sw=100%
BVW=0.1
BVW=0.08
BVW=0.06
BVW=0.04
Perf in red
3200-3300
Depth: 3200 - 3300
X:
Y:
a: 1
m: 2.5
n: 2
DEPTH
3250 - 3300
3230 - 3250
3212 - 3230
3208 - 3212
3190 - 3208
POROSITY
RESISTIVITY Ohm-m
Using cementation exponent, m, equals 2.5
- Pass #2
• Reduces pay to very top where perforated
• Lower zones have Sw ~ 50%
• Rw used, 0.02, may be higher
ACO
PERF: 3208-3212
IPP: 70 BOPD, 5 MCF, 512 BWPD

Pass #3 -- Adjusted Ro line to fit base of porosity using Rw now of 0.4 ohm-m, with m = 2.5

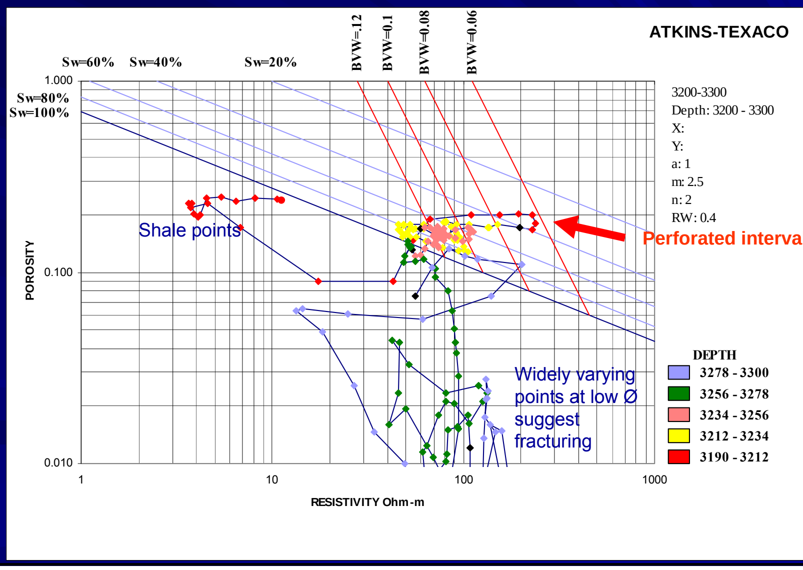

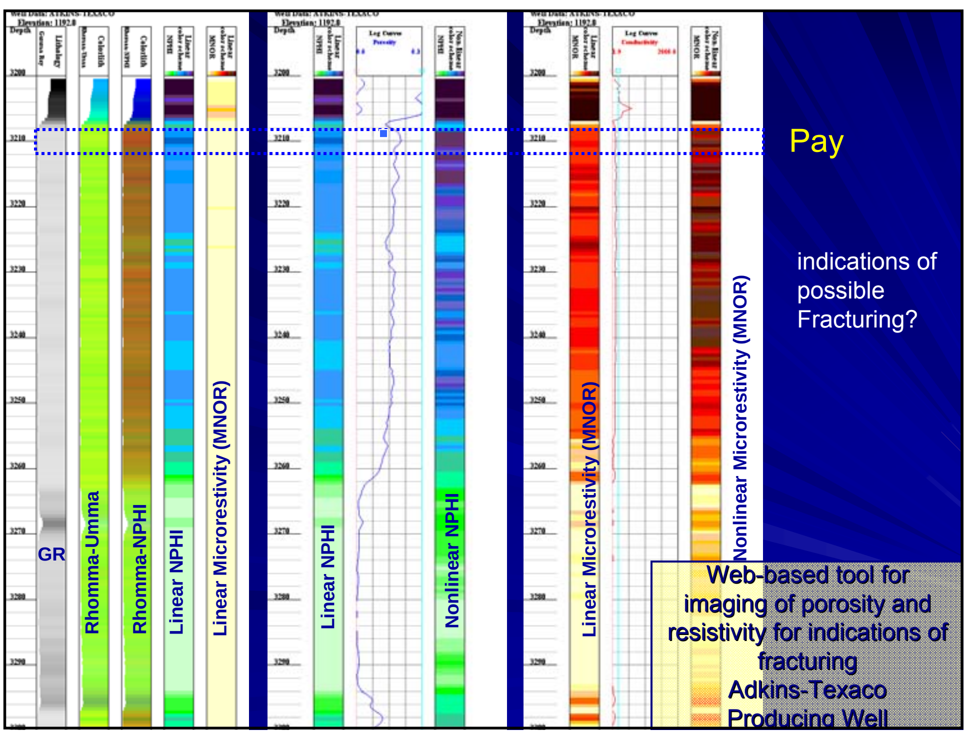

"Watfa-Nurmi chart"

$F = R_o/R_w$
$= a / Ø^m$

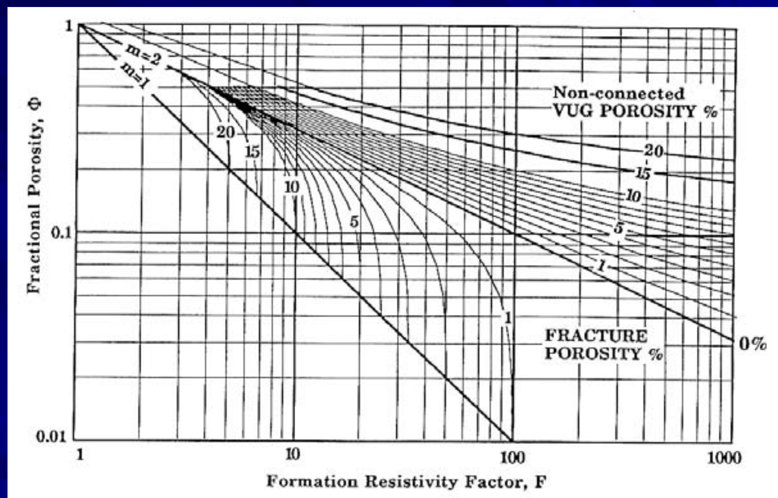

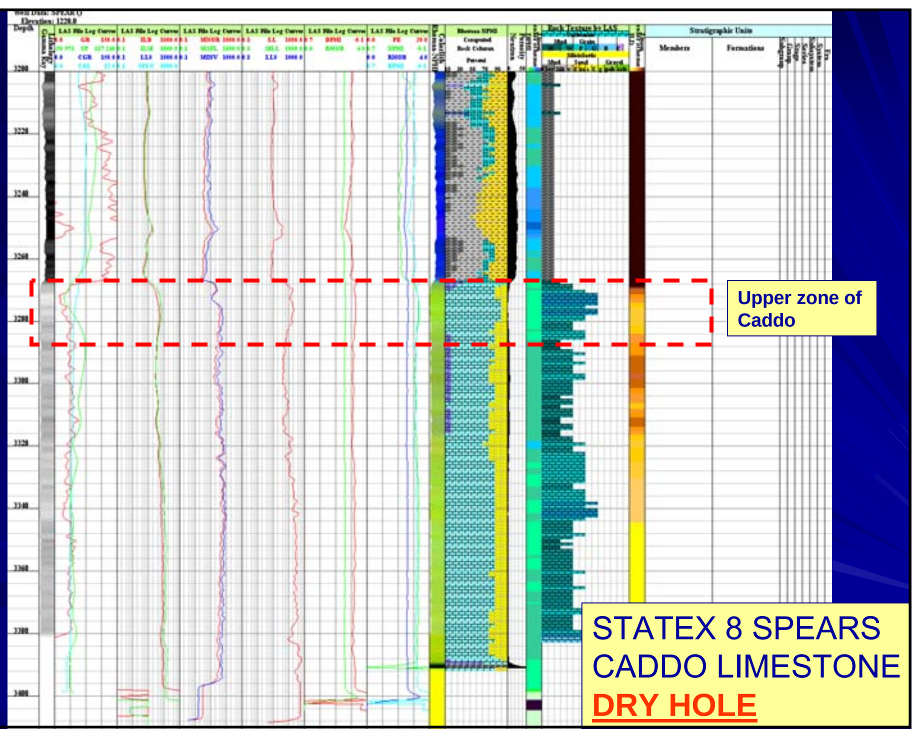

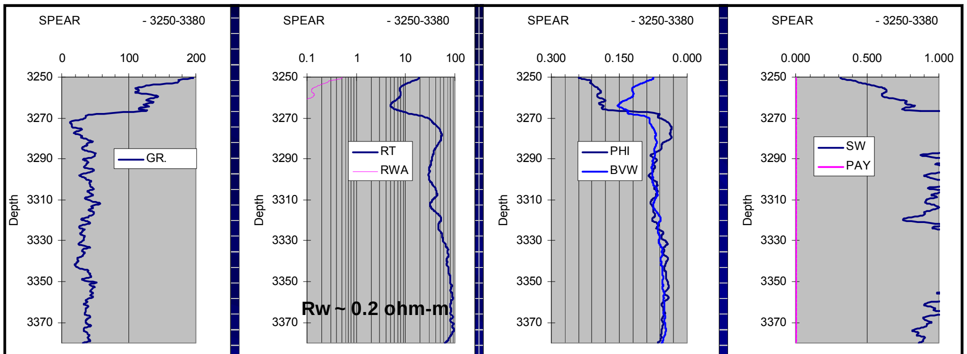

STATEX 8 SPEARS
CADDO LIMESTONE
DRY HOLE
-- Low porosity, tight
-- using m = 2.5, Rw = .05 ohm-m for best fit of points with Ro line

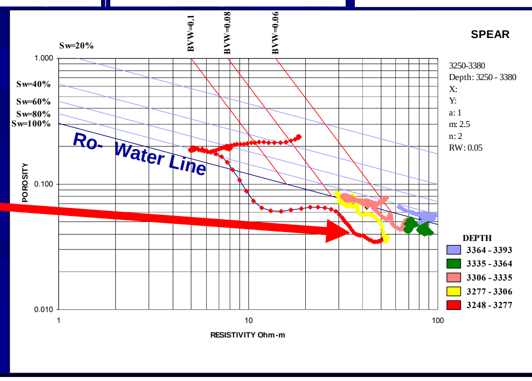

Petrophysical and Geophysical Characterization of Karst in a Permian San Andres Reservoir, Waddell Field, West Texas

by
Susan E. Nissen, John H. Doveton, and
W. Lynn Watney

presented at AAPG Annual Meeting
May 2008

Funded by the Department of Energy

Cooperative Agreement No.: DE-FC26-04NT15504

www.kgs.ku.edu/PRS/publication/2008/OFR08_5/

Acknowledgments

- Charlotte Sullivan, Chuck Blumentritt, Kurt Marfurt, and Qifeng Dou, for seismic attribute generation and geological insight
- Burlington Resources Oil & Gas Company and Schlumberger IPM, for providing seismic and well data
- Seismic Micro-Technology, Inc., for access to *The KINGDOM Suite+* seismic-interpretation software
- Hampson-Russell, for access to *STRATA* seismic inversion software
- IHS, for access to *PETRA* well-log correlation and mapping software
- The U. S. Department of Energy, for project funding under contract DE-FC26-04NT15504

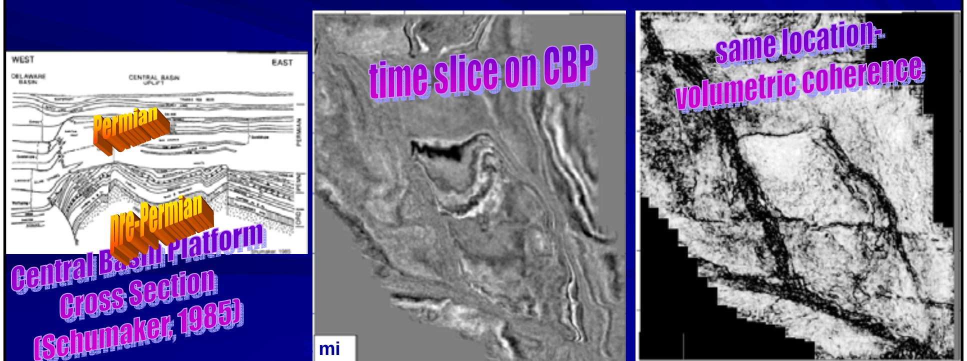

Blumentritt et al. (2003)

San Andres Reservoir on the Central Basin Platform

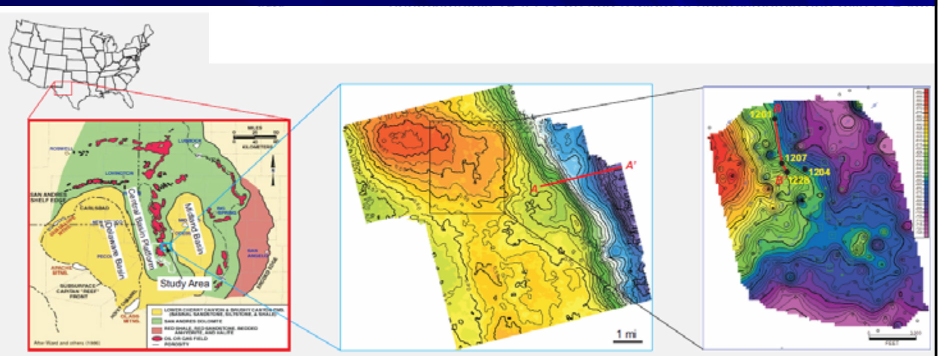

Simplified geological map of the San Andres Formation in the Permian Basin showing locations of major oil fields (Scholle, http://geoinfo.nmt.edu/staff/scholle/guadalupe.html; after Ward et al.,1986). Our study area is in Waddell Field, northern Crane County, TX, located on the east central flank of the Central Basin Platform.

A time structure map of the top of the Grayburg from a 3D seismic survey over Waddell Field shows the regional structural configuration. The black box highlights the "high volume area" study area.

Subsea depth map of the top of the San Andres Formation for the "high volume area" of Waddell Field.

Improving Geologic and Engineering Models of Midcontinent Fracture and Karst-Modified Reservoirs Using New 3-D Seismic Attributes
Kansas Geological Survey | Allied Geophysical Labs-University of Houston

Home | Project Info | Personnel | Attributes | Tech Transfer | Catalog

www.kgs.ku.edu/SEISKARST

Finding in Study

•. Karst impacts reservoir performance

• Highly compartmentalized reservoir and fluid production is extremely variable.

• Reservoir heterogeneity appears to be related to stratigraphy and diagenesis, as well as karst features associated with a subaerial exposure surface at the top of the San Andres Formation.

• Core data indicate that the uppermost San Andres consists of sporadically porous "macro" karst, characterized by intense chaotic brecciation and anhydrite replacement, followed by isolated, late stage anhydrite dissolution.

• The karst overprints high frequency sequences composed of gypsiferous oolitic, fusulinid, and skeletal packstone-grainstone reservoir rock with moldic, vug, and fracture porosity.

Nissen et al. (2008)

Findings (continued)

• Wireline log petrophysical solutions used to quantitatively discriminate anhydritic karst from the underlying packstone-grainstone strata in uncored wells.

• The base of the karst zone corresponds to a sharp decrease in seismic impedance, and 3D seismic data are used to map the base of karst between wells.

• The karst zone exhibits high variability in thickness; however, the zone is generally thicker on higher portions of a SE-trending anticline that runs through the study area, suggesting a structural control on karst development.

• Seismic data show that the karst zone truncates the base of the porous reservoir in some areas and seismic attributes reveal potential reservoir compartment boundaries.

• Better understanding of local karst control on fluid flow in this reservoir can improve reservoir management decisions.

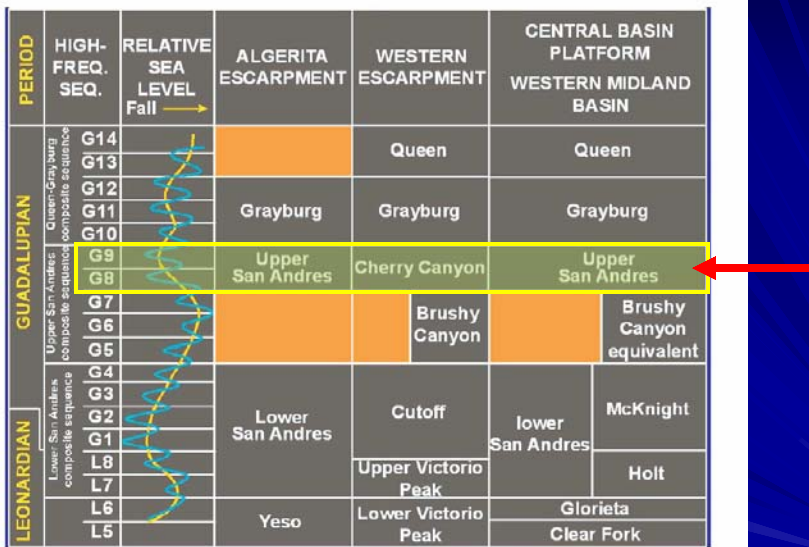

Stratigraphic column for upper Leonardian and lower Guadalupian section in the Permian Basin. After Ruppel and Bebout (2001).

Seismic profile A-A' across shelf margin of CBP

- Interval from Guadalupian 4 (G4) horizon to top of San Andres is part of a *transgressive systems tract (TST)*.
- Interval from Top San Andres to Grayburg is part of a *high stand systems tract (HST)*.

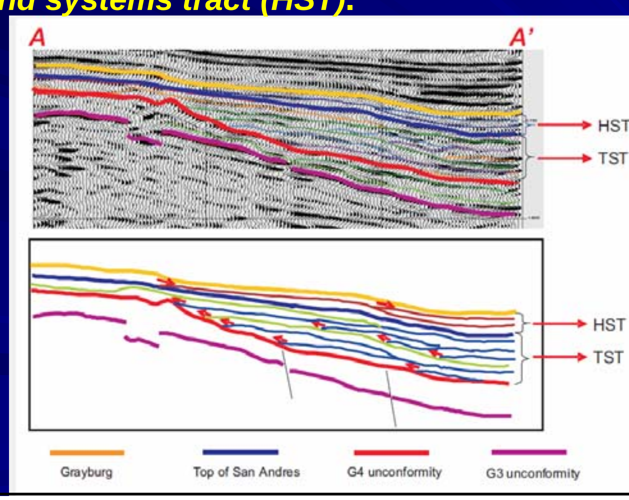

2 sq. mile "high volume" area of Waddell Field

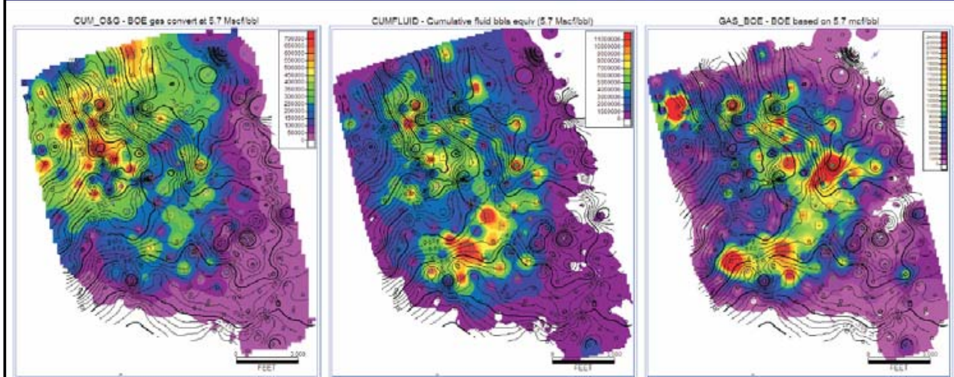

- **Multi-mineral models are essential for estimating effective porosities that provide good matches with core.**
- **Statistical zonation of well logs provides a consistent method for identifying the base of karst.**
- **Seismic horizon mapping provides details on the configuration of the reservoir interval.**
- **Seismic impedance allows us to determine interwell porosity variation.**
- **BVW profile analysis is useful for assessing spatial continuity of the reservoir.**
- **Multi-trace seismic attributes, such as volumetric curvature, provide added detail in our interpretation of reservoir compartmentalization.**

Enhanced Characterization of Reservoir Heterogeneity

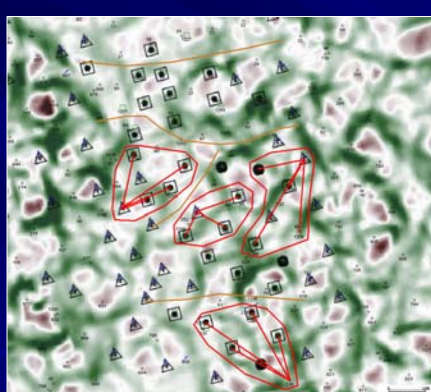

Most negative curvature map

WADDELL FIELD - Permian San Andres

Green = tight negative curvature (faults, fractures?)

Red outline = tracer survey outlines prominent flow areas

Orange lines = engineering interpreted permeability barriers

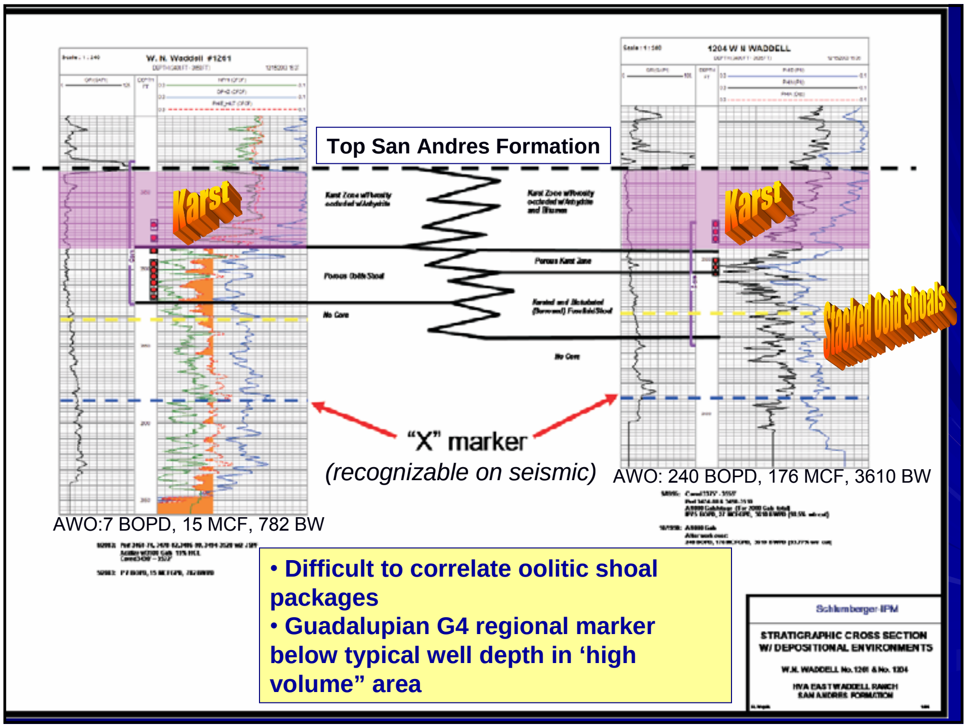
Top San Andres Formation
Karst
Karst
Stacked Ooid Shoals
"X" marker
(recognizable on seismic)
AWO:7 BOPD, 15 MCF, 782 BW
AWO: 240 BOPD, 176 MCF, 3610 BW
• Difficult to correlate oolitic shoal packages
• Guadalupian G4 regional marker below typical well depth in 'high volume" area
Schlumberger-IPM
STRATIGRAPHIC CROSS SECTION
W/ DEPOSITIONAL ENVIRONMENTS

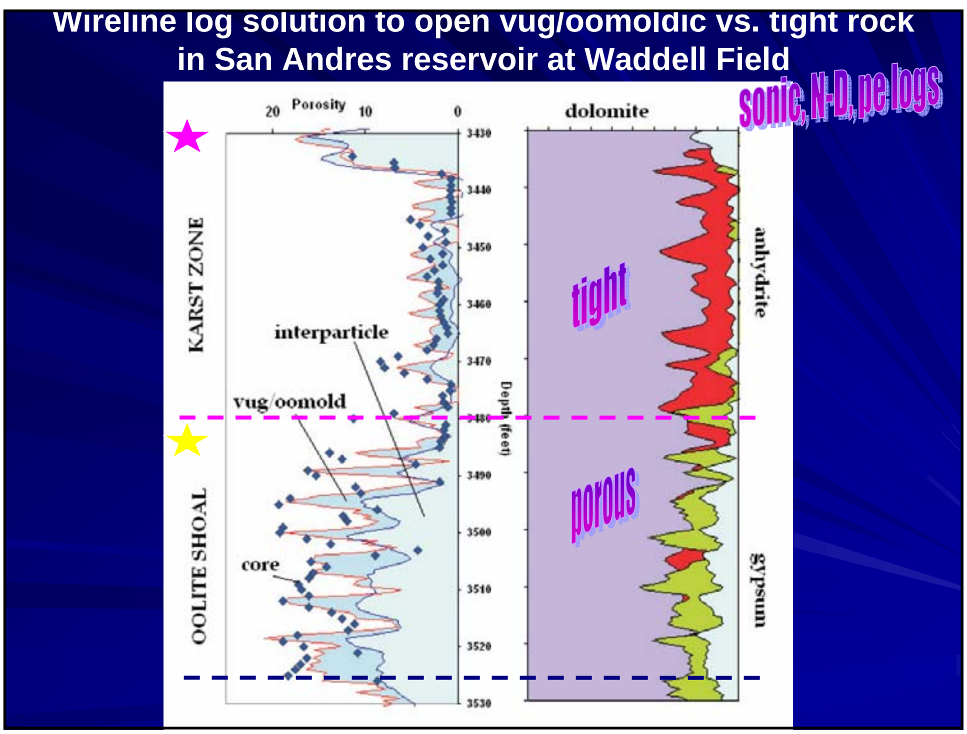
Wireline log solution to open vug/oomoldic vs. tight rock in San Andres reservoir at Waddell Field
sonic, N-D, pe logs
Porosity
20
10
0
dolomite
KARST ZONE
OOLITE SHOAL
interparticle
vug/oomold
core
Depth (feet)
3430
3440
3450
3460
3470
3480
3490
3500
3510
3520
3530
tight
porous
anhydrite
gypsum

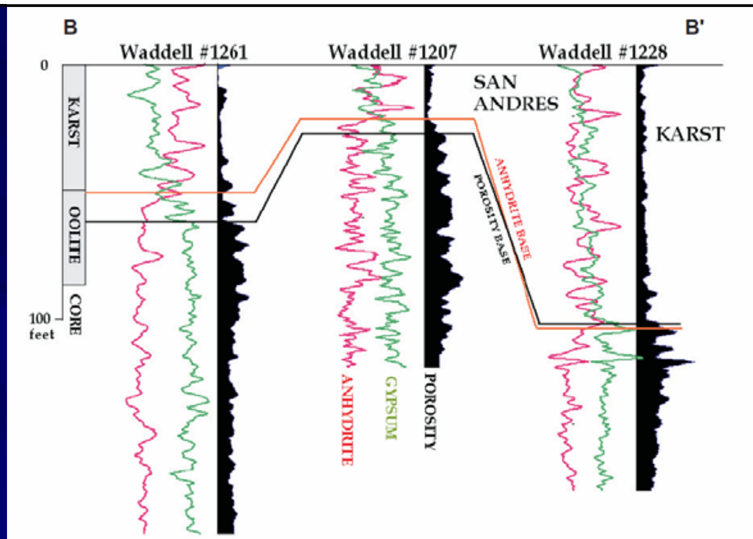

An example of the results of the karstic zone methodology is shown for the cored well #1261 well and two neighboring wells. In well #1261, the core description subdivision of the upper San Andres Formation between the karst zone and porous, oolitic shoal facies is closely matched by the zonation picks based on the sonic and estimated-anhydrite logs. Note the significant variation in thickness of the interpreted karst zone in the three wells.

Karst thickest along crest of current structural high

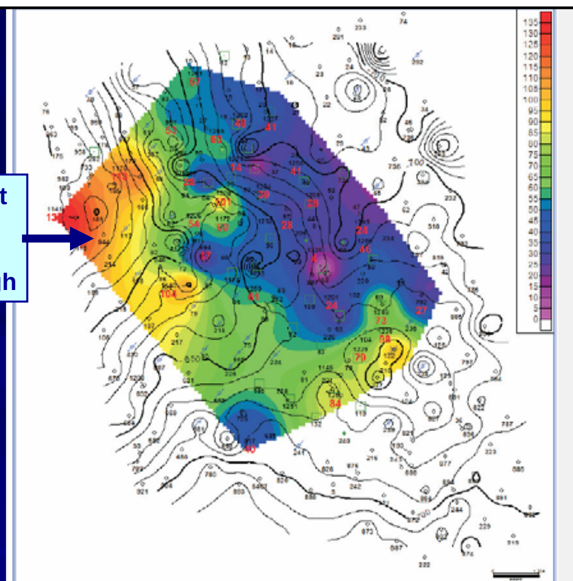

Isopach map of upper tight zone of San Andres Formation interpreted as karst, with top of San Andres Formation subsea depth contours superimposed.

Seismic Horizon Analysis and Reservoir Characterization

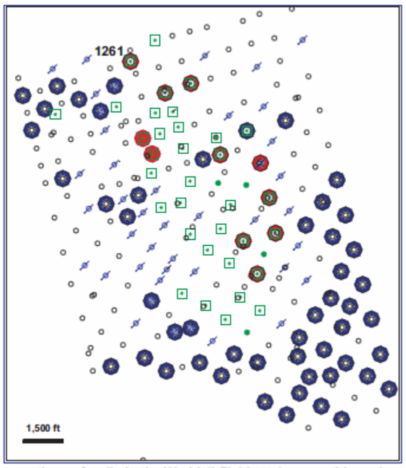

Locations of wells in the Waddell Field study area with sonic logs (blue) and both sonic and density logs (red).

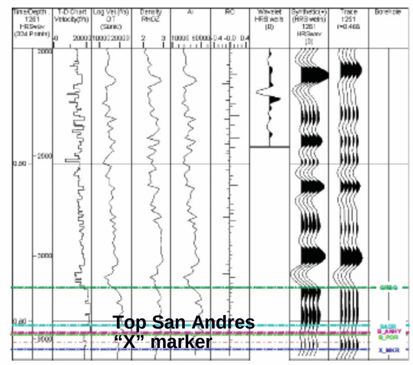

Synthetic seismogram for well #1261 showing tie with seismic data. Labeled tops are: top Grayburg (GRBG; dark green), top San Andres (SADR; cyan), base of anhydritic section beneath the top of San Andres (B_ANHY; magenta), base of tight zone beneath top of San Andres (B_POR; light green), "x" marker (X_MKR; blue).

Time structure at base of karst below top of San Andres Formation

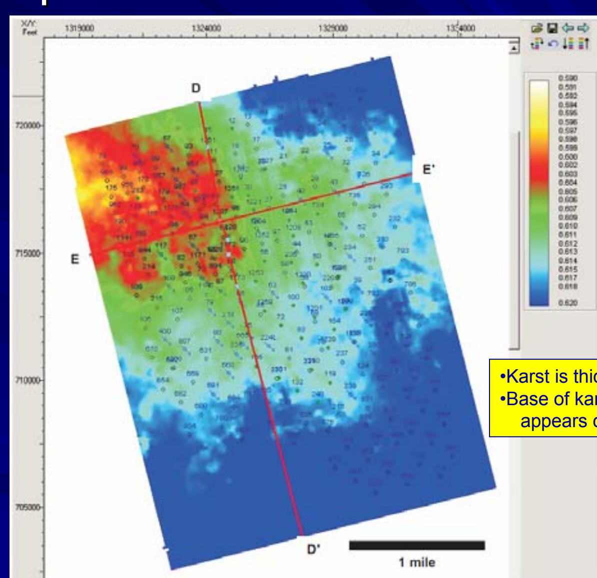

•Karst is thicker over structure
•Base of karst based on seismic appears consistent

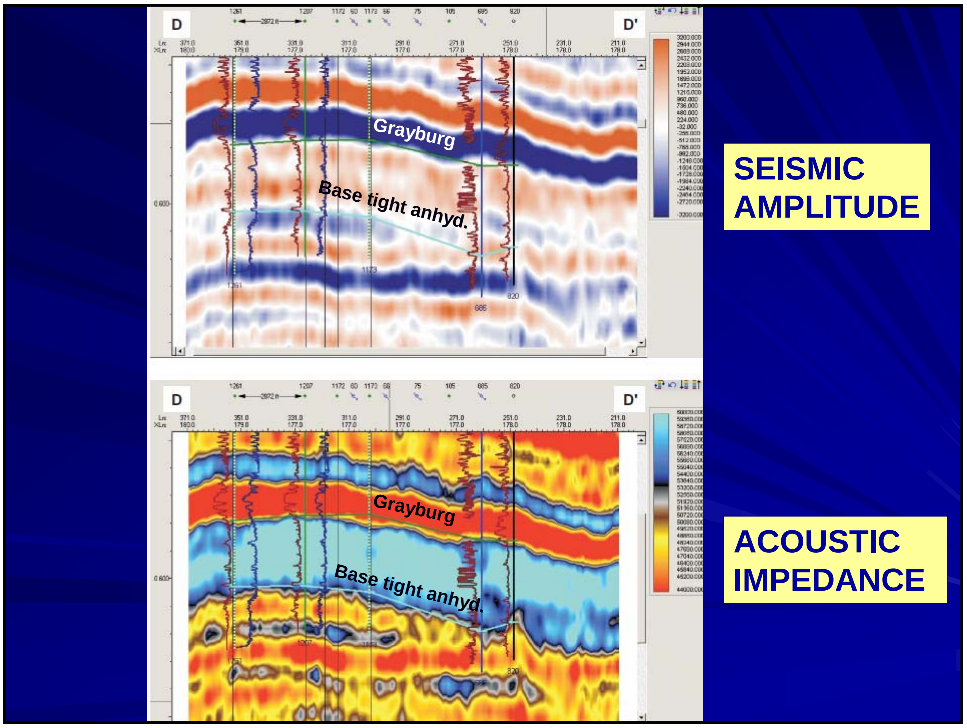
D
D'
Grayburg
Base tight anhyd.
SEISMIC AMPLITUDE
ACOUSTIC IMPEDANCE

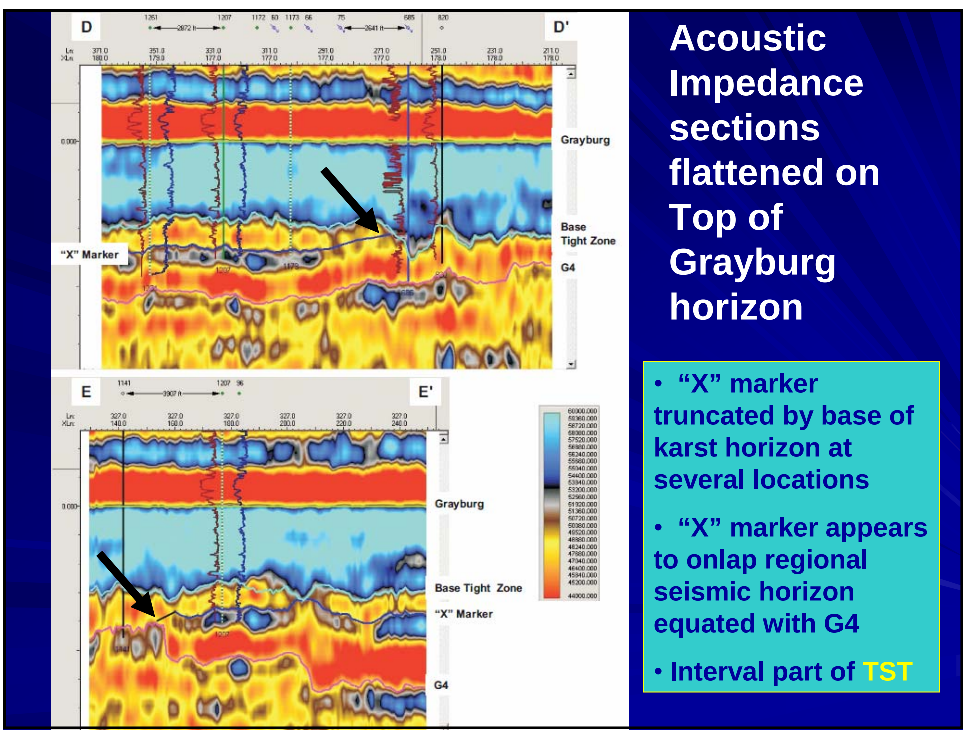
D
D'
Grayburg
Base Tight Zone
G4
"X" Marker
E
E'
Base Tight Zone
Acoustic Impedance sections flattened on Top of Grayburg horizon
• "X" marker truncated by base of karst horizon at several locations
• "X" marker appears to onlap regional seismic horizon equated with G4
• Interval part of TST

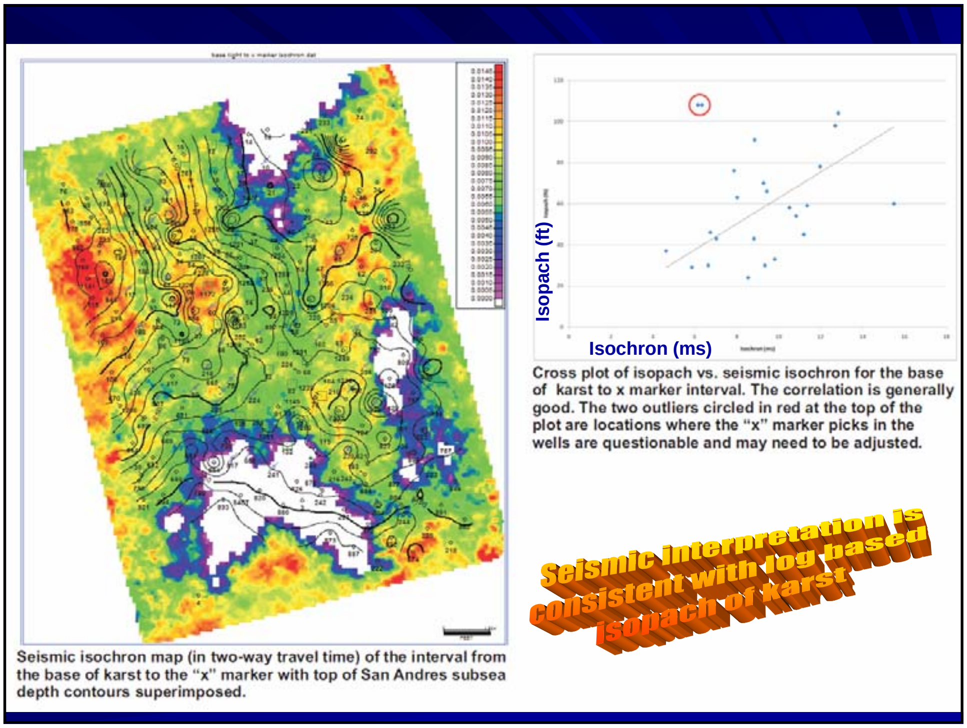
Isopach (ft)
Isochron (ms)
Cross plot of isopach vs. seismic isochron for the base of karst to x marker interval. The correlation is generally good. The two outliers circled in red at the top of the plot are locations where the "x" marker picks in the wells are questionable and may need to be adjusted.
Seismic interpretation is consistent with log based isopach of karst
Seismic isochron map (in two-way travel time) of the interval from the base of karst to the "x" marker with top of San Andres subsea depth contours superimposed.

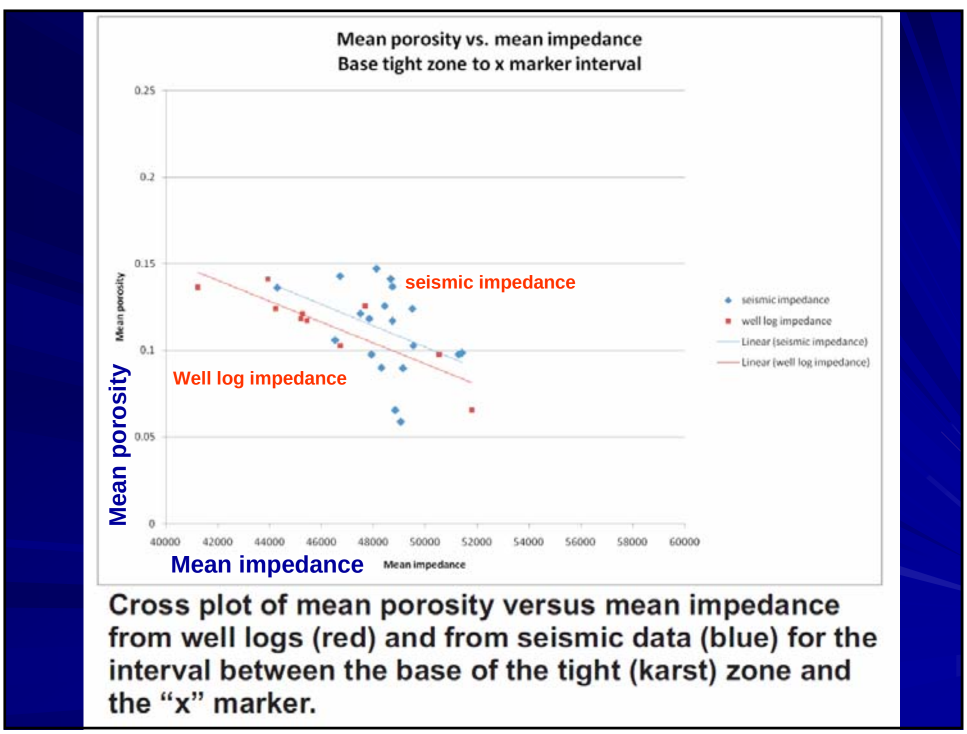
Mean porosity vs. mean impedance
Base tight zone to x marker interval
0.25
0.2
0.15
0.1
0.05
0
40000
42000
44000
46000
48000
50000
52000
54000
56000
58000
60000
seismic impedance
Well log impedance
Mean porosity
Mean impedance
seismic impedance
well log impedance
Linear (seismic impedance)
Linear (well log impedance)
Cross plot of mean porosity versus mean impedance from well logs (red) and from seismic data (blue) for the interval between the base of the tight (karst) zone and the "x" marker.

Porosity distribution appears to be preserved trend of ooid shoal or diagenetically enhancement along lineament (e.g., dissolution of pore filling gypsum cement)

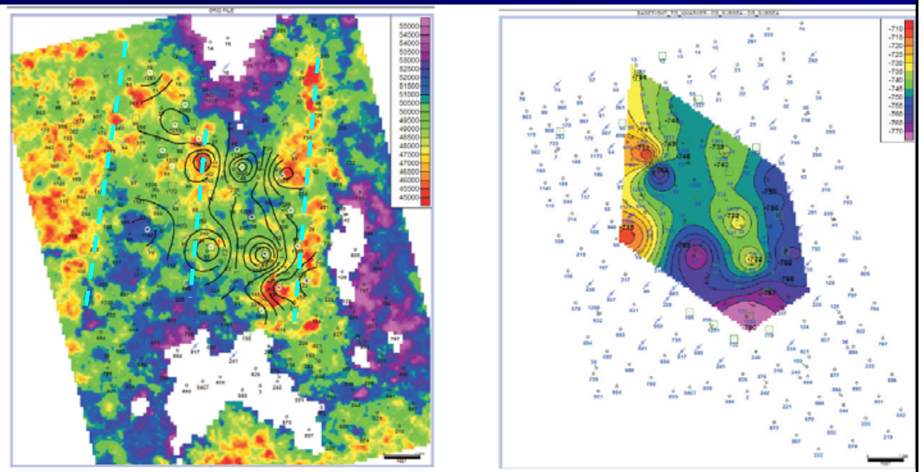

Map of mean seismic impedance for the interval from the base of karst to the "x" marker. Mean porosity contours from well logs are superimposed.

Center of gravity of porosity for the interval from the base of karst to the "x" marker measured in feet subsea. Lower center of gravity (blue) corresponds to higher mean porosity.

Reservoir Connectivity & Compartments

BVW ANALYSIS

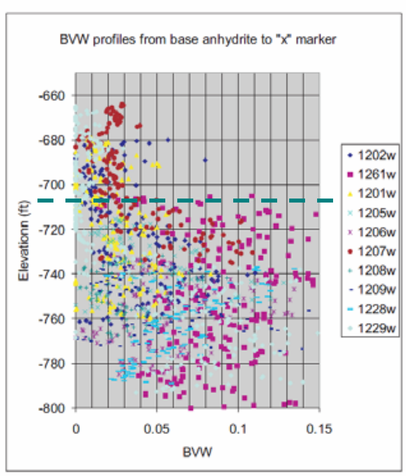

<u>BVW = Sw x Ø</u>

- In principal: Increase BVW with depth as approach oil-water contact in a transition zone
- BVW-depth pattern here is widely scattered, no pattern
- Lack of pattern suggests no common transition zone among wells, *or widely varying reservoir properties/pore types*

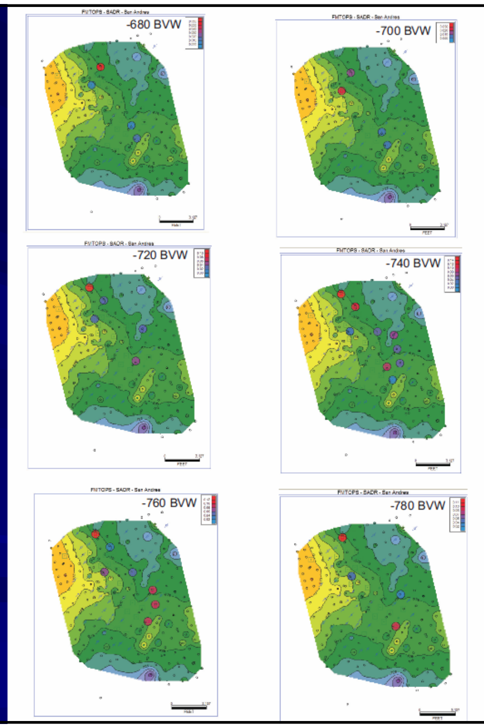

Bubble maps of *BVW* at given elevation (subsea) superimposed on top of San Andres structure map

- BVW values vary markedly by depth
- Depth slices show no pattern of BVW variation with depth
- No strong field-wide transition zone, but rather well-scale variations in reservoir properties

PHI-BVW ANALYSIS

Ø-BVW = ~So

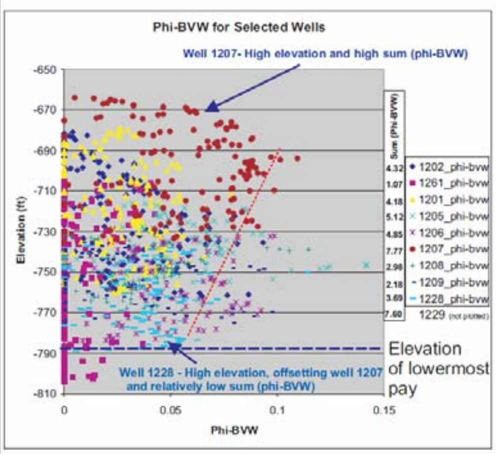

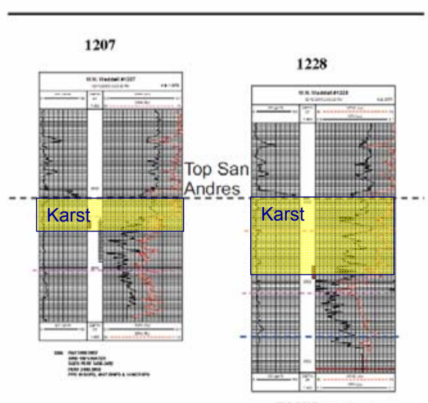

- Adjacent wells #1207 and #1228 are at opposite ends of depth plot vs. Ø-BVW.
  - Both wells at essentially the same elevation at top of the San Andres Fm.
  - #1228 is more tightly clustered with lower elevation wells due to thick karst.
- Base of pay corresponds with lowest Ø-BVW, suggesting proximity to water level.

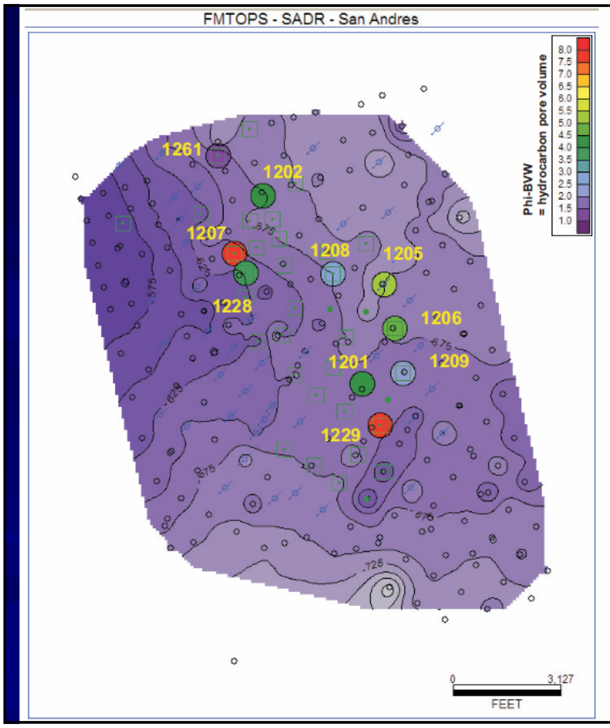

Structure map on Top San Andres Formation

- Bubbles depict cumulative Phi-BVW in pay intervals for each well.
- No clear pattern including offset wells
- Similar to maps of cumulative oil and gas production in "high volume area".

Most positive volumetric curvature extracted along a *Devonian horizon* superimposed on mean impedance map for base of karst to "X" marker

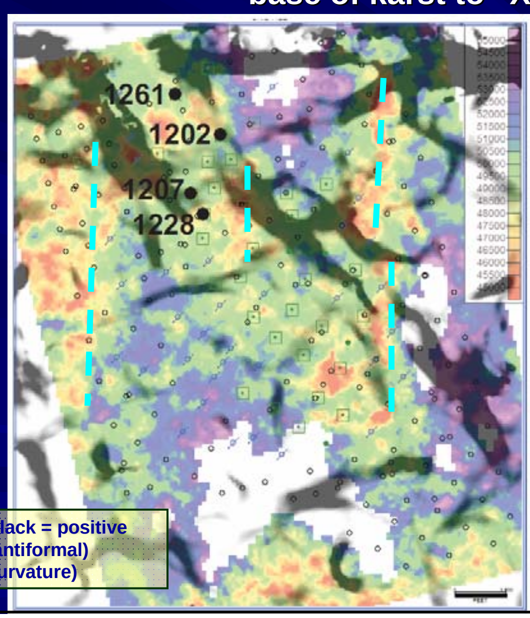

- **Significant deep-seated structural control to the northwest-trending features in the "high volume area".**
- **Crosscutting north to northeast-trending features on the Devonian surface appear to have impacted porosity development in the San Andres.**

Most positive volumetric curvature extracted *along "X" marker* superimposed on mean impedance map for base of karst to "X" marker

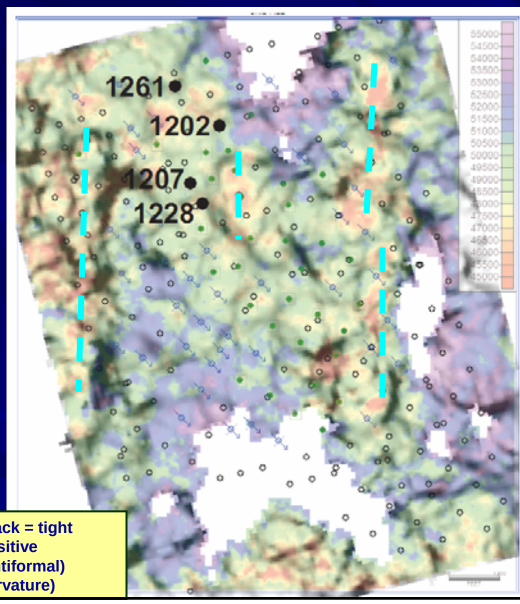

- **Some of the same structural trends as the Devonian horizon but also shows a *finer network of lineaments that enclose areas with diameters on the order of 1500 ft (450 m).***
- **These features may indicate reservoir compartmentalization at *a single-well scale*.**

Conclusions

- A wide range of fluid recoveries is noted in wells in the "high volume area" of Waddell Field. Higher production generally comes from:
  - 1) the main structural high,
  - 2) along the northeast flank of the southeast-trending anticline that runs through the area, and
  - 3) along a narrow northeast-trending area roughly corresponding to a structural saddle on the anticline.
- In the "high volume area", tight, anhydritic "macro" karst at the top of the San Andres Formation cuts down into the underlying porous reservoir.
- The karst zone exhibits high variability in thickness but is generally thicker on the higher portions of the southeast-trending anticline.
- The porous carbonate reservoir interval below the karst is on the saddle area of the anticline.
- A seismic horizon corresponding to the "x" marker (base of porous reservoir) can be interpreted across the impedance volume. This horizon is truncated by the base of karst in some areas, suggesting an associated change in reservoir type/quality in these areas.

Conclusions (continued)

- A comparison of mean and center of gravity measures of porosity indicates that higher porosity is developed lower in the pay interval.
- The mean seismic impedance of the reservoir interval corresponds well with mean porosity from well logs and allows porosity approximation in areas of poor well control.
- The impedance maps suggest that the porous San Andres shoals that comprise the pay appear to have N-NE trends, oblique to the main San Andres structure. The pattern of shoal development may be controlled by deep- seated structure.
- Local karst development appears to be at a well scale, greatly reducing the reservoir quality, which causes variability in oil and gas production, even within this high volume area.
- A combination of factors appears to be responsible for the pay distribution in the high volume area of Waddell Field.

Seismic amplitude map showing rectilinear porosity pattern in San Andres Formation

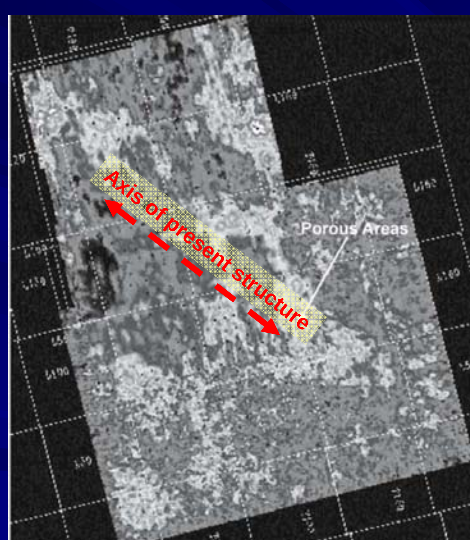

- **another example of compartmentalization attributed in part to structural control**
- **amplitude/porosity pattern believed controlled by access to burial fluids migrating along fractures leading to anhydrite dissolution**

From Lucia (1999)

Isopach of number of fracture feet in a 20 ft slice map of the *Yates San Andres field*

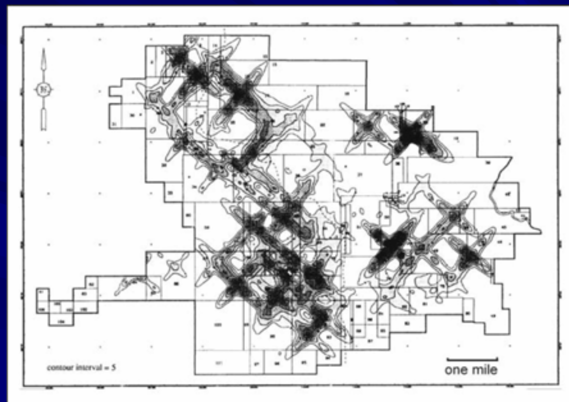

- NW-SE and orthogonal NE-SW fracture and karst trend overprint matrix porosity accompanied by numerous caves below top of San Andres
- grainstone and grain-dominated packstone have highest porosity
- grainstone concentrated on ramp crest
- 4 Billion bbl reservoir

Tinker and Mruk (1995)

NW-SE cross section across Taylor-Link San Andres reservoir

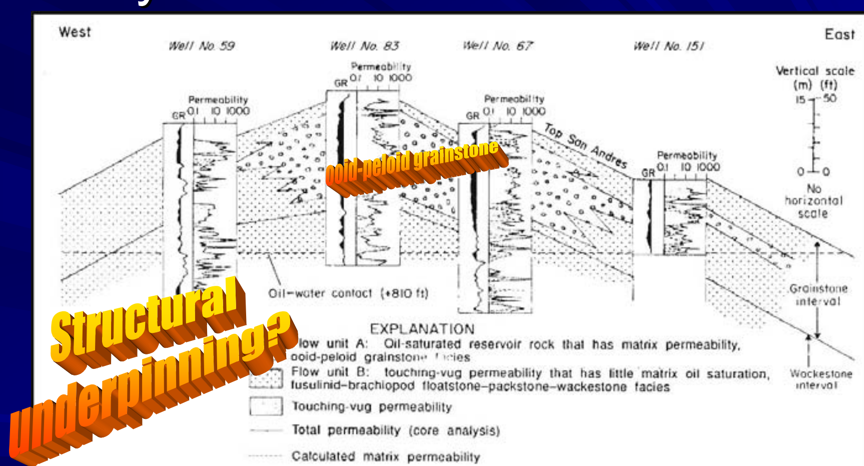

- ooid grainstone rock fabric facies and fractured fusulinid wackestone facies
- grainstone dolomitized with interooid porosity, ~60 ft thick, amalgamation of several shoaling-upward cycles
- 50 million bbl reservoir

Lucia et al. (1992)

Additional Information for Part 4 – Lithofacies and Petrofacies

Illustrations that follow provide additional geological background to this paper

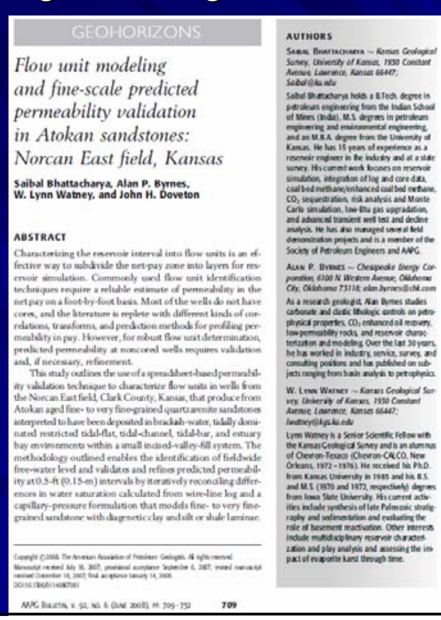

GEOHORIZONS

Flow unit modeling and fine-scale predicted permeability validation in Atokan sandstones: Norcan East field, Kansas

Saibal Bhattacharya, Alan P. Byrnes, W. Lynn Watney, and John H. Doveton

ABSTRACT

Characterizing the reservoir interval into flow units is an effective way to subdivide the net-pay zone into layers for reservoir simulation. Commonly used flow unit identification techniques require a reliable estimate of permeability in the net pay on a foot-by-foot basis. Most of the wells do not have cores, and the literature is replete with different kinds of correlations, transforms, and prediction methods for profiling permeability in pay. However, for robust flow unit determination, predicted permeability at noncored wells requires validation and, if necessary, refinement.

This study outlines the use of a spreadsheet-based permeability validation technique to characterize flow units in wells from the Norcan East field, Clark County, Kansas, that produce from Atokan aged fine- to very fine-grained quartzarenite sandstones interpreted to have been deposited in brackish-water, tidally dominated restricted tidal-flat, tidal-channel, tidal-bar, and estuary bay environments within a small incised-valley-fill system. The methodology outlined enables the identification of fieldwide free-water level and validates and refines predicted permeability at 0.5-ft (0.15-m) intervals by iteratively reconciling differences in water saturation calculated from wire-line log and a capillary-pressure formulation that models fine- to very fine-grained sandstone with diagnetic clay and silt or shale laminae.

Manuscript received July 18, 2007; provisional acceptance September 6, 2007; revised manuscript received December 18, 2007; final acceptance January 14, 2008.
DOI:10.1306/01140807081

AUTHORS

Saibal Bhattacharya ~ *Kansas Geological Survey, University of Kansas, 1930 Constant Avenue, Lawrence, Kansas 66047; Saibal@ku.edu*

Saibal Bhattacharya holds a B.Tech. degree in petroleum engineering from the Indian School of Mines (India), M.S. degrees in petroleum engineering and environmental engineering, and an M.B.A. degree from the University of Kansas. He has 15 years of experience as a reservoir engineer in the industry and at a state survey. His current work focuses on reservoir simulation, integration of log and core data, coal bed methane/enhanced coal bed methane, CO_2 sequestration, risk analysis and Monte Carlo simulation, low-Btu gas upgradation, and advanced transient well test and decline analysis. He has also managed several field demonstration projects and is a member of the Society of Petroleum Engineers and AAPG.

Alan P. Byrnes ~ *Chesapeake Energy Corporation, 6100 N. Western Avenue, Oklahoma City, Oklahoma 73118; alan.byrnes@chk.com*

As a research geologist, Alan Byrnes studies carbonate and clastic lithologic controls on petrophysical properties, CO_2 enhanced oil recovery, low-permeability rocks, and reservoir characterization and modeling. Over the last 30 years, he has worked in industry, service, survey, and consulting positions and has published on subjects ranging from basin analysis to petrophysics.

W. Lynn Watney ~ *Kansas Geological Survey, University of Kansas, 1930 Constant Avenue, Lawrence, Kansas 66047; lwatney@kgs.ku.edu*

Lynn Watney is a Senior Scientific Fellow with the Kansas Geological Survey and is an alumnus of Chevron-Texaco (Chevron-CALCO, New Orleans, 1972–1976). He received his Ph.D. from Kansas University in 1985 and his B.S. and M.S. (1970 and 1972, respectively) degrees from Iowa State University. His current activities include synthesis of late Paleozoic stratigraphy and sedimentation and evaluating the role of basement reactivation. Other interests include multidisciplinary reservoir characterization and play analysis and assessing the impact of evaporite karst through time.

AAPG Bulletin, v. 92, no. 6 (June 2008), pp. 709–732 709

Geo-Engineering Modeling of Morrow/Atoka Incised-Valley Fill Deposits Using Web-Based Freeware for Incremental Field Exploitation

W. Lynn Watney[1,3], Saibal Bhattacharya[1], Alan Byrnes[1], John Doveton[1],
John Victorine[1], Rick Brownrigg[2]

[1]Kansas Geological Survey
[2]Electrical Engineering & Computer Science Department
[3]KU Energy Research Center
The University of Kansas
Lawrence, KS 66047

Objectives

- Regional framework of Pennsylvanian incised valleys in western Kansas
- Sequence stratigraphy of Atokan Stage
- Lithofacies and high-frequency cycles controlling production in Minneola/Norcan East Field
- Flow units, waterflood performance, refined reservoir model
  - Correlation and mapping
  - Controls
- Summary

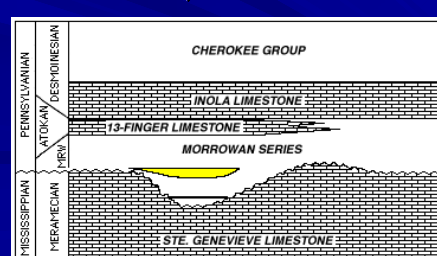

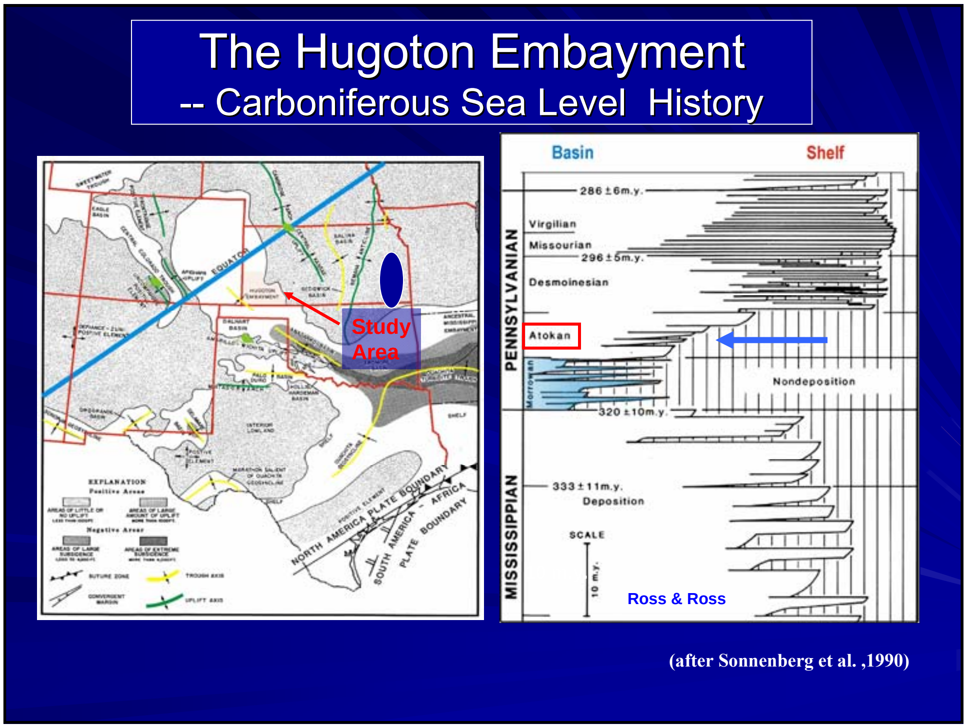
The Hugoton Embayment
-- Carboniferous Sea Level History
Study Area
Basin
Shelf
PENNSYLVANIAN
MISSISSIPPIAN
Virgilian
Missourian
Desmoinesian
Atokan
Morrowan
286 ±6m.y.
296 ±5m.y.
320 ±10m.y.
333 ±11m.y.
Nondeposition
Deposition
SCALE
10 m.y.
Ross & Ross
NORTH AMERICA PLATE BOUNDARY
SOUTH AMERICA - AFRICA PLATE BOUNDARY
EQUATOR
(after Sonnenberg et al. ,1990)

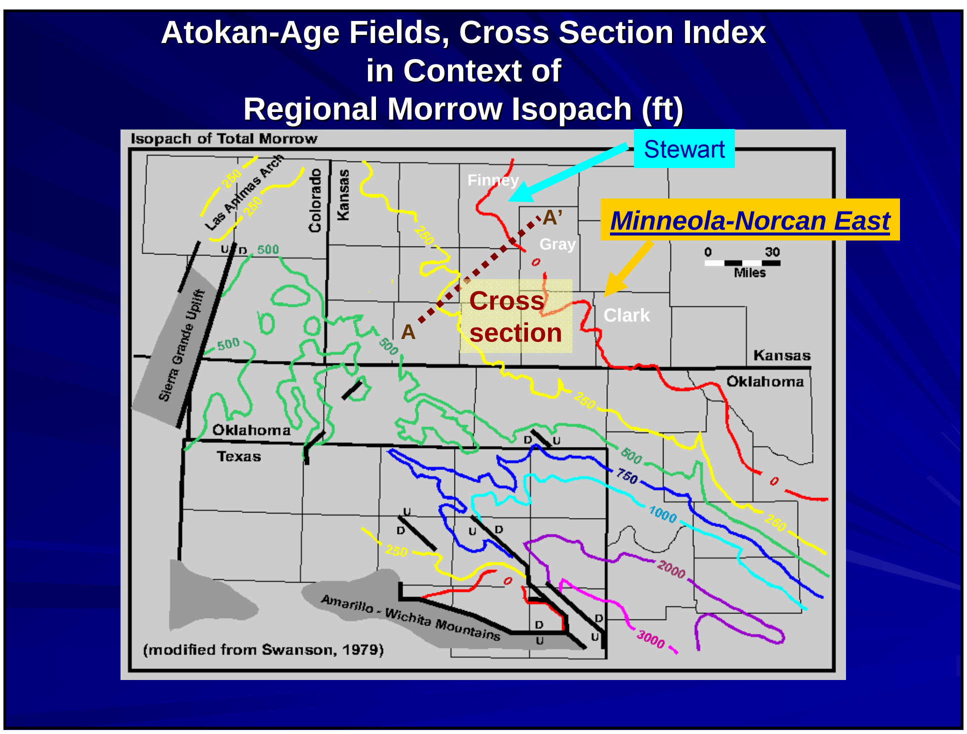
Atokan-Age Fields, Cross Section Index
in Context of
Regional Morrow Isopach (ft)
Isopach of Total Morrow
Stewart
Minneola-Norcan East
Finney
Gray
Clark
A'
A
Cross section
Las Animas Arch
Sierra Grande Uplift
Colorado
Kansas
Oklahoma
Texas
0 30 Miles
Amarillo - Wichita Mountains
(modified from Swanson, 1979)

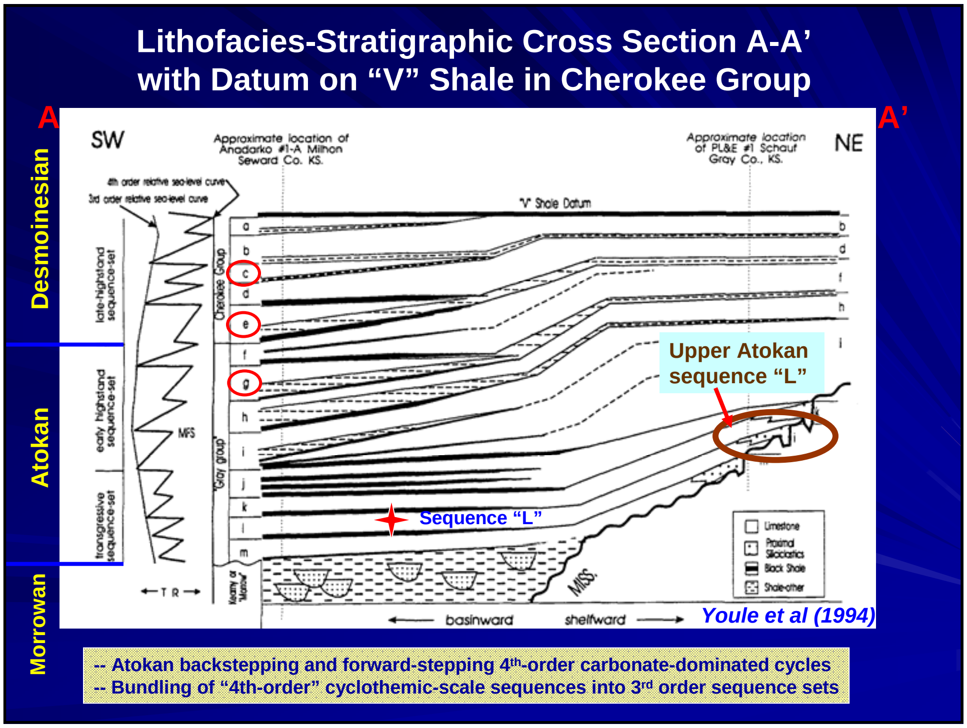
Lithofacies-Stratigraphic Cross Section A-A' with Datum on "V" Shale in Cherokee Group
A
A'
Desmoinesian
Atokan
Morrowan
SW
NE
Approximate location of Anadarko #1-A Milhon Seward Co. KS.
Approximate location of PL&E #1 Schauf Gray Co., KS.
4th order relative sea-level curve
3rd order relative sea-level curve
"V" Shale Datum
late-highstand sequence-set
early highstand sequence-set
transgressive sequence-set
MFS
Cherokee Group
"Gray group"
Upper Atokan sequence "L"
Sequence "L"
MISS.
Limestone
Proximal Siliciclastics
Black Shale
Shale-other
basinward
shelfward
Youle et al (1994)
-- Atokan backstepping and forward-stepping 4th-order carbonate-dominated cycles
-- Bundling of "4th-order" cyclothemic-scale sequences into 3rd order sequence sets

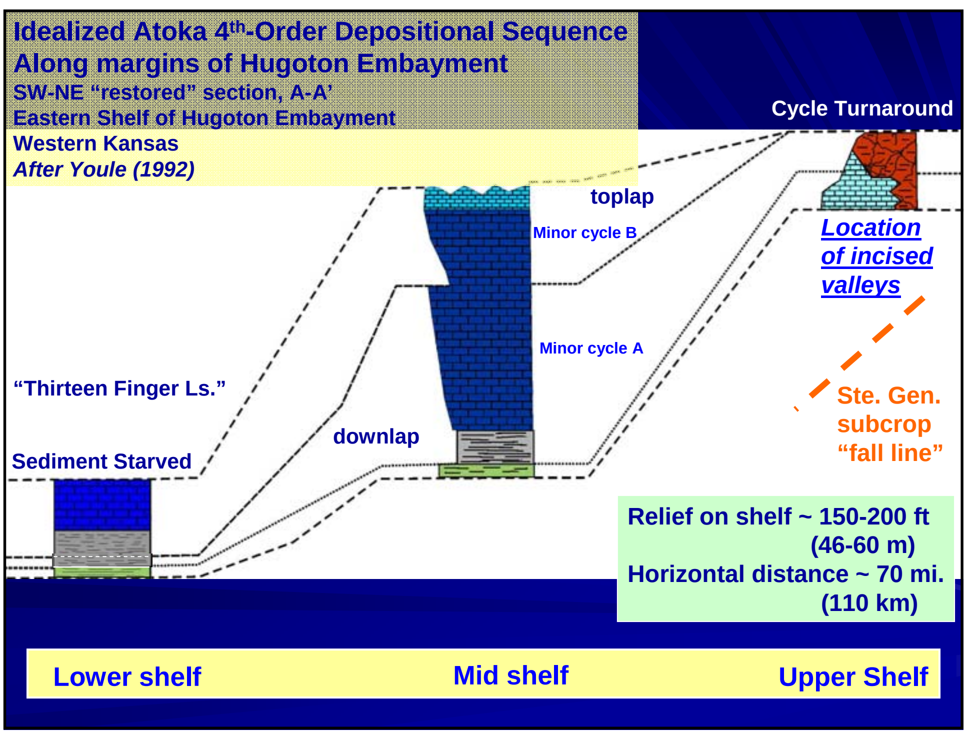
Idealized Atoka 4th-Order Depositional Sequence
Along margins of Hugoton Embayment
SW-NE "restored" section, A-A'
Eastern Shelf of Hugoton Embayment
Western Kansas
After Youle (1992)
Cycle Turnaround
toplap
Minor cycle B
Minor cycle A
Location of incised valleys
"Thirteen Finger Ls."
downlap
Sediment Starved
Ste. Gen. subcrop "fall line"
Relief on shelf ~ 150-200 ft (46-60 m)
Horizontal distance ~ 70 mi. (110 km)
Lower shelf
Mid shelf
Upper Shelf

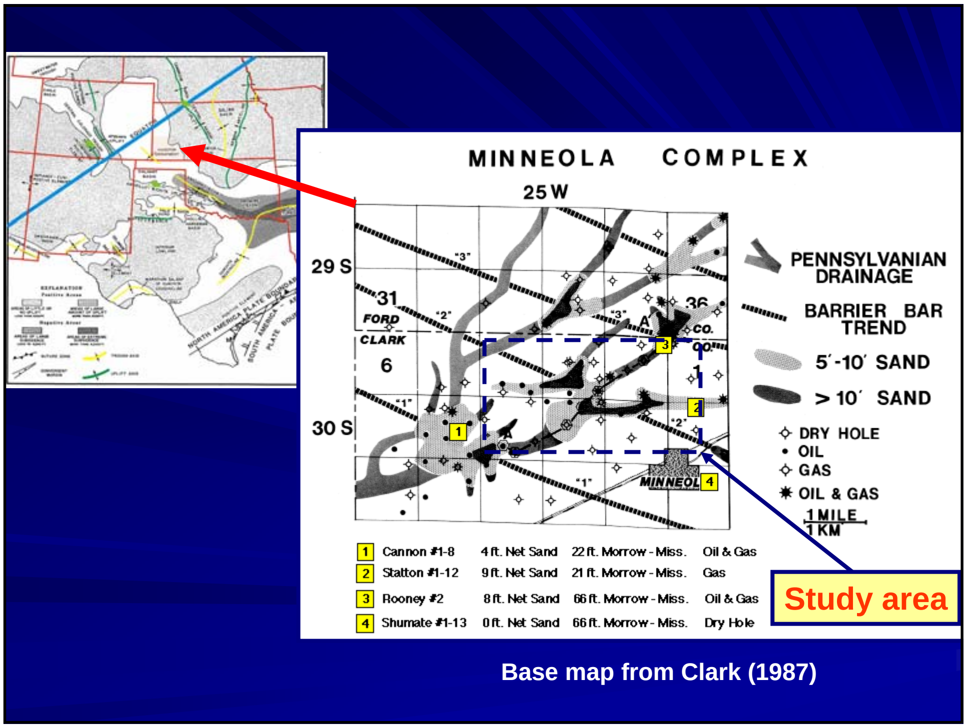
MINNEOLA COMPLEX
25 W
29 S
30 S
PENNSYLVANIAN DRAINAGE
BARRIER BAR TREND
5´-10´ SAND
> 10´ SAND
DRY HOLE
OIL
GAS
OIL & GAS
1 MILE
1 KM
1 Cannon #1-8 4 ft. Net Sand 22 ft. Morrow - Miss. Oil & Gas
2 Statton #1-12 9 ft. Net Sand 21 ft. Morrow - Miss. Gas
3 Rooney #2 8 ft. Net Sand 66 ft. Morrow - Miss. Oil & Gas
4 Shumate #1-13 0 ft. Net Sand 66 ft. Morrow - Miss. Dry Hole
Study area
Base map from Clark (1987)

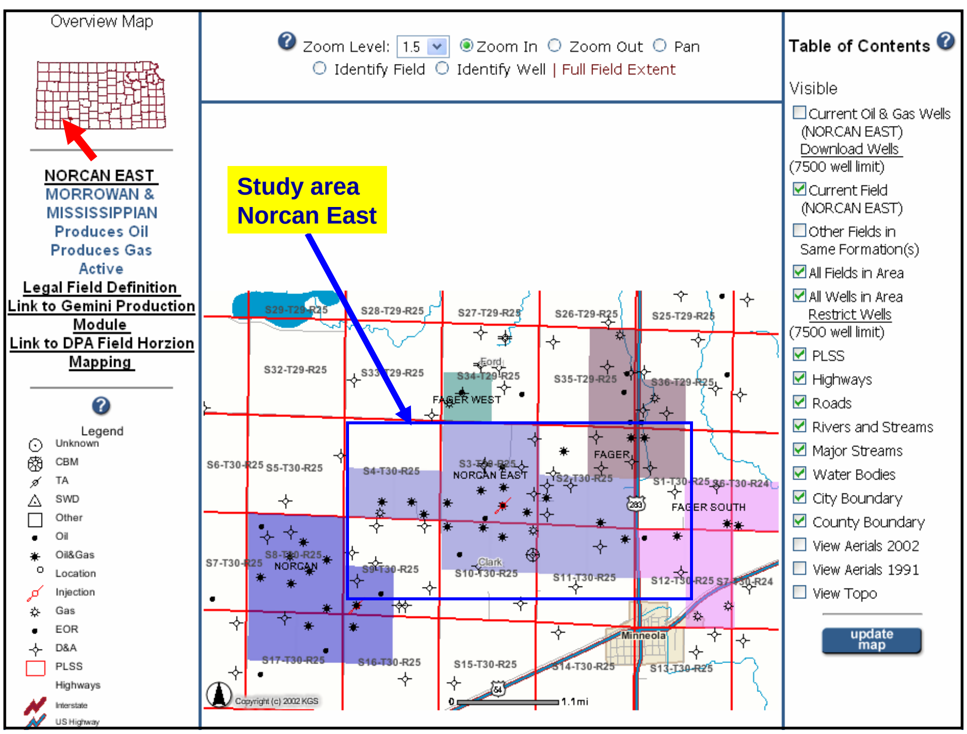
Overview Map
NORCAN EAST
MORROWAN & MISSISSIPPIAN
Produces Oil
Produces Gas
Active
Legal Field Definition
Link to Gemini Production Module
Link to DPA Field Horzion Mapping
Zoom Level: 1.5
Zoom In
Zoom Out
Pan
Identify Field
Identify Well | Full Field Extent
Study area
Norcan East
Table of Contents
Visible
Current Oil & Gas Wells (NORCAN EAST)
Download Wells
(7500 well limit)
Current Field (NORCAN EAST)
Other Fields in Same Formation(s)
All Fields in Area
All Wells in Area
Restrict Wells
(7500 well limit)
PLSS
Highways
Roads
Rivers and Streams
Major Streams
Water Bodies
City Boundary
County Boundary
View Aerials 2002
View Aerials 1991
View Topo
update map

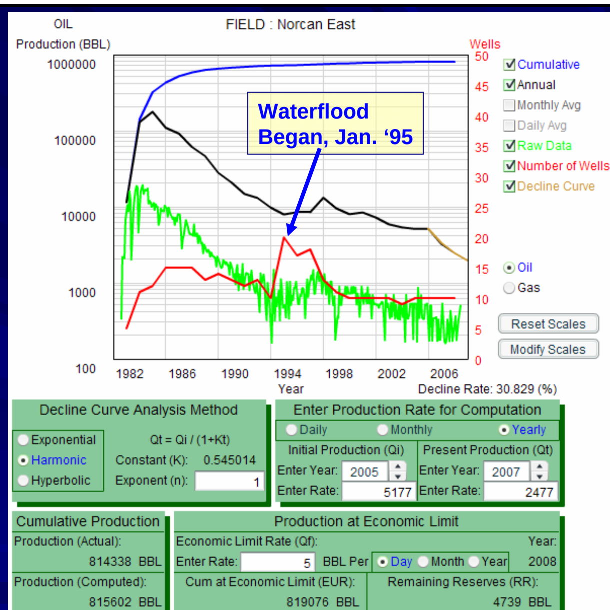

Cumulative Oil Production: 814,000 bbls

Projections: Estimated remaining reserves: 21k bbls

Economic limit at 5 BOPD reached: ~2008…

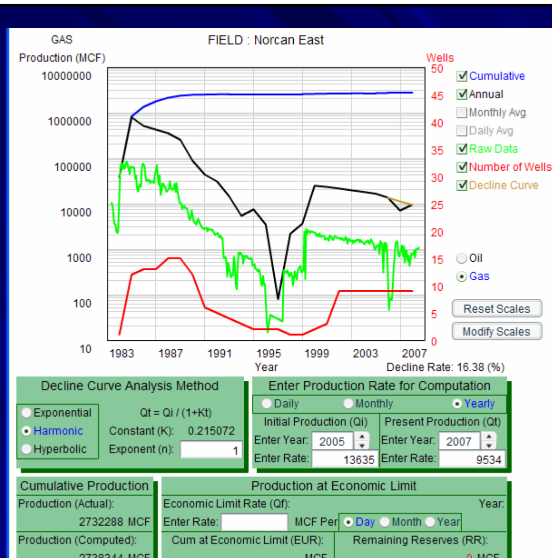

Cumulative Gas Production: 2.7 BCF

Projections: Estimated remaining reserves: 147 MMCF

Cumulative oil and gas = 1,164 MBOE

Compared to nearby Stewart Field = 9.6 MMbbls

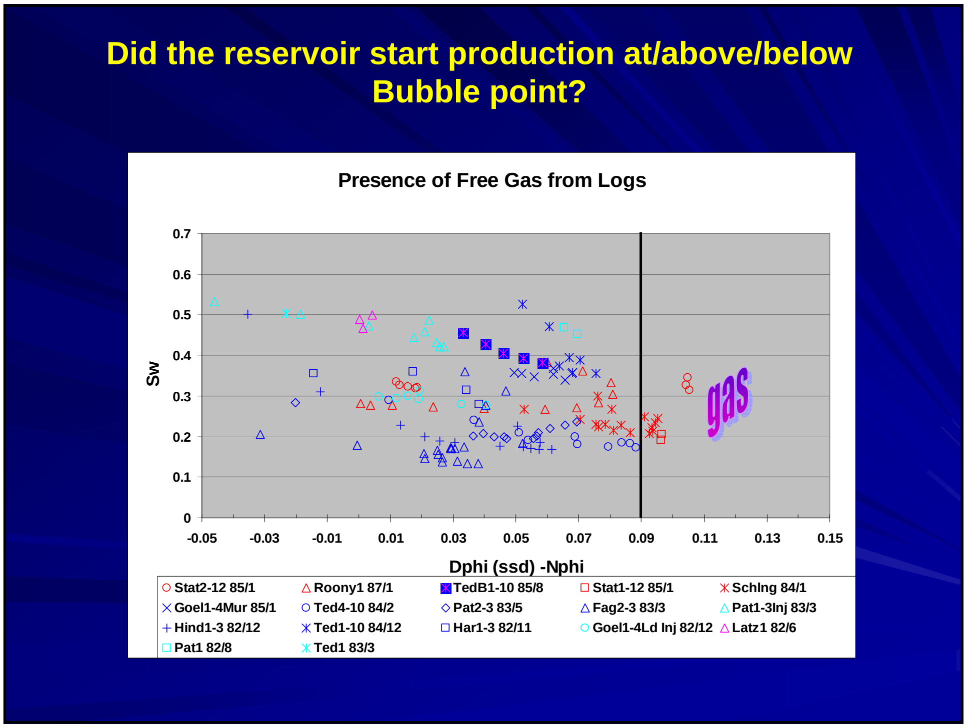
Did the reservoir start production at/above/below Bubble point?
Presence of Free Gas from Logs
Sw
0.7
0.6
0.5
0.4
0.3
0.2
0.1
0
-0.05
-0.03
-0.01
0.01
0.03
0.05
0.07
0.09
0.11
0.13
0.15
Dphi (ssd) -Nphi
gas
Stat2-12 85/1
Roony1 87/1
TedB1-10 85/8
Stat1-12 85/1
Schlng 84/1
Goel1-4Mur 85/1
Ted4-10 84/2
Pat2-3 83/5
Fag2-3 83/3
Pat1-3Inj 83/3
Hind1-3 82/12
Ted1-10 84/12
Har1-3 82/11
Goel1-4Ld Inj 82/12
Latz1 82/6
Pat1 82/8
Ted1 83/3

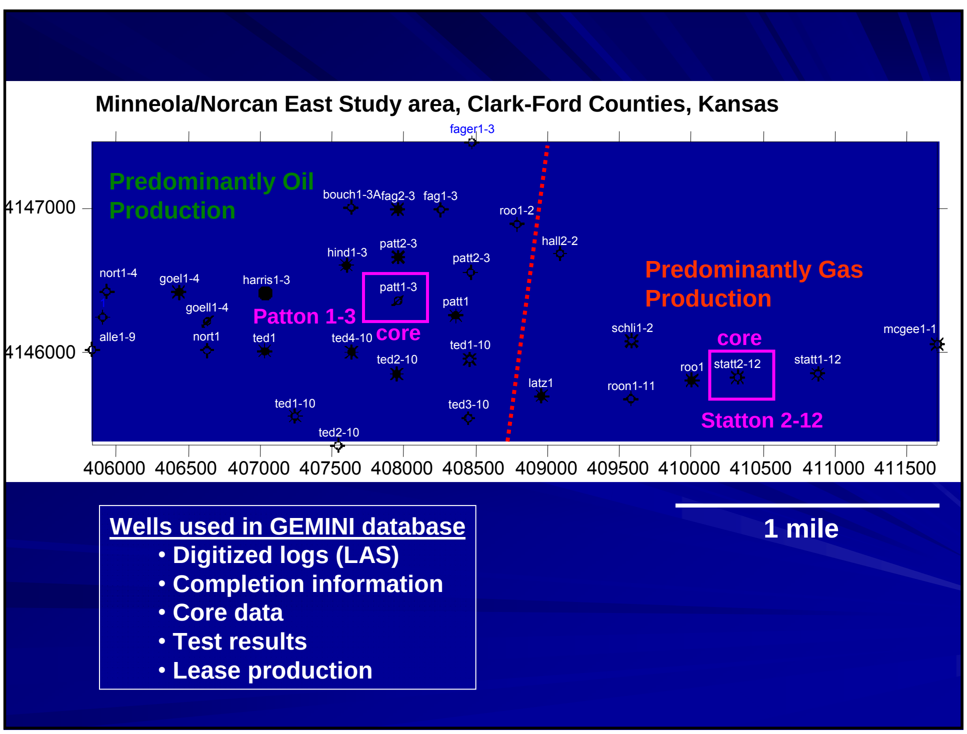
Minneola/Norcan East Study area, Clark-Ford Counties, Kansas
Predominantly Oil Production
Predominantly Gas Production
Patton 1-3
core
Statton 2-12
core
4147000
4146000
fager1-3
bouch1-3A
fag2-3
fag1-3
roo1-2
hall2-2
hind1-3
patt2-3
patt2-3
nort1-4
goel1-4
harris1-3
patt1-3
goell1-4
patt1
alle1-9
nort1
ted1
ted4-10
ted1-10
ted2-10
schli1-2
mcgee1-1
roo1
statt2-12
statt1-12
roon1-11
latz1
ted1-10
ted3-10
ted2-10
406000 406500 407000 407500 408000 408500 409000 409500 410000 410500 411000 411500
Wells used in GEMINI database
• Digitized logs (LAS)
• Completion information
• Core data
• Test results
• Lease production
1 mile

Total magnetic field intensity with oil fields

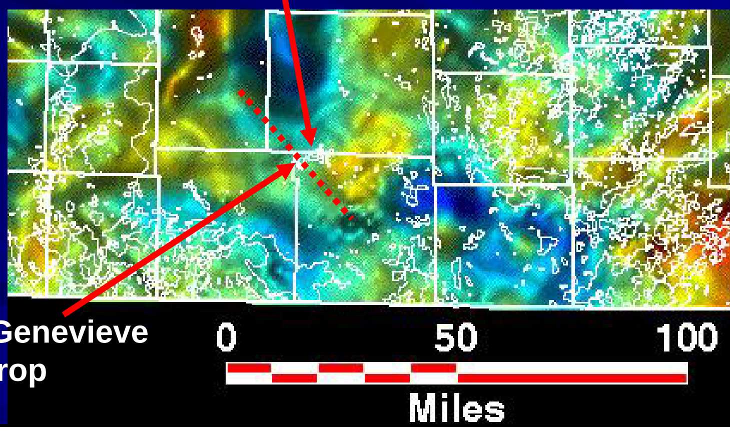

High-Resolution Seismic Survey of the
Minneola Complex
Southwest Kansas
Kansas Geological Survey Open-File Report OFR 98-44
Joseph M. Kruger, Kansas Geological Survey

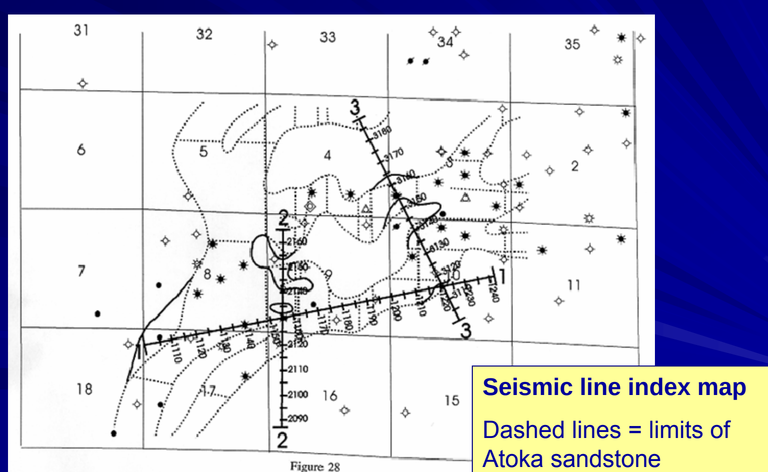

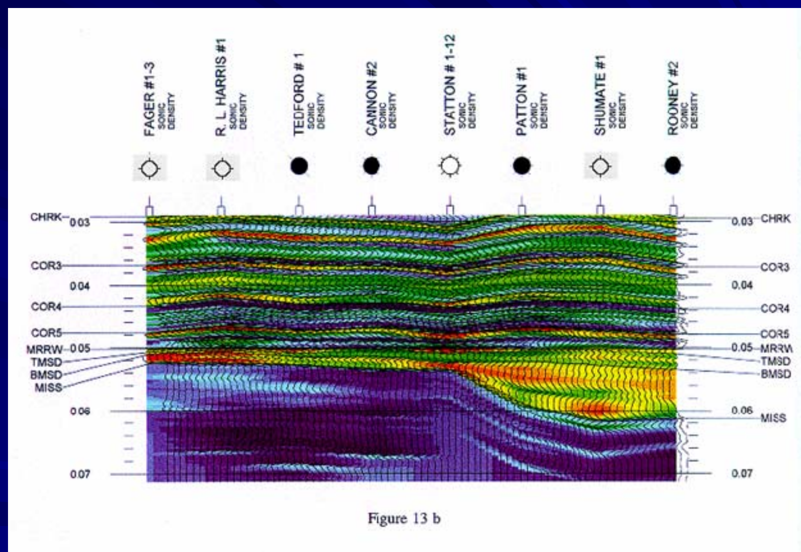

Acoustic impedance interpolation of sonic and density logs from wells

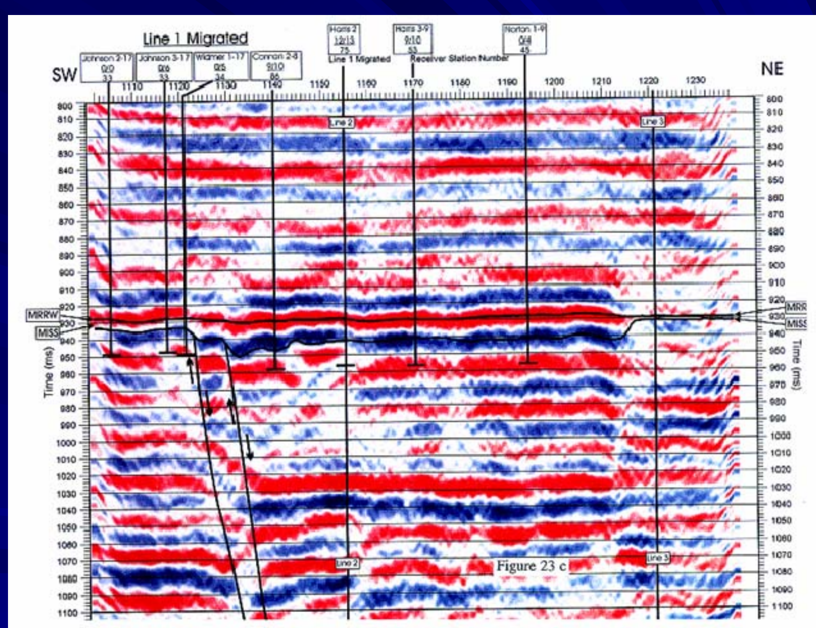

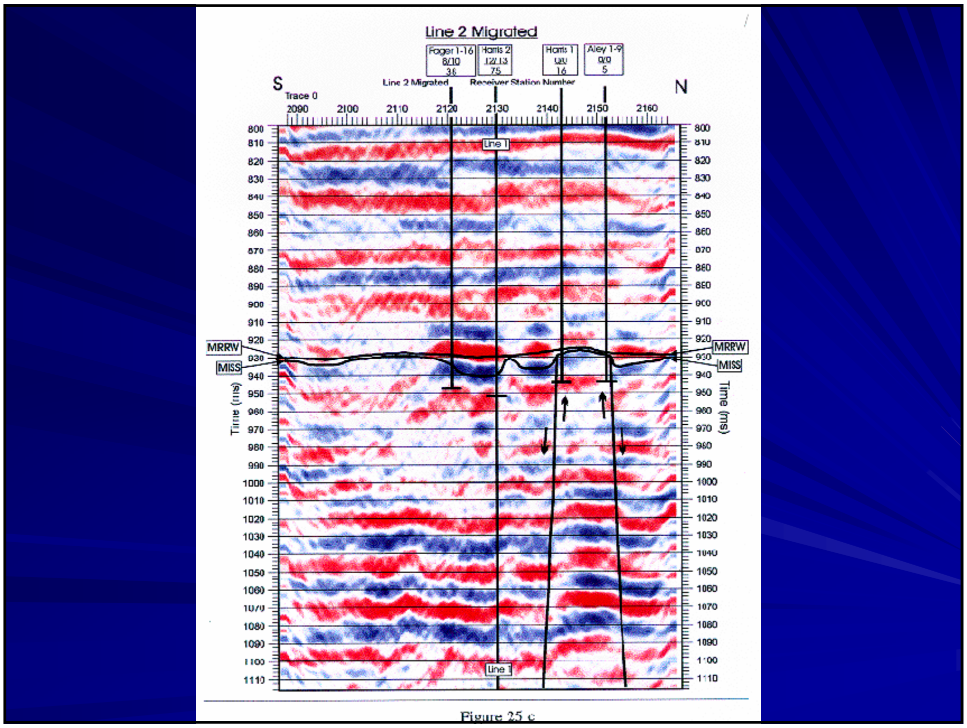
Line 2 Migrated
S
N
Trace 0
Line 2 Migrated
Receiver Station Number
MRRW
MISS
Time (ms)
Line 1
Figure 25 c

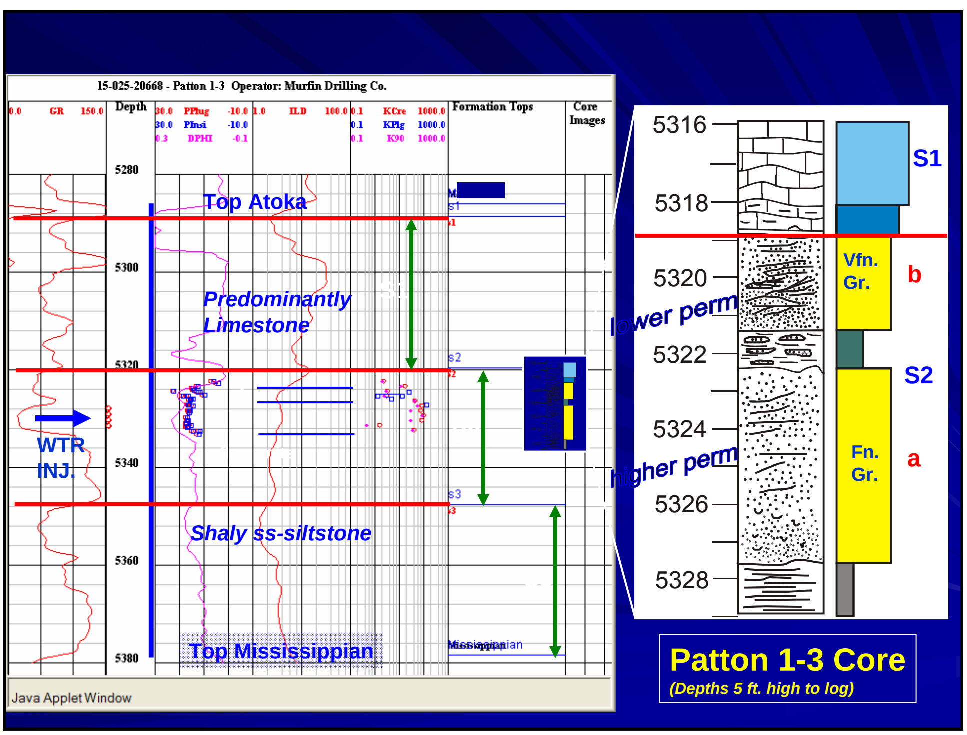
15-025-20668 - Patton 1-3 Operator: Murfin Drilling Co.
GR
Depth
ILD
Formation Tops
Core Images
Top Atoka
Predominantly Limestone
WTR INJ.
Shaly ss-siltstone
Top Mississippian
Java Applet Window
lower perm
higher perm
5316
5318
5320
5322
5324
5326
5328
S1
S2
Vfn. Gr.
Fn. Gr.
b
a
Patton 1-3 Core
(Depths 5 ft. high to log)

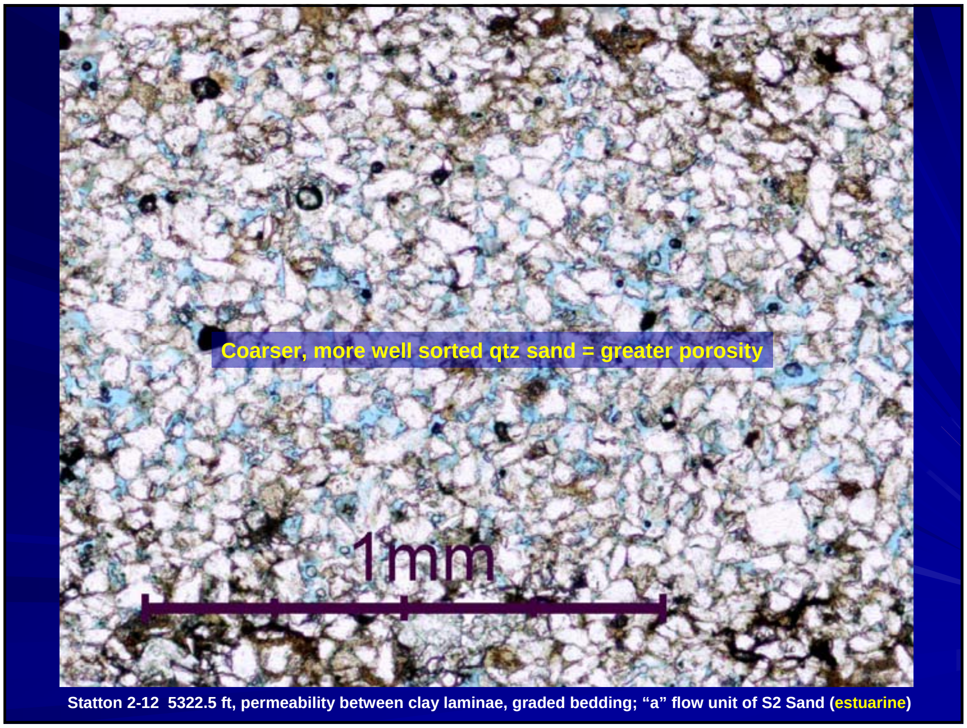
Coarser, more well sorted qtz sand = greater porosity
1mm
Statton 2-12 5322.5 ft, permeability between clay laminae, graded bedding; “a” flow unit of S2 Sand (estuarine)

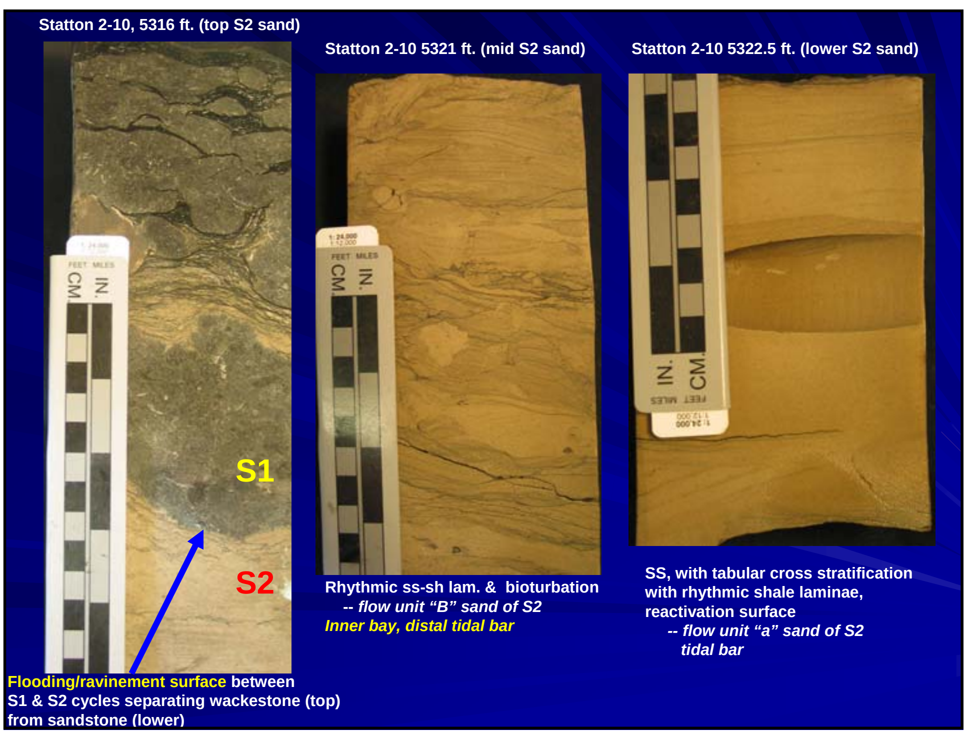
Statton 2-10, 5316 ft. (top S2 sand)
Statton 2-10 5321 ft. (mid S2 sand)
Statton 2-10 5322.5 ft. (lower S2 sand)
S1
S2
Rhythmic ss-sh lam. & bioturbation
-- flow unit “B” sand of S2
Inner bay, distal tidal bar
SS, with tabular cross stratification with rhythmic shale laminae, reactivation surface
-- flow unit “a” sand of S2
tidal bar
Flooding/ravinement surface between S1 & S2 cycles separating wackestone (top) from sandstone (lower)

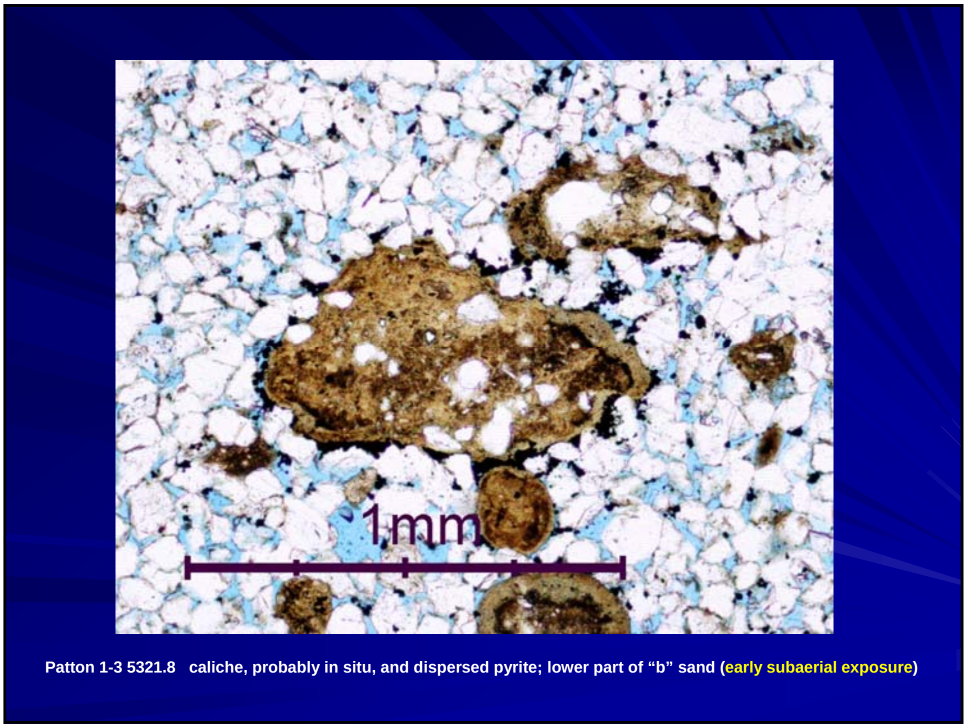
1mm
Patton 1-3 5321.8 caliche, probably in situ, and dispersed pyrite; lower part of "b" sand (early subaerial exposure)

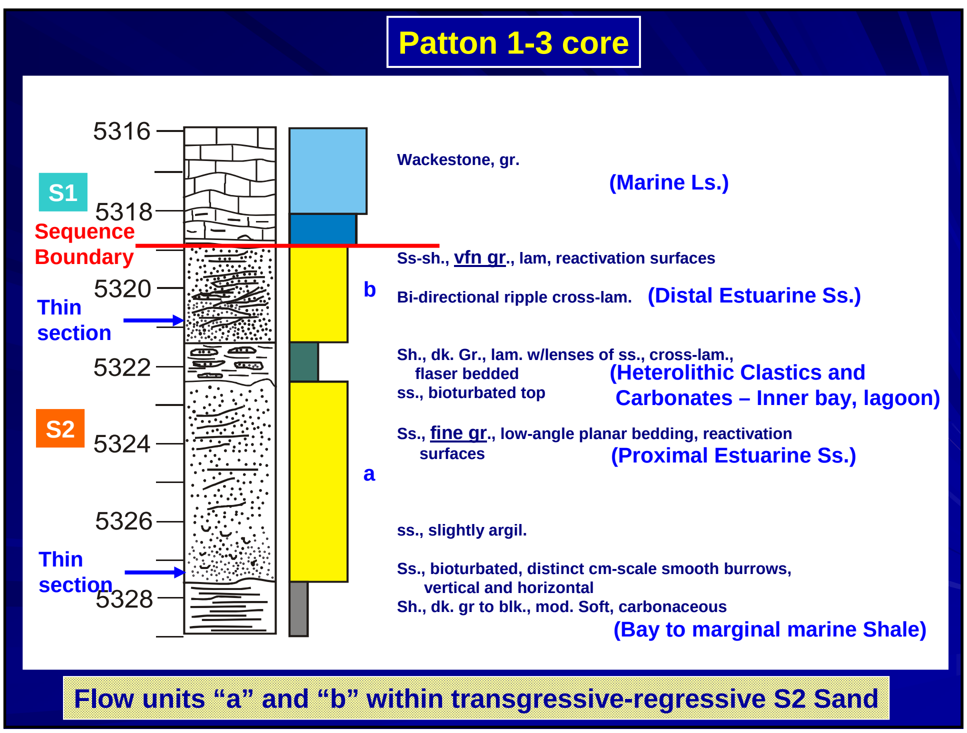
Patton 1-3 core
5316
5318
5320
5322
5324
5326
5328
S1
S2
Sequence Boundary
Thin section
Thin section
b
a
Wackestone, gr.
(Marine Ls.)
Ss-sh., vfn gr., lam, reactivation surfaces
Bi-directional ripple cross-lam.
(Distal Estuarine Ss.)
Sh., dk. Gr., lam. w/lenses of ss., cross-lam., flaser bedded
ss., bioturbated top
(Heterolithic Clastics and Carbonates – Inner bay, lagoon)
Ss., fine gr., low-angle planar bedding, reactivation surfaces
(Proximal Estuarine Ss.)
ss., slightly argil.
Ss., bioturbated, distinct cm-scale smooth burrows, vertical and horizontal
Sh., dk. gr to blk., mod. Soft, carbonaceous
(Bay to marginal marine Shale)
Flow units "a" and "b" within transgressive-regressive S2 Sand

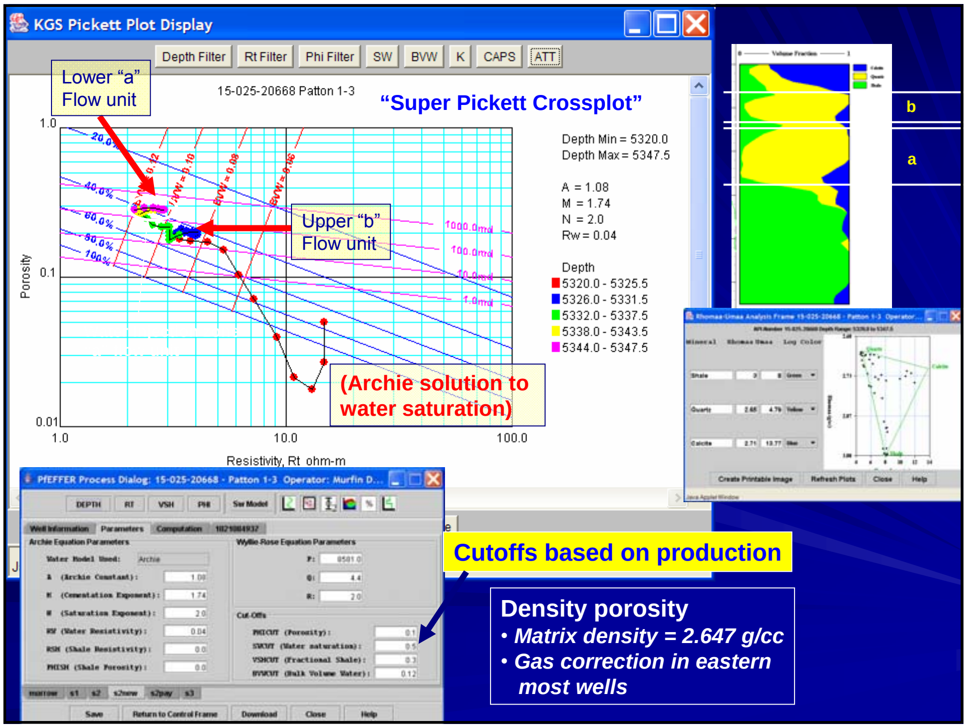
KGS Pickett Plot Display
Lower "a" Flow unit
15-025-20668 Patton 1-3
"Super Pickett Crossplot"
Upper "b" Flow unit
(Archie solution to water saturation)
Depth Min = 5320.0
Depth Max = 5347.5
A = 1.08
M = 1.74
N = 2.0
Rw = 0.04
Depth
5320.0 - 5325.5
5326.0 - 5331.5
5332.0 - 5337.5
5338.0 - 5343.5
5344.0 - 5347.5
Porosity
Resistivity, Rt ohm-m
b
a
Cutoffs based on production
Density porosity
• Matrix density = 2.647 g/cc
• Gas correction in eastern most wells

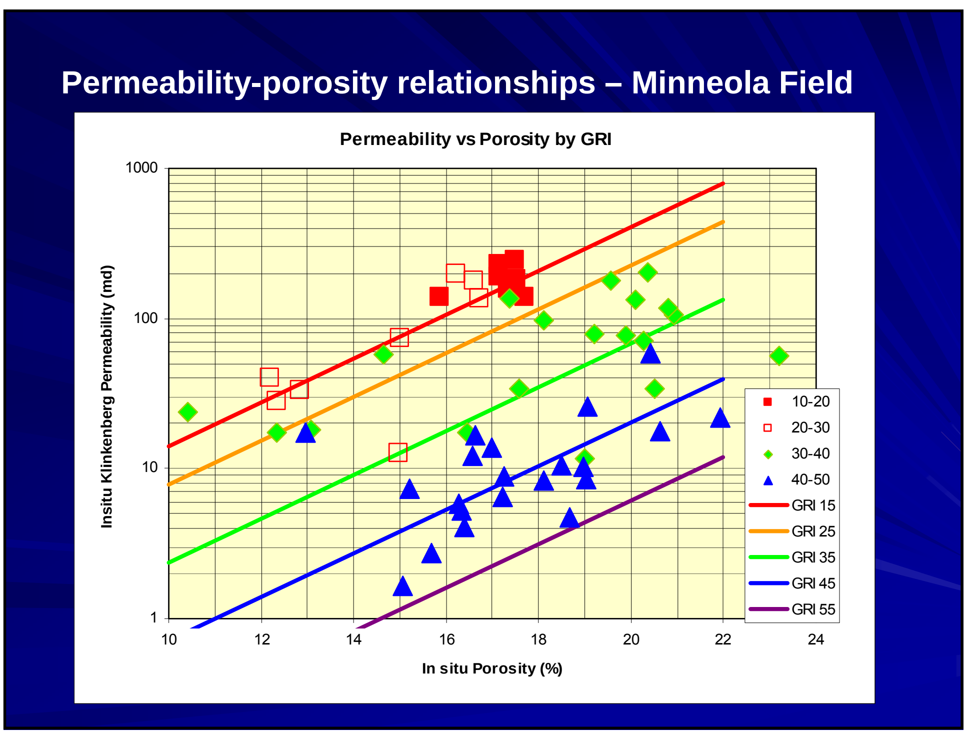
Permeability-porosity relationships – Minneola Field
Permeability vs Porosity by GRI
Insitu Klinkenberg Permeability (md)
In situ Porosity (%)
10-20
20-30
30-40
40-50
GRI 15
GRI 25
GRI 35
GRI 45
GRI 55

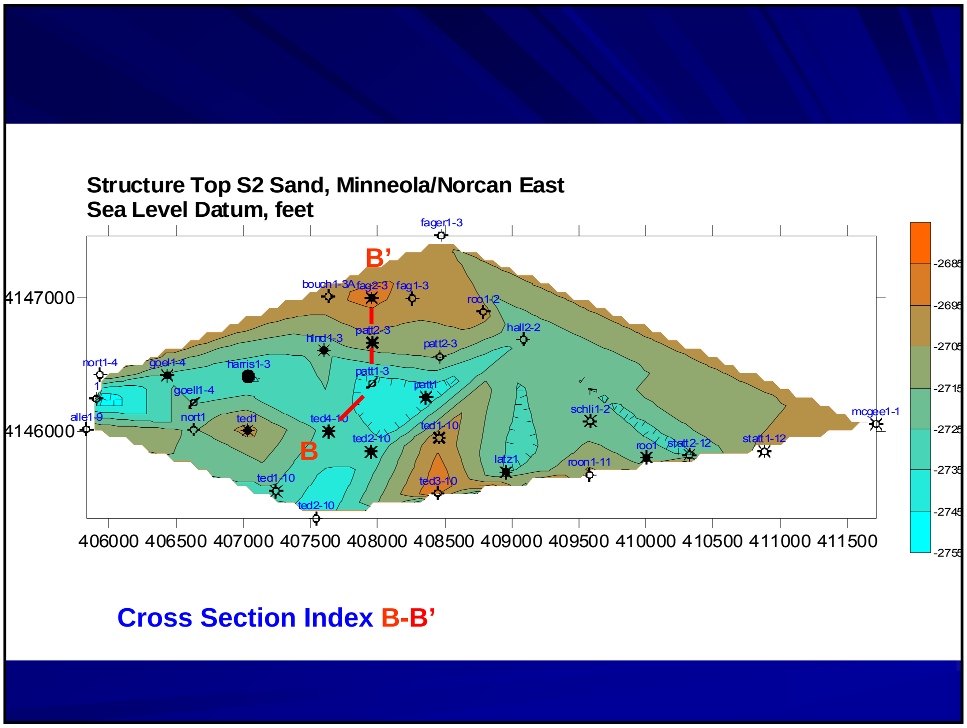
Structure Top S2 Sand, Minneola/Norcan East
Sea Level Datum, feet
B'
B
4147000
4146000
406000 406500 407000 407500 408000 408500 409000 409500 410000 410500 411000 411500
Cross Section Index B-B'

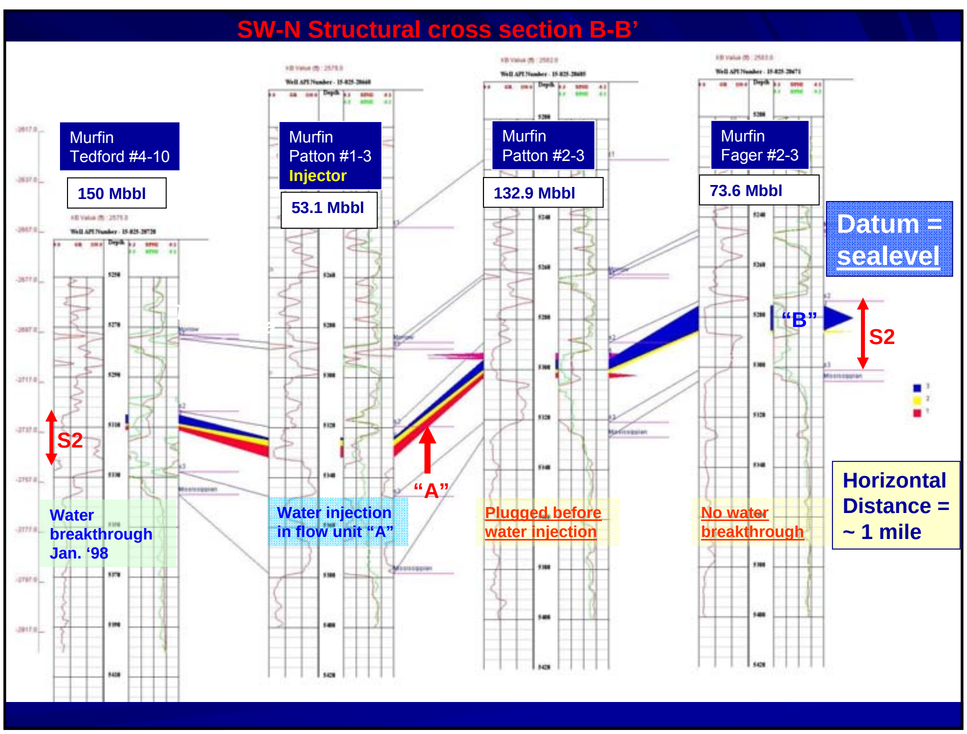
SW-N Structural cross section B-B'
Murfin
Tedford #4-10
150 Mbbl
Murfin
Patton #1-3
Injector
53.1 Mbbl
Murfin
Patton #2-3
132.9 Mbbl
Murfin
Fager #2-3
73.6 Mbbl
Datum = sealevel
"B"
S2
S2
"A"
Water breakthrough Jan. '98
Water injection in flow unit "A"
Plugged before water injection
No water breakthrough
Horizontal Distance = ~ 1 mile

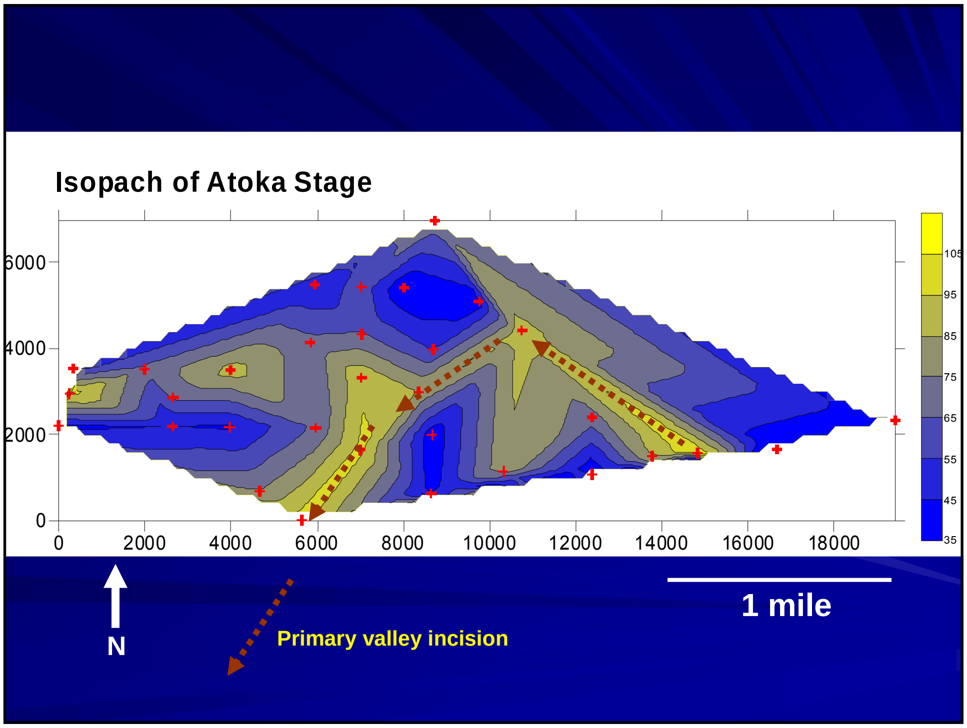
Isopach of Atoka Stage
6000
4000
2000
0
0
2000
4000
6000
8000
10000
12000
14000
16000
18000
105
95
85
75
65
55
45
35
N
Primary valley incision
1 mile

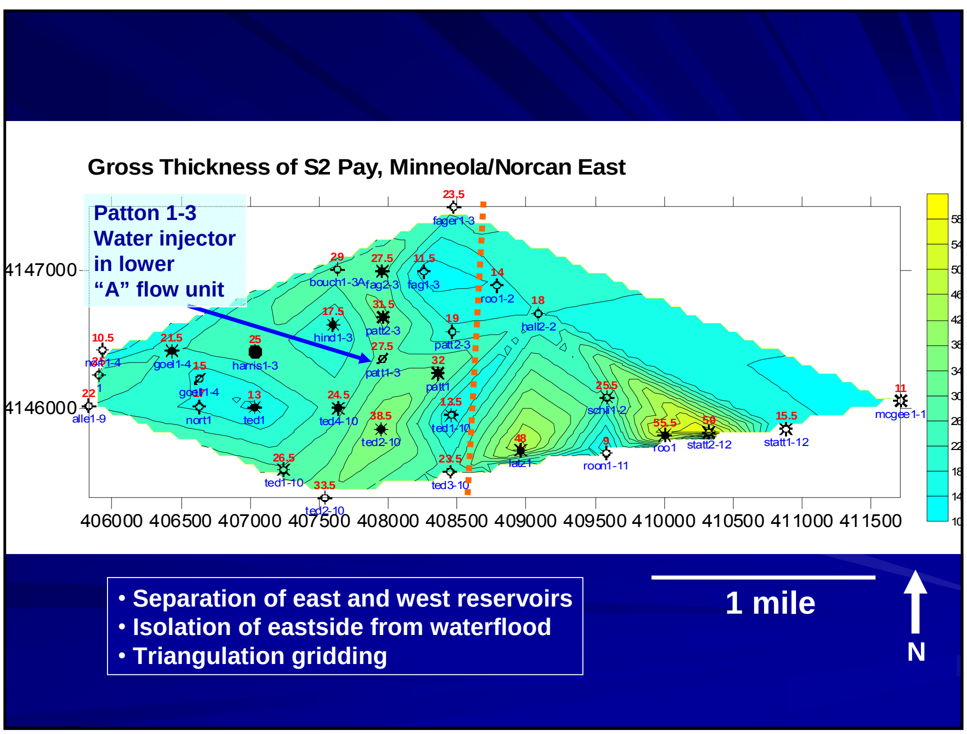
Gross Thickness of S2 Pay, Minneola/Norcan East
Patton 1-3
Water injector
in lower
"A" flow unit
4147000
4146000
406000 406500 407000 407500 408000 408500 409000 409500 410000 410500 411000 411500
• Separation of east and west reservoirs
• Isolation of eastside from waterflood
• Triangulation gridding
1 mile
N

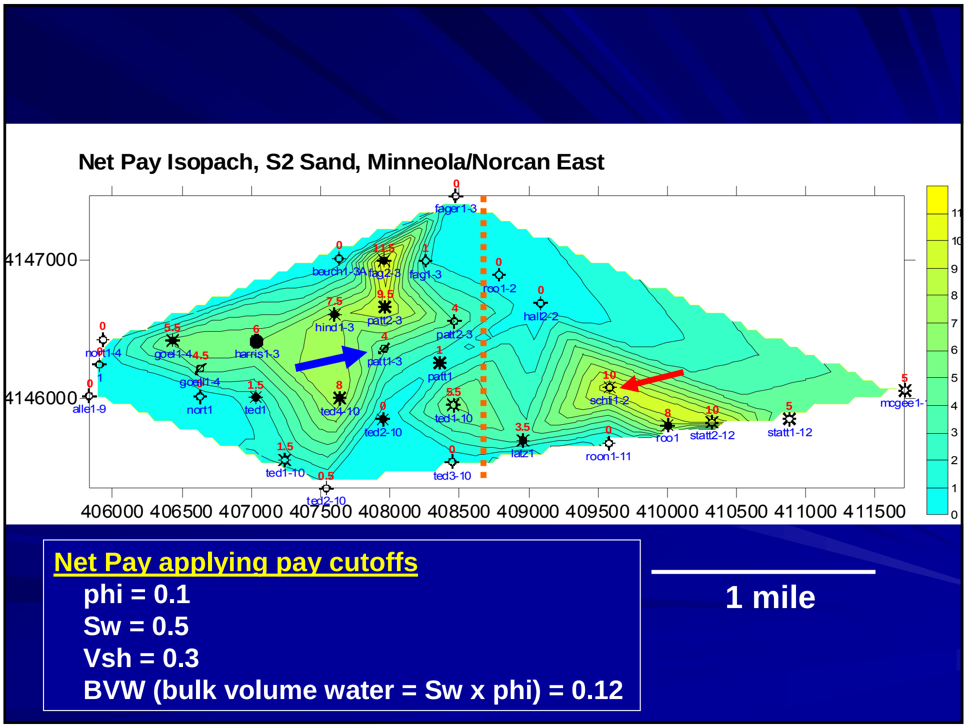
Net Pay Isopach, S2 Sand, Minneola/Norcan East
4147000
4146000
406000 406500 407000 407500 408000 408500 409000 409500 410000 410500 411000 411500
Net Pay applying pay cutoffs
phi = 0.1
Sw = 0.5
Vsh = 0.3
BVW (bulk volume water = Sw x phi) = 0.12
1 mile

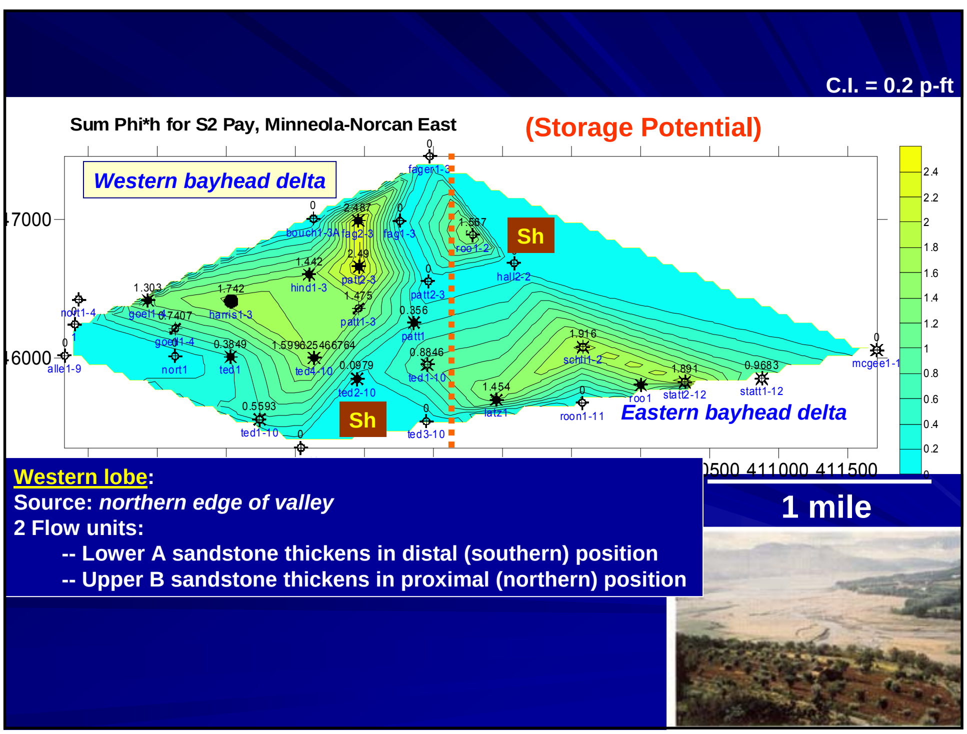
C.I. = 0.2 p-ft
Sum Phi*h for S2 Pay, Minneola-Norcan East
(Storage Potential)
Western bayhead delta
Sh
Sh
Eastern bayhead delta
Western lobe:
Source: northern edge of valley
2 Flow units:
-- Lower A sandstone thickens in distal (southern) position
-- Upper B sandstone thickens in proximal (northern) position
1 mile

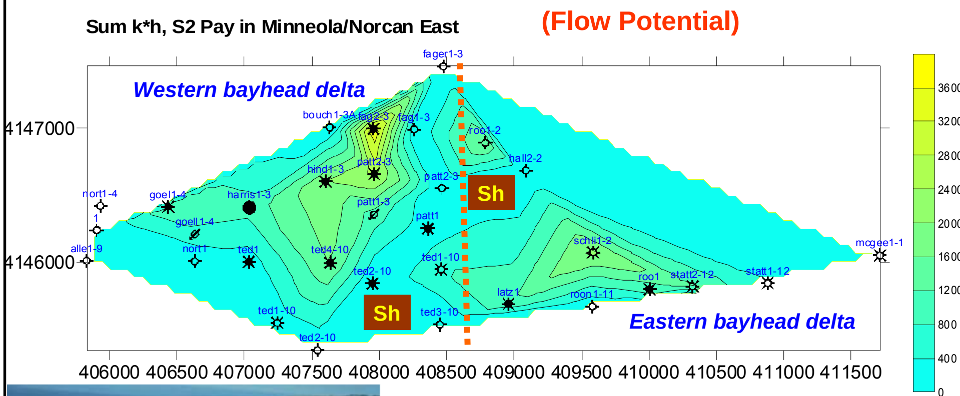

1 mile

Eastern Lobe:

- Source: *southeastern edge of valley*
- 3 flow units:
  - -- Lower A and B sandstones are laterally extensive before grading into limestone to west
  - -- Upper C sandstone limited to proximal position in southeast

Volumetrics of S2 Sand

- *OOIP ~8 MMBBLS*
- *Compared to cumulative production of ~1.1 MMBOE (14% of OOIP)*

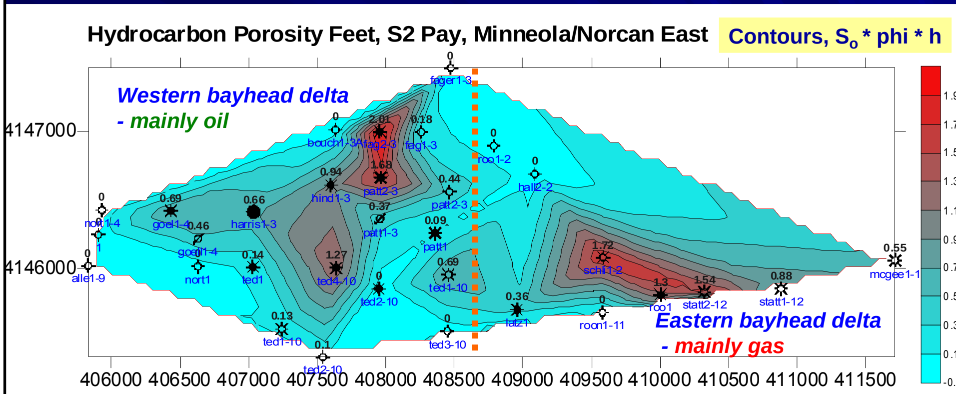

Comparison of this volumetric map with the a map of the cumulative BOE shows a high degree of correlation.

1 mile

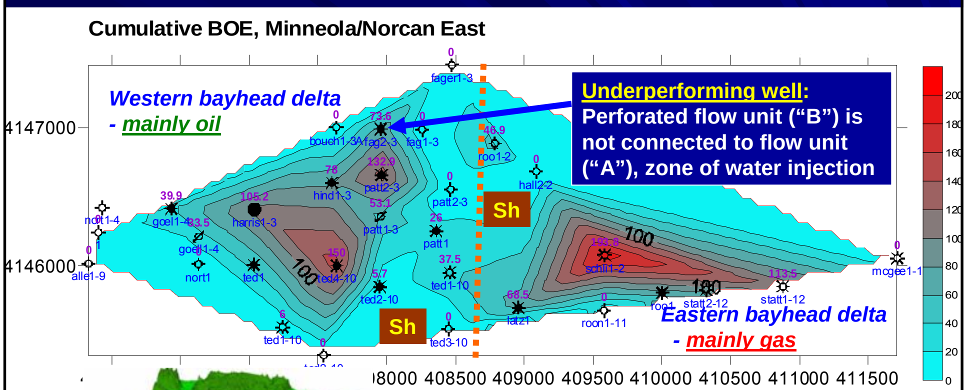

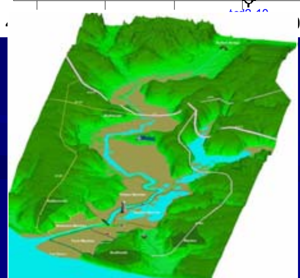

1 mile

http://www.suffolkestuaries.co.uk/Blyth/images/Option1-NAI.jpg

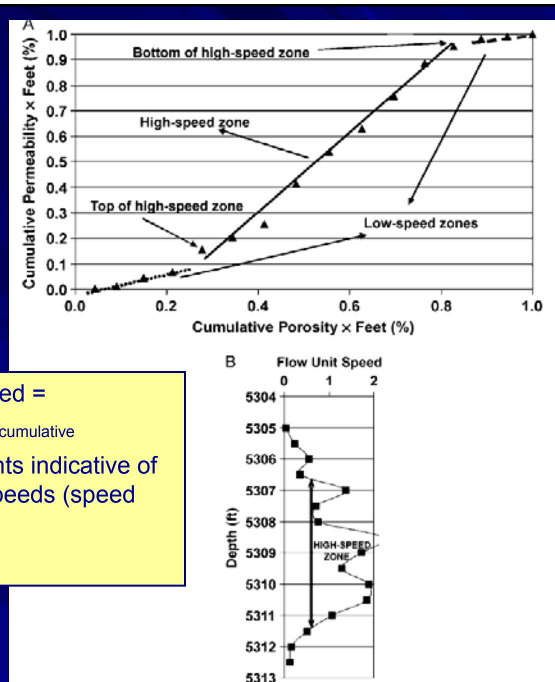

- Flow unit speed = $K_{cumulative}$*ft/Ø*$ft_{cumulative}$
- Inflection points indicative of different flow speeds (speed zones)

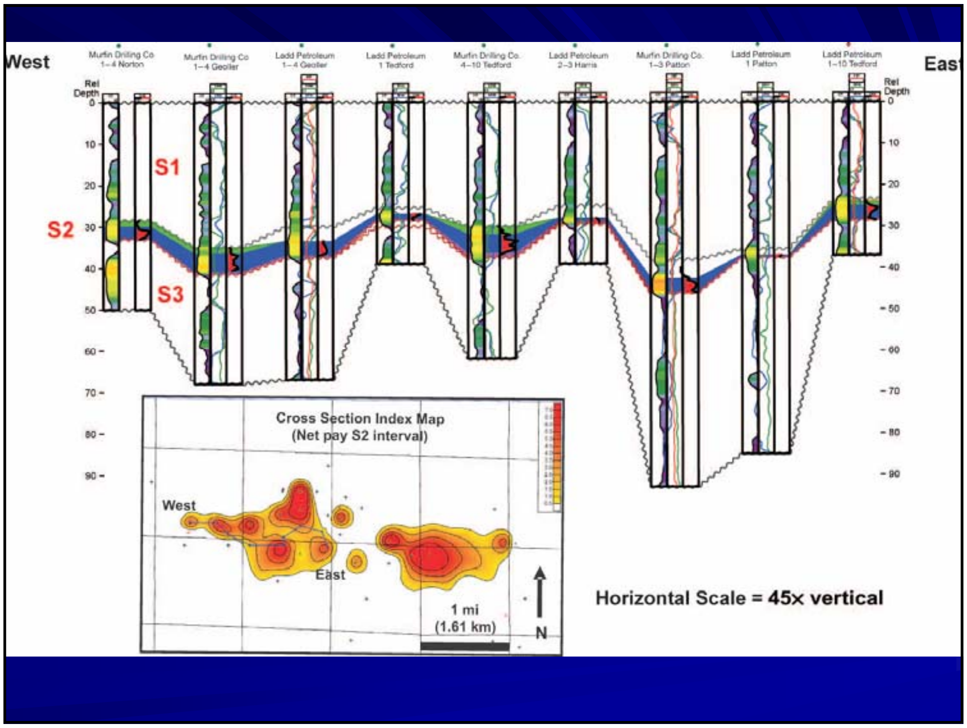

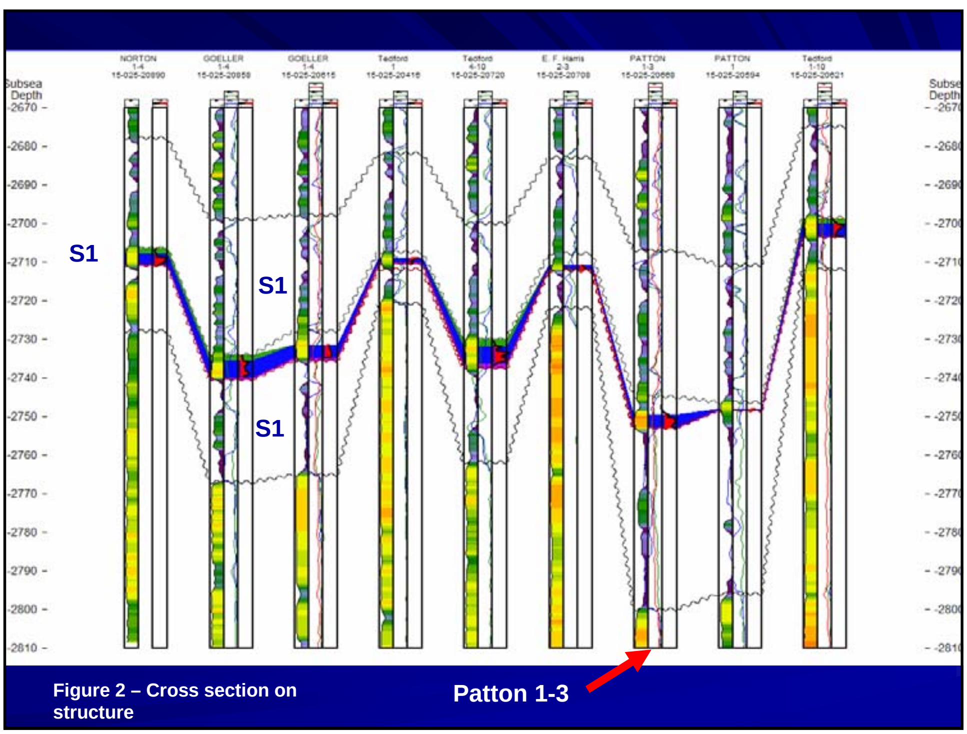

Figure 2 – Cross section on structure

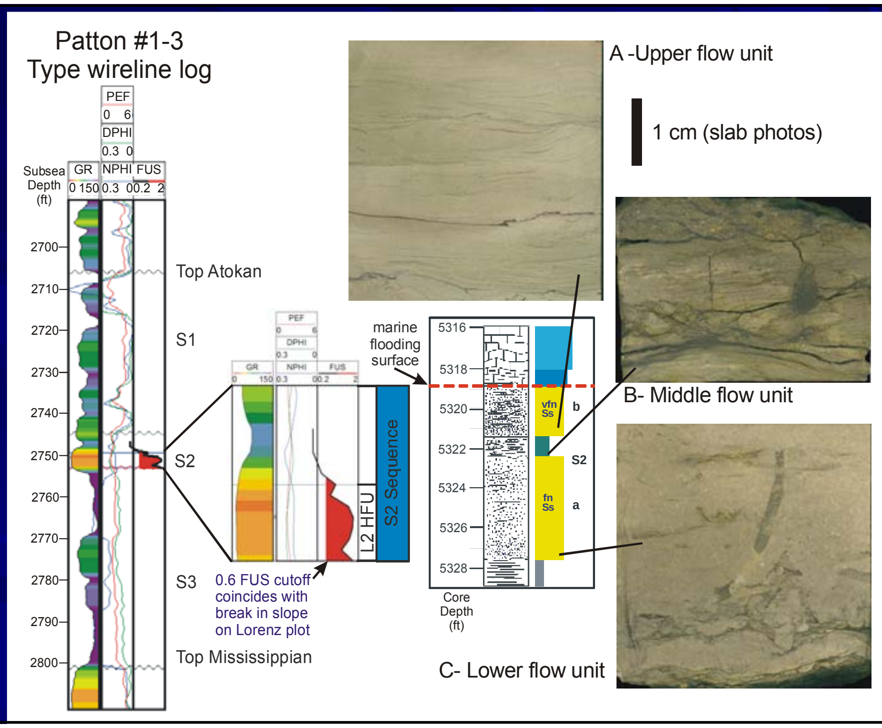

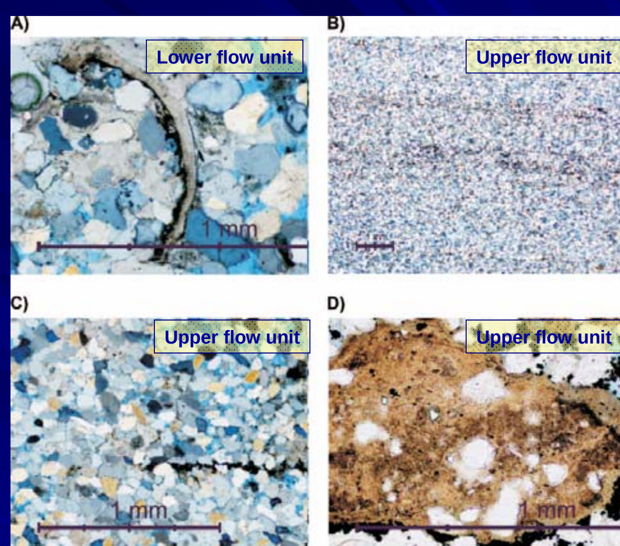

Thin-section photomicrographs of lower and upper flow units of S2 in Murfin Drilling Company 1-3 Patton well. (A) Patton 5327.3 ft (1623.76 m) (lower flow unit): bivalve in quartz sandstone. (B) Fine-grained sandstone with millimeter-shaly laminations (Patton 5320.1 ft [1621.56 m], upper flow unit). Blue epoxy impregnated under cross nicols. The scale bar (1 mm; 0.03 in.) is in the lower left. (C) Patton 5321.8 ft (1622.08 m): quartose sandstone (lower upper flow unit). (D) Patton 5321.8 ft (1622.08 m) (lower upper flow unit): caliche nodule (microcrystalline calcite) containing displaced sand grains suggesting in-situ formation. Blue epoxy impregnation under cross nicols. Porosity developed on the right and bottom of the photomicrograph. Scale bar shown is 1.0 mm (0.03 in.) long.

Positive correlation in net pay with cumulative production

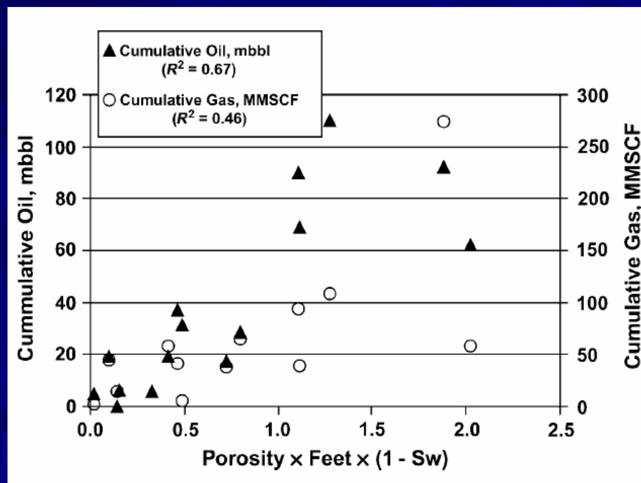

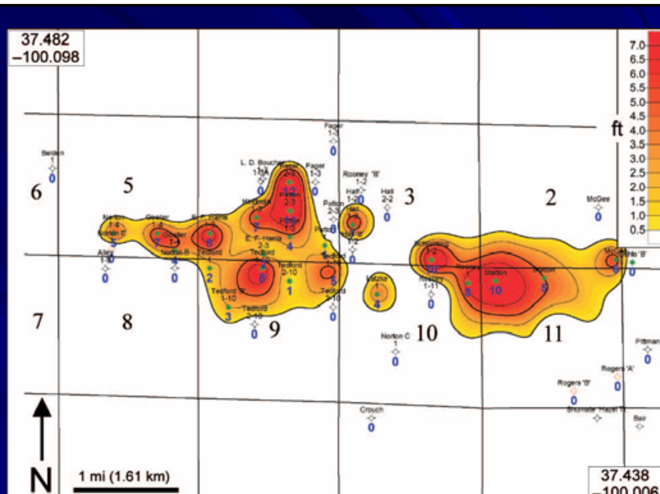

S2 net-pay isopach map of the Norcan East field. The thickness is expressed in feet, and the square grid is 1 mi (1.61 km) on a side. The S2 sandstone is limited to confines of the incised valley, and two discrete sandstone accumulations (an eastern and a western lobe) are visible.

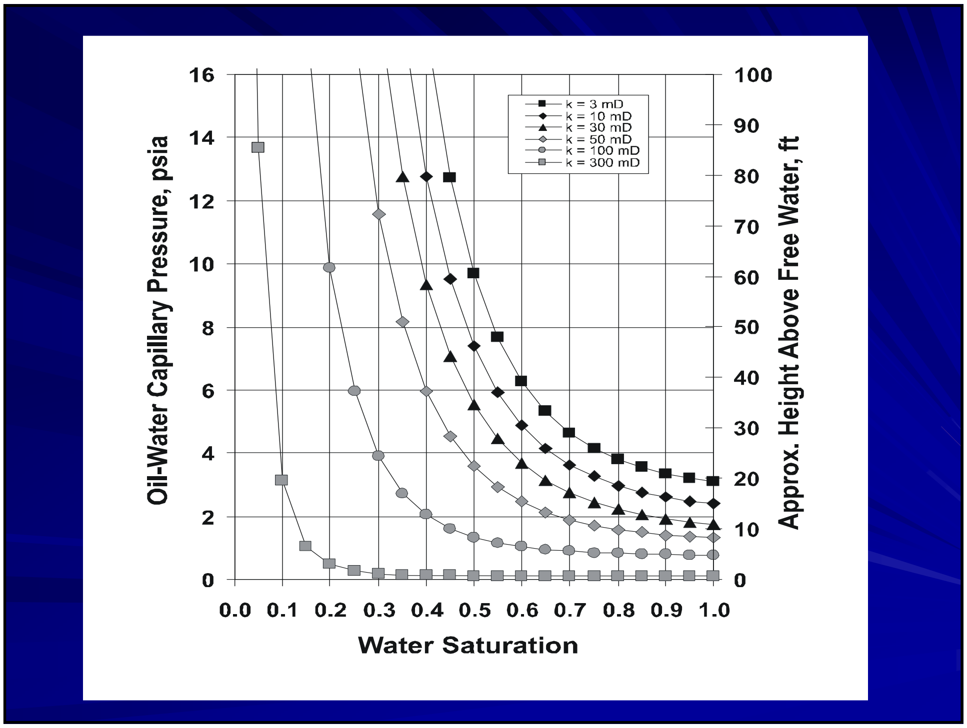
Oil-Water Capillary Pressure, psia
Approx. Height Above Free Water, ft
Water Saturation
k = 3 mD
k = 10 mD
k = 30 mD
k = 50 mD
k = 100 mD
k = 300 mD

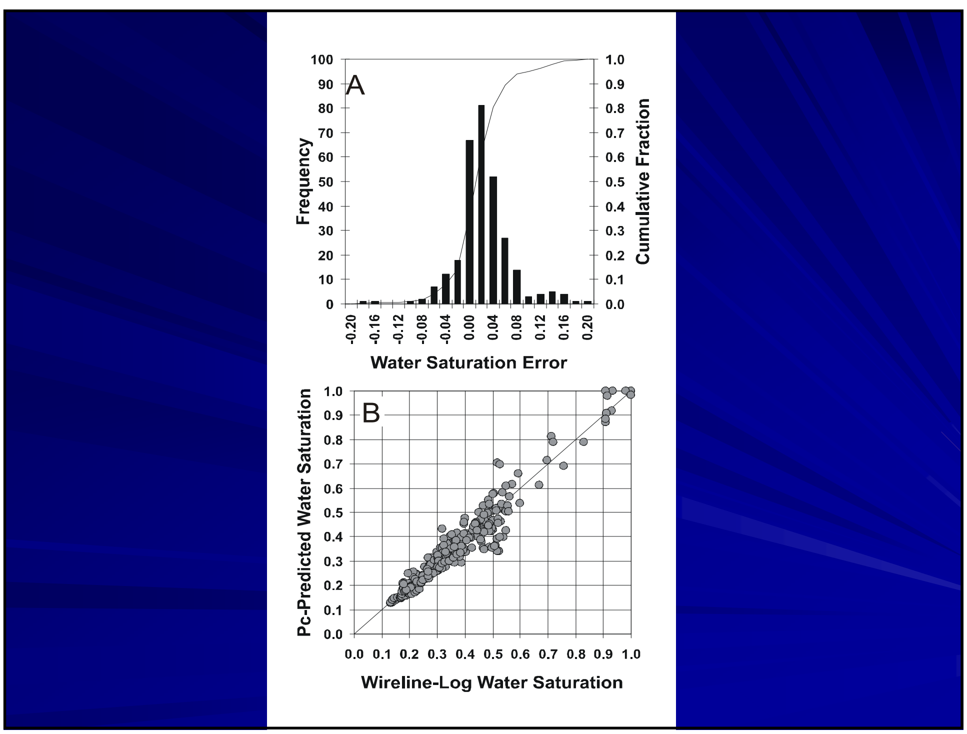
A
Frequency
Cumulative Fraction
Water Saturation Error
B
Pc-Predicted Water Saturation
Wireline-Log Water Saturation

Is BVW related to structure or pore characteristics?

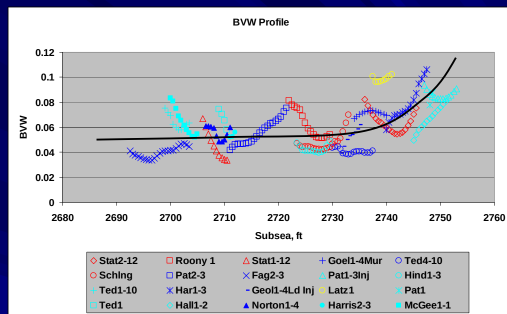

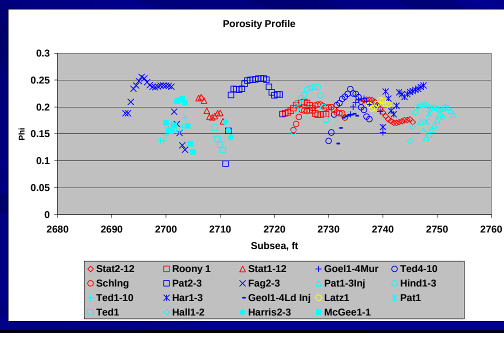

Log derived Sw vs elevation for S2 pay

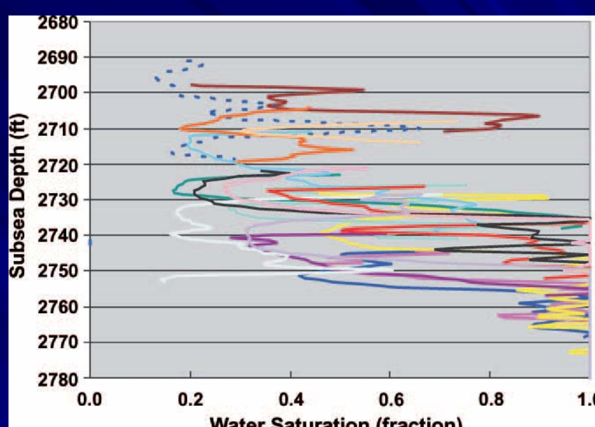

- Colors represent saturation profiles of different wells.
- In some wells, the logs stop before saturation gets to or near 1, whereas at others, the saturation reaches or is close to 1 at different subsea depths.

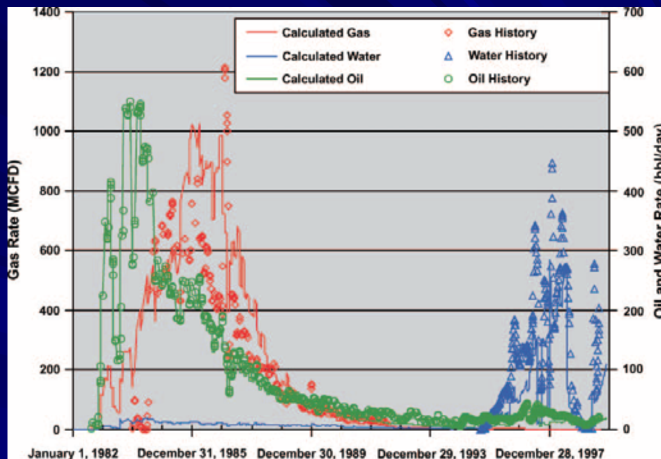

- History match of fluid production from the western segment of the Norcan East field.
- The green circles and line represent the historic oil rate and that calculated by the simulator.

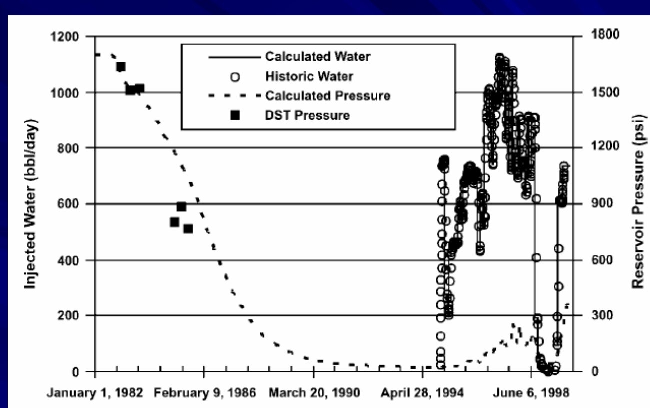

- History match between simulator-calculated water injection volumes and historic volumes of injected water in western segment of the field
- Broken black line = simulator calculated field pressure

Depositional & Petrofacies Model for Atoka sandstone Reservoirs

GEMINI Geo-Engineering Modeling through INternet Informatics

- The classic tripartite estuary mouth, inner estuary, and alluvial plain depositional model for the IVF systems is modified to accommodate reservoir compartmentalization introduced by multiple, tributary drainage into an estuary at Minneola Field forming subordinate bayhead estuarine deltas
- Cyclothemic-scale (4th-order) changes in sea level during the Pennsylvanian resulted in unconformity-bounded depositional sequences
  - –most clearly defined on well logs in this estuarine system by correlatable marine flooding surfaces.
- A transgressive-regressive lithofacies succession in the reservoir-bearing cycle often consists of (from bottom to top): 1) bay-fill shale, 2) tidal-dominated bay mouth bar to fluvial; 3) heterolithic intertidal central bay muds, silts,sands, and carbonates; and 4) fluvial to bay mouth bar lithofacies.
- Local depositional conditions vary depending on the local elevation and position in the valley, proximity to the sediment source, and the mouth of the valley.
- Lithofacies reflect the landward terminus of the Atokan marine cycle
- Coarser, better sorted sandstones are better reservoirs:
  - – reflected by lower GR, higher porosity and permeability, lower Sw and BVW
  - – in proximal positions in bayfill deltas in Norcan East in Minneola Field complex

Additional example of Pennsylvanian Ooid Shoal – Collier Flats, Missourian Swope Limestone, Comanche County, Kansas

Collier Flats Field – lower shelf ooid shoal on structural break

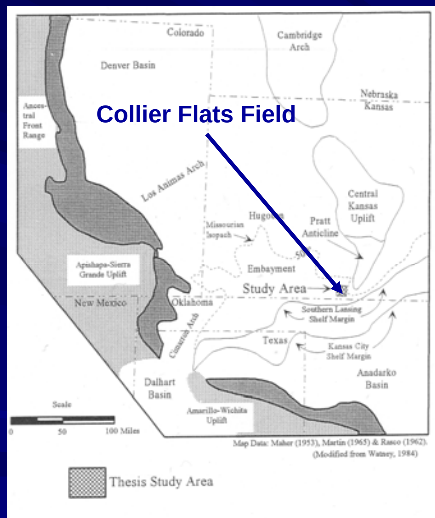

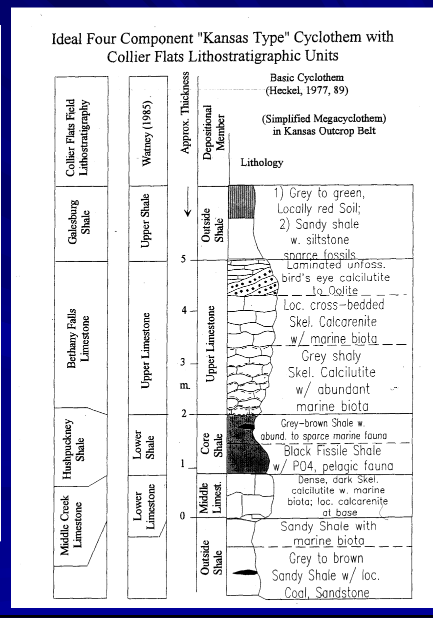

Lebeau (1997)

Collier Flats – Bethany Falls Ooid Shoal

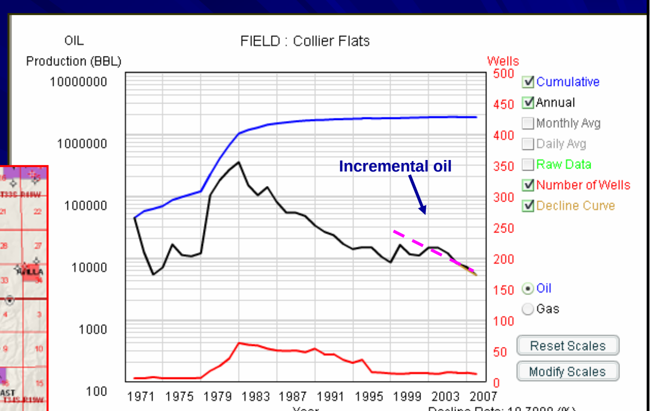

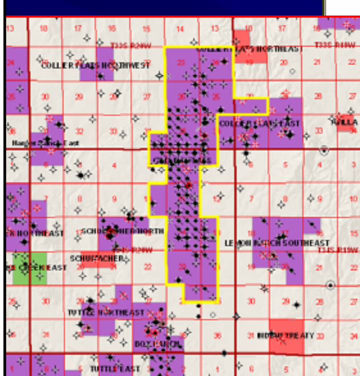

- 11 wells (62 max in 1982),
- Cumulative production = 2 MM bbls oil and 7.8 BCF
- Discovered 1970
- Waterflood initiated in 1998

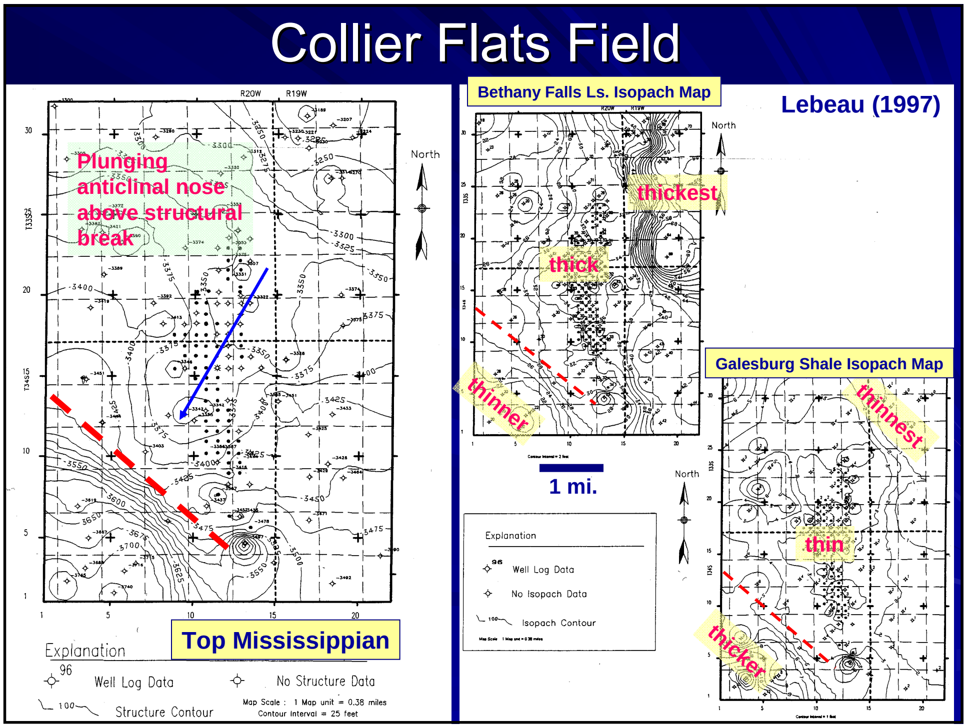
Collier Flats Field
Plunging anticlinal nose above structural break
Top Mississippian
Explanation
Well Log Data
No Structure Data
Structure Contour
Map Scale : 1 Map unit = 0.38 miles
Contour Interval = 25 feet
North
Bethany Falls Ls. Isopach Map
Lebeau (1997)
thickest
thick
thinner
1 mi.
Explanation
Well Log Data
No Isopach Data
Isopach Contour
Galesburg Shale Isopach Map
thinnest
thin
thicker

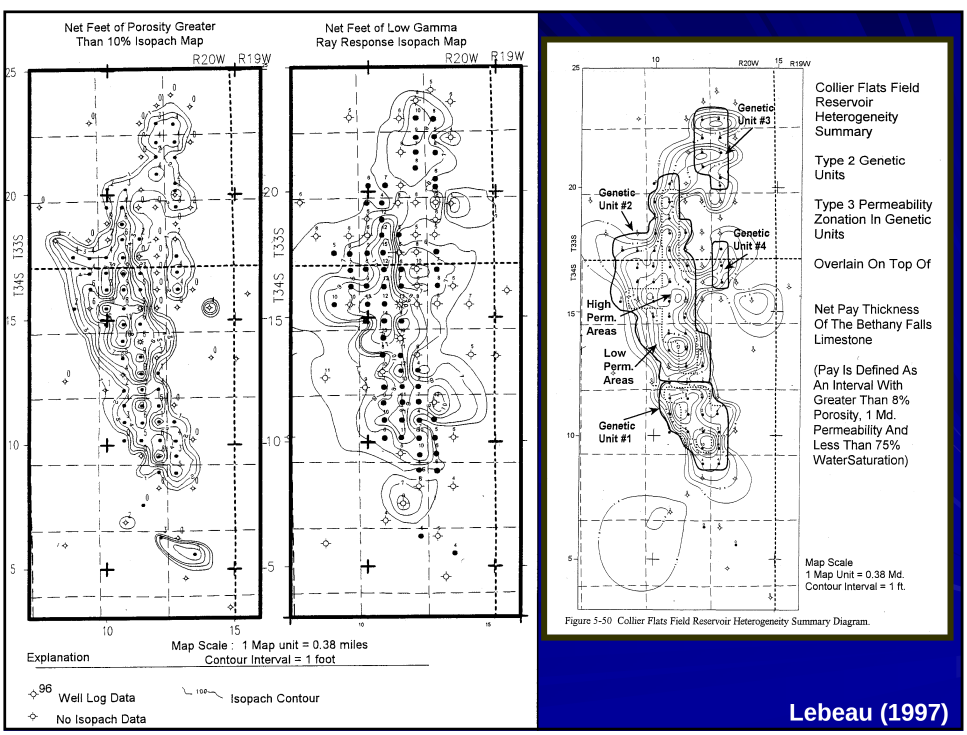
Net Feet of Porosity Greater Than 10% Isopach Map
Net Feet of Low Gamma Ray Response Isopach Map
R20W
R19W
T33S
T34S
Map Scale : 1 Map unit = 0.38 miles
Contour Interval = 1 foot
Explanation
Well Log Data
Isopach Contour
No Isopach Data
Genetic Unit #3
Genetic Unit #2
Genetic Unit #4
High Perm. Areas
Low Perm. Areas
Genetic Unit #1
Collier Flats Field Reservoir Heterogeneity Summary
Type 2 Genetic Units
Type 3 Permeability Zonation In Genetic Units
Overlain On Top Of
Net Pay Thickness Of The Bethany Falls Limestone
(Pay Is Defined As An Interval With Greater Than 8% Porosity, 1 Md. Permeability And Less Than 75% WaterSaturation)
Map Scale
1 Map Unit = 0.38 Md.
Contour Interval = 1 ft.
Figure 5-50 Collier Flats Field Reservoir Heterogeneity Summary Diagram.
Lebeau (1997)

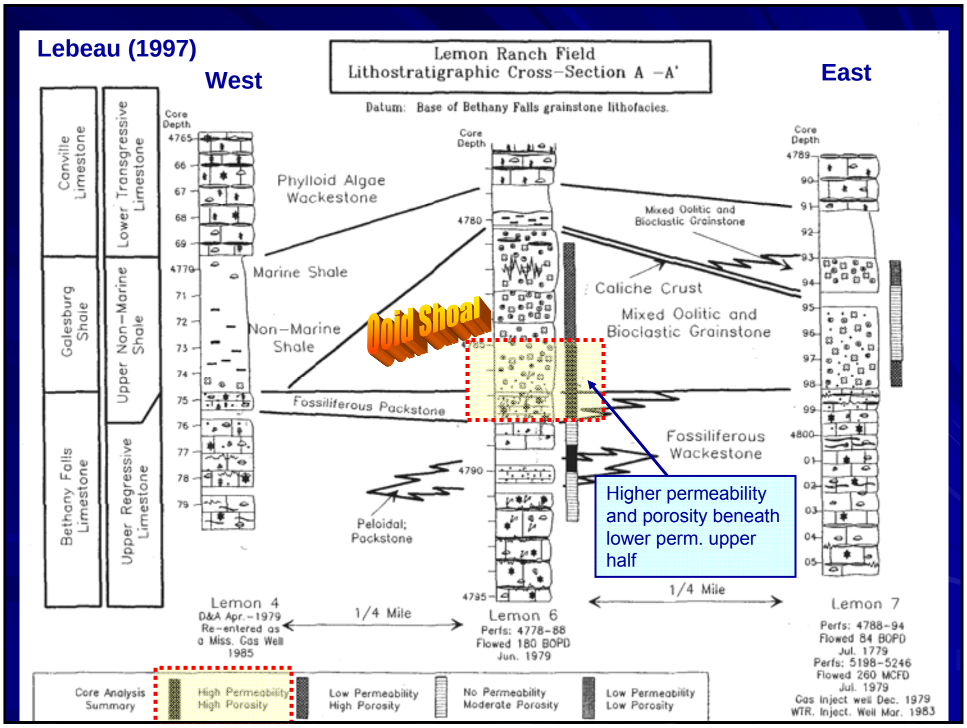
Lebeau (1997)
West
East
Lemon Ranch Field
Lithostratigraphic Cross-Section A -A'
Datum: Base of Bethany Falls grainstone lithofacies.
Canville Limestone
Galesburg Shale
Bethany Falls Limestone
Lower Transgressive Limestone
Upper Non-Marine Shale
Upper Regressive Limestone
Phylloid Algae Wackestone
Marine Shale
Non-Marine Shale
Ooid Shoal
Fossiliferous Packstone
Peloidal; Packstone
Mixed Oolitic and Bioclastic Grainstone
Caliche Crust
Mixed Oolitic and Bioclastic Grainstone
Fossiliferous Wackestone
Higher permeability and porosity beneath lower perm. upper half
Lemon 4
D&A Apr.-1979
Re-entered as a Miss. Gas Well 1985
1/4 Mile
Lemon 6
Perfs: 4778-88
Flowed 180 BOPD
Jun. 1979
1/4 Mile
Lemon 7
Perfs: 4788-94
Flowed 84 BOPD
Jul. 1779
Perfs: 5198-5246
Flowed 260 MCFD
Jul. 1979
Gas Inject well Dec. 1979
WTR. Inject. Well Mar. 1983
Core Analysis Summary
High Permeability High Porosity
Low Permeability High Porosity
No Permeability Moderate Porosity
Low Permeability Low Porosity